DISPLACEMENT-BASED SEISMIC DESIGN OF BRIDGES WITH ISOLATION AND ENERGY DISSIPATION DEVICES

A Dissertation Presented

by

FERNANDO SANCHEZ-FLORES

to

THE GRADUATE SCHOOL OF ENGINEERING

of

KYOTO UNIVERSITY

In Partial Fulfillment of the Requirements for the Degree of Doctor of Engineering

Specializing in Seismic Structural Engineering

September, 2011

京都大学

This dissertation is devoted to my mother Julia Flores

Querida mami: Gracias por tu infinito amor que ha coloreado con alegría y esperanza mis días más aciagos...

ABSTRACT

Since the *Performance-Based Seismic Engineering* (PBSE) was issued, several design methods has been proposed to fulfill its requirements. Within the PBSE framework, one of the most promising methods is based on the control of displacements, namely displacement-based design (DBD). In DBD, the inelastic structure is simplified into an equivalent elastic single degree of freedom system characterized by equivalent properties. Recently, this philosophy of design has been adopted for several major design codes in the world. In this study, new equivalent linearization equations and a novel displacement-based approach for isolated bridges with seismic energy dissipation devices are developed with emphasis on their application to the Japanese Design Specifications for Highway Bridges.

In the first part of this study, equations for equivalent properties are developed and defined in terms of the initial period of the structure. The results show that they can estimate the maximum inelastic displacement between the limits of conservative errors set as -10% and 20%. The results also suggest that the equivalent properties should be derived for specific types of earthquakes, hysteretic models and one specific soil conditions.

In the second part of this research, a displacement-based design method is developed for isolated bridges with seismic dampers. The performance objectives were defined by the elastic behavior of the piers and the inelastic behavior of the isolators. Viscous dampers, either linear or nonlinear, are used as seismic energy dissipation devices. It was verified that the bridges and piers designed with the proposed DBD method achieve the desired performance objectives since the resulting displacements are kept under the target values. Based on the results, the method is shown to be efficient and accurate design instrument. Moreover, with the proposed methodology the iterative nonlinear analyses required in the current force-based design to calculate the viscous damper coefficients are avoided.

The last part of this study addresses the bidirectional effects of the earthquake in isolated skewed piers of bridges with supplemental dampers. A design methodology is presented and verified by nonlinear time history analysis. Based on the results, the approach is accurate enough for preliminary design of new bridges or for assessment of existing structures.

ACKNOWLEDGEMENTS

For the past three years an incredible amount of time and work has been put into this final research as a member of the Structural Dynamics Laboratory of Kyoto University. Throughout the years, some individuals voluntarily offered generous amounts of time, helpful advice, and selfless support that encouraged me to complete this study. For this, I offer my sincerest thanks.

I would like to take time to thank certain individuals for their particularly support during my research.

First, I would like to acknowledge my academic advisor Prof. Akira Igarashi for his kind support during my six and half years of stay in Japan. I would also like to thank Prof. Takeshi Koike and Prof. Sumio Sawada for the reviews and critical comments that contributed to improve the final version of this dissertation.

It is a pleasure to thank Prof. Izuru Takewaki and to Prof. Minehiro Nishiyama for the encouragement and support I received.

I would like to thank the member of the ICSS Bridge Research Committee with whom I learned the current state-of-practice of design bridges in Japan. Especially, I would like to thank to Mr. Tetsuo Matsuda (West Nippon Expressway Engineering Kyushu Co.), Mr. Hiroshi Matsuda (JIP Techno Science Corp.), Mr. Hiroshige Uno (Oiles Corp.), and Mr. Yoshinori Wada and other related engineers of NEXCO-West.

I am truly indebted and thankful to my Prof. Amador Terán-Gilmore (UAM-A, México) for his friendship, support and encouragement since I was undergraduate student.

I would like to thank the Japanese Government for their financial support provided through the Minister of Education, Culture, Sport, Science and Technology by a Monbukagakusho scholarship.

I would like to show my deepest gratitude to my mother Julia Flores. I could not be where I am today without her love, patience, and kindness. She has been there for me every step of the way, and her encouragement means the world to me.

I would like to express my deep gratitude to Keiko, whose invaluable support, time, understanding and encouragement, during all this time enabled me to complete this work. I believe that without her presence this work would not have been possible. I would also like to thank my friends who not only boosted morally but also assisted me during the toughest moments; especially I would like to thank my dearest friends Eliza, Noriko, Patricia, Sherliza, Meagan and Yves.

Lastly, I offer my regards and thanks to all those who supported me in any respect throughout my life and graduate studies.

Fernando Sanchez-Flores

Kyoto, Japan

September, 2011

TABLE OF CONTENTS

LIST OF FIGURES

LIST OF TABLES

CHAPTER 1

INTRODUCTION

1.1 GENERAL REMARKS

Historically, earthquakes have been the most destructive natural disasters in the world for civil structures. To illustrate the magnitude of the damage that earthquake may cause, the reader is referred to USGS (2011), where detailed information on historic earthquakes, their magnitude and the economic losses they caused as well as the number of fatalities can be found. It is well-known the social and economic impact due to large earthquakes, and that the structural damage may cause extremely negative consequences. For instance, for the particular case of bridges, they generally provide vital links in transportation systems so they are extremely important lifelines that should be operating in the immediate aftermath for emergency response operations. The failure of one structural member yields a high probability of severe damage - or even collapse - due to the lack of structural redundancy (Moehle and Eberhard, 2000). Therefore, the structural damage must be reduced in these type of structures.

Throughout the years extensive research has been conducted on design approaches and seismic-protection technologies not only for bridges but also for buildings and other civil structures. One of the most relevant achievements is the concept of the Performance-Based Seismic Engineering (PBSE) (SEAOC, 1995). The PBSE has been adopted by some major codes in the world to enhance the seismic behavior of structures. In order to fulfill its requirements, several simplified design methods have been proposed. Among these, the displacement-based design is one of the most promising design methods that more realistically captures the inelastic structural behavior.

Recently, PBSE has been adopted in practicing engineering in combination with earthquake-resistant protective devices added to the structure. As a result, some displacement-based design approaches for structures with these devices have been developed. However, further research is need for the design of bridges with seismic isolators and viscous dampers under the concept of displacements control.

This Chapter introduces the aforementioned ideas and concepts into the context of this research.

1.2 PERFORMANCE-BASED SEISMIC DESIGN

One of the first documents to lay out tentative guidelines for *Performance-Based Seismic Engineering* (PBSE) is *Vision 2000*, published by the Structural Engineers Association of California (SEAOC, 1995). This document provided a conceptual framework for the development of performance-based seismic engineering. The primary objective of PBSE is to design a structure to achieve predefined levels of performance (*i.e.* levels of damage) when it is subjected to specific seismic hazard levels (*i.e.* earthquake intensities) within definable levels of reliability. Levels of performance are described in terms of displacements since damage is better correlated with displacements rather than forces (Bertero and Bertero 2000, Priestley 2000) while the earthquake and the levels of damage are defined by the design codes. One of the first multidisciplinary reviews of performance-based design in earthquake engineering can be found in Chandler and Lam (2001).

The performance levels are defined as follows:

- **Functional**. After the earthquake the structure is in operation with negligible damage.
- **Operational**. The structure continues in operation although with minor damage and disruption in nonessential services.
- **Life Safety**. Damage is moderate to extensive but some margin exists before total or partial structural collapse. Life safety is substantially protected.
- **Near Collapse**. Damage is severe although structural collapse is prevented. Life safety is at risk.

The earthquake ground motion demand is generally defined as the engineering characteristic of the shaking at a site for a given earthquake that has a certain probability of occurrence (BSSC, 1997). The demand is generally classified into three categories:

- **Serviceability Earthquake**. Ground motion with 50% of probability of being exceeded in 50 years.
- **Design Earthquake**. Ground motion with 10% of probability of being exceeded in 50 years.
- **Maximum Earthquake**. Ground motion with 5% of probability of being exceeded in 50 years, or the maximum level of ground motion expected within the known geologic framework.

The Performance Objectives are all possible combinations of structural performance and seismic demand (Figure 1.1). Performance Objectives may be assigned dependent upon the function and importance of the structure, cost considerations, etc. There can be a single Performance Objective or multiple Performance Objectives (one for different Seismic Demands).

To satisfy the mentioned requirements of PBSD, the most recurrent approaches are: (a) force-based design, (b) energy-based design, and (c) displacement-based design, (SEAOC, 1995). From these, the latter, based on the control of displacements, is one of the most promising design methods that more realistically captures the inelastic structural behavior.

In the following sections the design approaches based on forces and displacements will be described into the context of the present study.

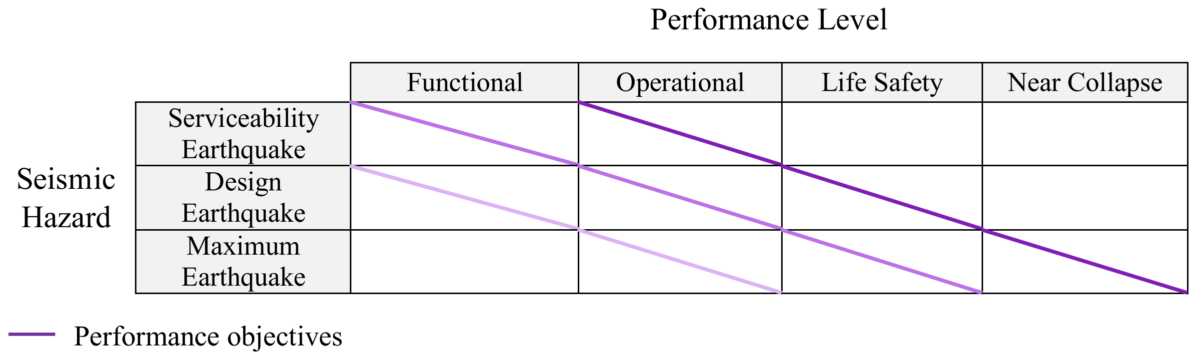

Figure 1.1 Performance Objectives for Performance-Based Seismic Engineering

1.3 Force-Based Design

1.3.1 Methodology

Force-based design is the current state of practice in seismic design. This method is based on the assumption that the earthquake force can be determined from the elastic acceleration response spectra at the estimated period of the structure (Figure 1.2). The elements are then designed to resist the seismic forces and the displacements verified until the end of the design process.

In general, it consists of the following steps:

i. *Selection of the preliminary pier cross section*

Define the bridge characteristics. In this step the initial parameters are chosen based on structure geometry and location. A preliminary design for gravity loadings is conducted and a preliminary member size is obtained.

ii. *Set member stiffness*

The member stiffness (gross or reduced) is calculated based on the size estimated from step one and design assumptions.

iii. *Dynamic characteristics of the structure*

Based on member stiffness and mass, either the fundamental period is computed in the case of an equivalent lateral force approach, or periods corresponding to a number of modes are computed through modal analysis. For a structure of weight W and stiffness K simplified as a single-degree-of-freedom (SDOF) system, the fundamental period (T_0) is calculated by expressions of this form:

$$T_0 = 2\pi\sqrt{\frac{W}{gK}} \tag{1.1}$$

where g is the gravitational acceleration.

iv. *Define the ductility and the reduction factor*

The ductility (μ) and the reduction factor (R_μ) for the structure are defined to ensure inelastic structural behavior.

v. *Obtain the elastic forces from acceleration spectrum*

First, the acceleration S_a, for the system with weight W and elastic period T_0 is obtained (Figure 1-2). Consequently, the elastic base shear, V_e, is calculated as

$$V_e = S_a(W)I \tag{1.2}$$

where I is the importance factor of the structure specified in seismic Codes.

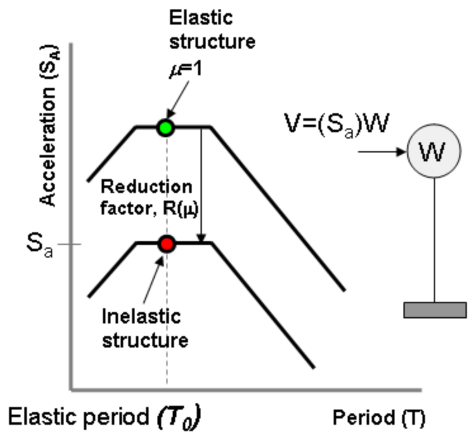

Figure 1.2 Conceptual base of force-based design

vi. *Calculate the seismic forces*

The design shear is obtained by multiplying the base shear by a reduction factor defined in terms of the ductility of the system $R(\mu)$ as

$$V_{ge} = \frac{V_e}{R(\mu)} \tag{1.3}$$

vii. *Structural analysis and design of plastic hinge locations*

The structure is analyzed under seismic forces to determine the required moment capacities and locations of plastic hinges.

viii. *Verification of the displacements*

Verify that the obtained displacements do not exceed code-allowable limits. If the computed displacements do not exceed code-limits, the design is completed; otherwise it is modified in an iterative process.

ix. *Capacity design of structural members*

After this step the displacements under seismic forces can be computed.

These steps are summarized in Figure 1.3.

1.3.2 LIMITATIONS

Although force-based design has been improved throughout the years, it is still having inherent conceptual limitations. A complete list of them can be found in Oguzmert, (2006) and Priestley *et al.* (2007). In this section, only the most significant ones for this research are listed as follows:

- It is based on the elastic structural period. For inelastic structures, the analysis should be carried out with the inelastic period. However, this is not a common calculation in the engineering practice.
- Unique ductility capacities and force-reduction factors can be assigned to different structural systems.
- In bridges where the superstructure is designed at the column yield displacement, the girders could possibly be under-designed.

- The distribution of base shear strength between piers is based on the assumption that piers can be forced to yield at the same displacement despite having different stiffness.
- Structural and nonstructural damage experienced during an earthquake are primarily due to lateral displacements, therefore the force-based procedures may not provide a reliable indication of damage potential.

As can be observed, the FBD method is based on the base shear as the one and only design parameter at one specific level of earthquake ground motion. However, designs based on just one ground motion level not necessarily may lead to acceptable performance in service, damageability or safety limit states when the structure is subjected to different levels of earthquakes.

Summarizing, since damage is more sensitive to displacement (strain), rather than strength (stress) (Bertero and Bertero, 2001), the current force-based design method cannot achieve the performance objectives defined in the PBSE (Priestley *et al*., 2000). Thus the FBD procedure is not appropriate for a seismic design philosophy based on damage control. Therefore, the displacement-based design is the most promising method to achieve the performance objectives of the performance-based seismic engineering (Priestley *et al*., 2007).

1.3.3 FORCE-BASED DESIGN FOR BRIDGES WITH VISCOUS DAMPERS

Among the large number of energy dissipation devices available in the current state-of-practice, in this work only viscous dampers are considered due their characteristics reducing the displacement response of the structure without significantly changing the initial period of vibration (Chapter 2).

Although there is a well-established routine for the design of base-isolated structures with viscous dampers, generally the characteristics of the viscous dampers are initially assumed (Figure 1.4). If the displacements exceed the allowable value the characteristics of the dampers have to be modified. Then, the conventional practice of carrying out a series of trial and error process for design of supplemental dampers requires a lot of computation time (Kim and Choi, 2003) due the inelastic time history analyses. For models with small number of nodes/elements, these can be carried out in a relatively short time. However, for models with a large number of nodes/elements, nonlinear time history analyses are usually time consuming and expensive. Then, the force-based design is not an efficient tool to calculate the amount of damping provided by viscous dampers. As it will be shown in this work, the displacement-based design procedure is an efficient option to easily obtain the characteristics of the dampers, in such a way that the displacements are kept below predefined values.

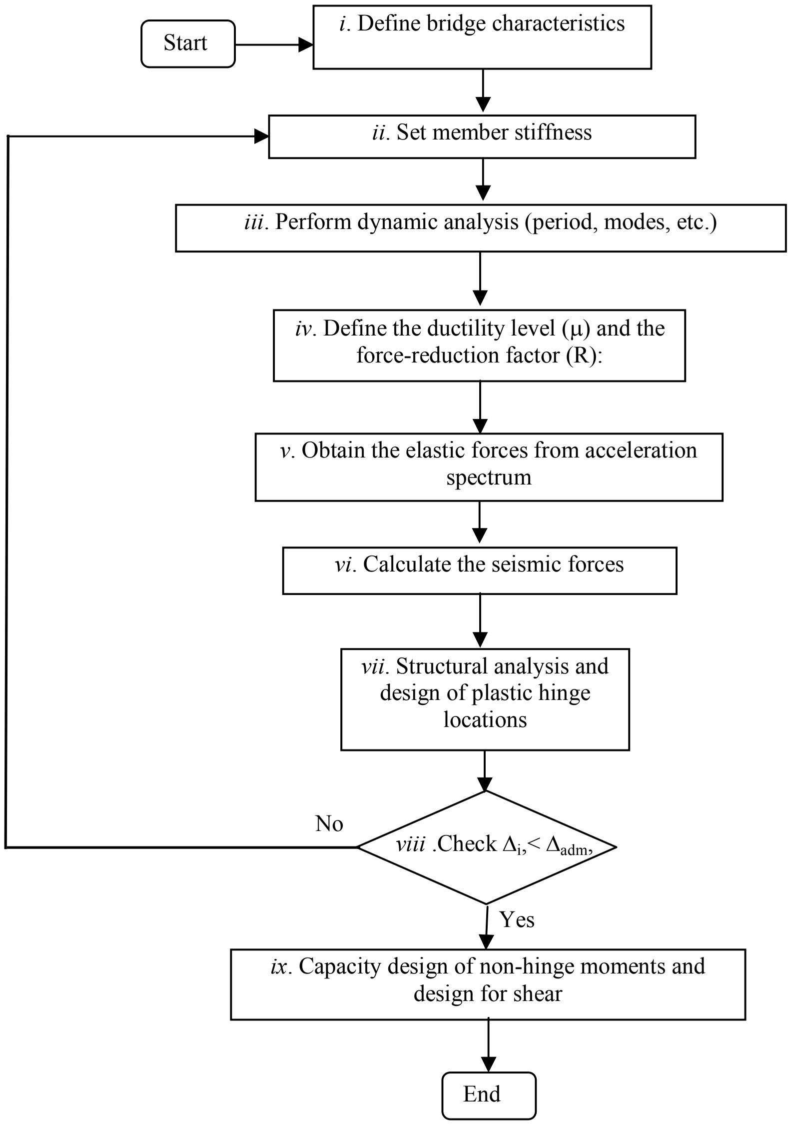

Figure 1.3 Force-based design methodology

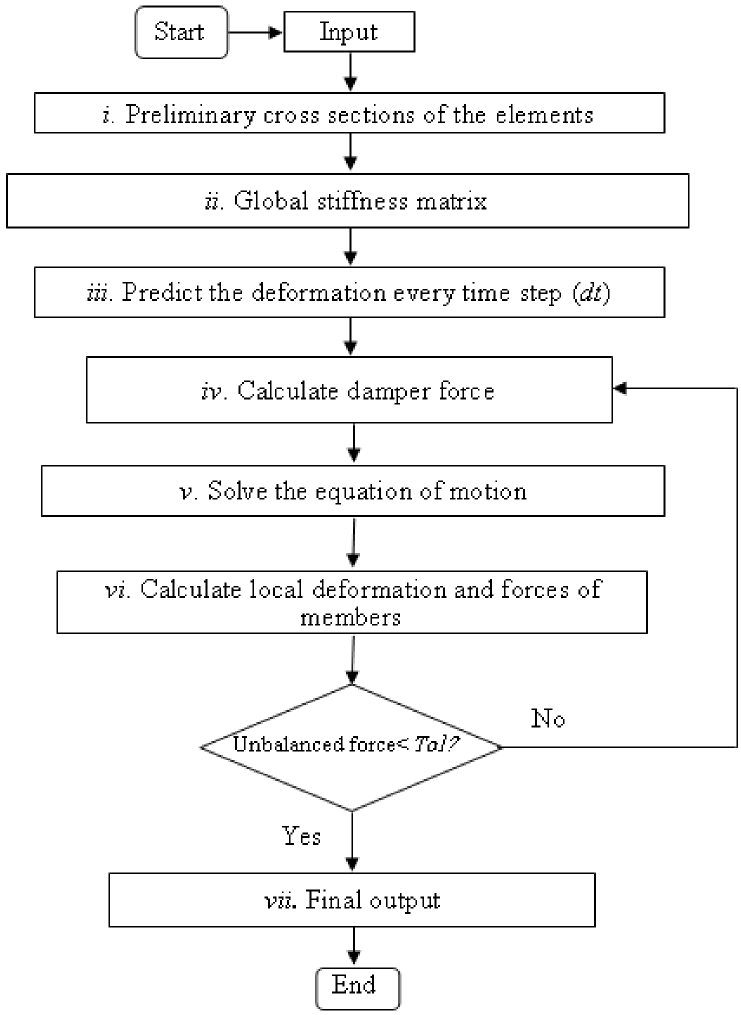

Figure 1.4 FBD design methodology for structures with dampers (modified from Wada et al. 2000)

1.4 DISPLACEMENT-BASED DESIGN

1.4.1 METHODOLOGY

In displacement-based procedures, seismic displacement is the primary response parameter for design. This means the acceptance criteria are expressed in terms of displacements rather than forces.

The first equivalent structure approach was suggested by Jacobsen (1930), some decades later the *substitute structure* approach was developed by Shibata and Sozen (1976). However, the modern concepts of displacement-based design were introduced in the 1990s (Moehle 1992, Priestley 1993, SEAOC 1995). The state-of-the-art of displacement-based design (DBD) for structures was presented in Appendix I (*Tentative Guidelines for Performance-Based Seismic Engineering*) and Part B (*Force–Displacement Approach*) of the 1999 SEAOC Blue Book (SEAOC, 1999). Appendix I refers to the *Direct displacement-based design* procedure and to the *Equal-displacement-based* (EBD) method. The former uses a substitute elastic structure to relate displacement demands to the effective period at peak response. The latter, uses the *equal displacement rule* to relate peak displacements to the period of the cracked elastic structure.

Since 1990s, extensive research on displacement-based design have been carried out for conventional structures (Moehle 1992, Wallace 1995a, Wallace 1995b, Medhekar and Kennedy 2000, Chopra and Goel 2001, Panagiotakos and Fardis 2001, Pang and Rosowsky 2007, Priestley *et al.*, 2007). Recently, displacement-based design has been extended to structures with base isolation (Jara and Casas 2006, Priestley *et al*. 2007, Pietra *et al*. 2008, Cardone *et al*. 2009), and structures with supplemental damping (Kim *et al*. 2006, Teran-Gilmore and Virto-Cambray 2006, Priestley *et al*. 2007, Shinde *et al*. 2008, Lin *et al*. 2008).

In DBD, the structure is designed to achieve a specified target displacement profile while subjected to earthquakes consistent with a given reference response spectrum. The DBD utilizes *equivalent linearization* techniques (Chapter 3) to characterize an equivalent simplified structure as a linear single-degree-of freedom (SDOF) system. Then, the design forces are obtained with the equivalent stiffness and the target displacement (Figure 1.5). The DBD approach aims to design a structure that achieves a selected performance limit state under selected earthquake intensity. For inelastic structures, the procedure must be combined with capacity design principles to ensure that the formation of plastic hinges occur in the design locations, and to prevent any non-ductile modes of inelastic deformation from occurring.

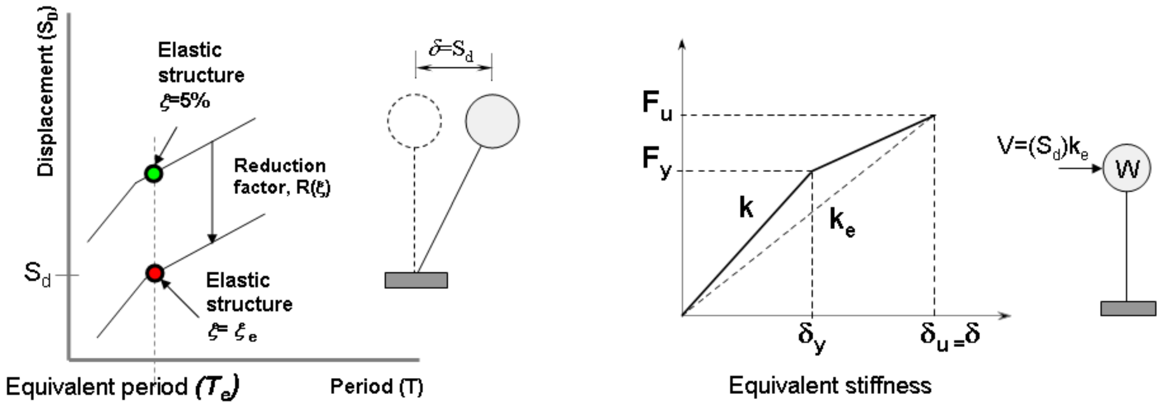

Figure 1.5 Conceptual base of displacement-based design

The general procedure for a SDOF system is described as follows:

i. Estimate the yield displacement of the structure, δ_y

This is done with semi-empirical relationships.

ii. Select an appropriate maximum inelastic displacement, δ_u

δ_u depends on the deformation capacity of the structural elements.

iii. Calculate the maximum displacement of the SDOF system, δ_{max}

δ_{max} is the sum of the yield displacement, δ_y, and the maximum inelastic displacement, δ_u.

iv. Select an appropriate value of effective structural damping, ξ_{eq}

ξ_{eq}, depends on the ductility level.

v. Calculate the equivalent period, T_{eq}

T_{eq} corresponds to the maximum displacement, δ_{max}, and the effective damping, ξ_{eq}.

vi. Calculate the equivalent stiffness, K_{eq}

The equivalent stiffness of the SDOF system is calculated with the equivalent mass.

vii. Calculate the base shear, V_b

The design base shear is calculated and distributed to the structural elements in accordance with their secant stiffness at maximum response.

viii. Design with capacity principles

The structure is then designed according to capacity design principles in order to guarantee the development of the desired failure mechanism.

The outline of the method is shown in Figure 1.6.

1.4.2 DISPLACEMENT-BASED DESIGN FOR BRIDGES WITH VISCOUS DAMPERS

Kim and Choi (2003) presented one of the first approaches to straightforwardly calculate the damping provided by viscous dampers in inelastic MDOF systems in the context of PBSD. To this end, Kim and Choi (2003) used capacity spectrum method and the equivalent damping capacity of the structure originated from plastic deformation of each structural member. For displacement-based design, however, few approaches have been presented. For buildings with viscous dampers, Lin *et al*. (2003), Kim *et al*. (2006), Lin *et al*. (2008) and Shinde *et al.* (2008) presented iterative procedures. For bridges, however, as the author knowledge, no approaches have been issued yet.

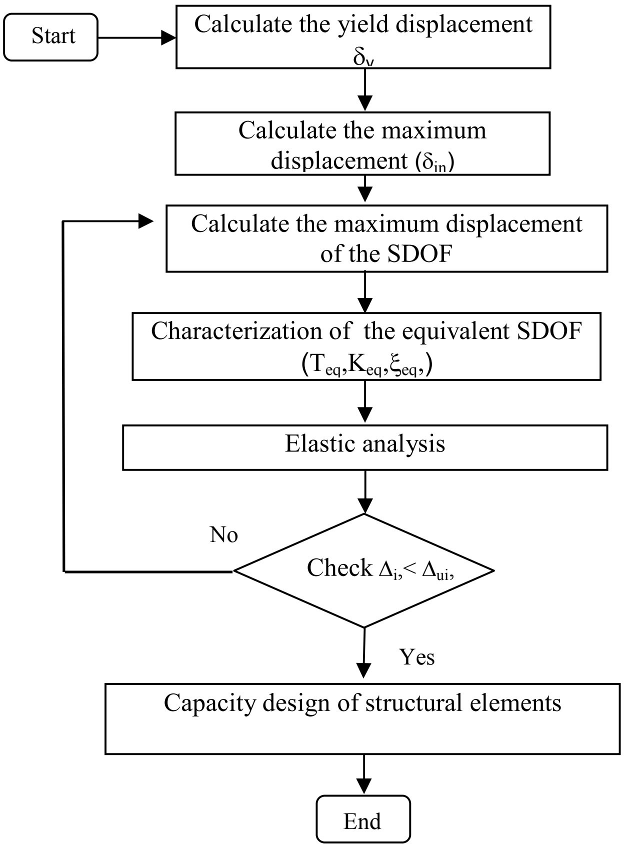

Figure 1.6 Displacement-based design methodology

1.4.3 DISPLACEMENT BASED DESIGN IN GUIDELINES FOR BRIDGES

The displacement-based design has been widely adopted in codes from the United States of America (USA). The California Department of Transportation presented one of the most remarkable challenges in the design philosophy for new bridges in the Seismic Design Criteria (SDC) (Caltrans, 2006), with the shift from force-based assessment to a displacement-based assessment following the ATC-32 recommendations (ATC, 1996). The SDC of Caltrans assumes the lateral strength of the system (size and reinforcement of the substructure sections) at the beginning of the process. Then, by displacement demand analysis and displacement verifications, it is confirmed that the structural seismic performance of the bridge is acceptable. Otherwise, the strength is revised and the process repeated. The maximum inelastic displacement is estimated from a linear elastic response spectrum analysis of the bridge with cracked section stiffness. Then, it is converted to peak inelastic displacements using the Displacement Modification Method. Once the displacement demands are estimated, the verification of the displacement capacity of each pier is done by means of a pushover analysis. Finally, the structural elements are designed and detailed according to capacity design principles.

Another well-known bridge code in the USA, the AASHTO LRFD Bridge Design Specifications (AASHTO, 2004) included improvements and the recommendations from the ATC (ATC, 1998), SDC (Caltrans, 2006), and other AASHTO committees for seismic design (AASHTO, 2002). In the LRFD Seismic Guide the objective is to prevent the structure collapse and loss of life. It recognizes the variability of seismic hazard over the US territory and specifies different Seismic Design Categories. The design procedure is in concept similar to the procedure by Caltrans, described in the previous paragraph. For regular bridges, the demand analysis is performed by uniform load methods. For other bridges, including regular ones, the spectral modal analysis can be used.

The aforementioned design methodologies have similarities such as:

- The use of displacement as a parameter to control damage and seismic demand.
- They require the bridge shows a specific value of ductility. This contrasts with the force-based approach in which the use of force reduction factors generalizes the ductility capacity.

- The structural members are designed by capacity principles to assure that the damage will only occur in predefined locations.

Thus, even though the details of a specific displacement-based methodology may change, the concepts and principles remain the same assuring satisfactory structural performance as can be observed in Figure 1.7

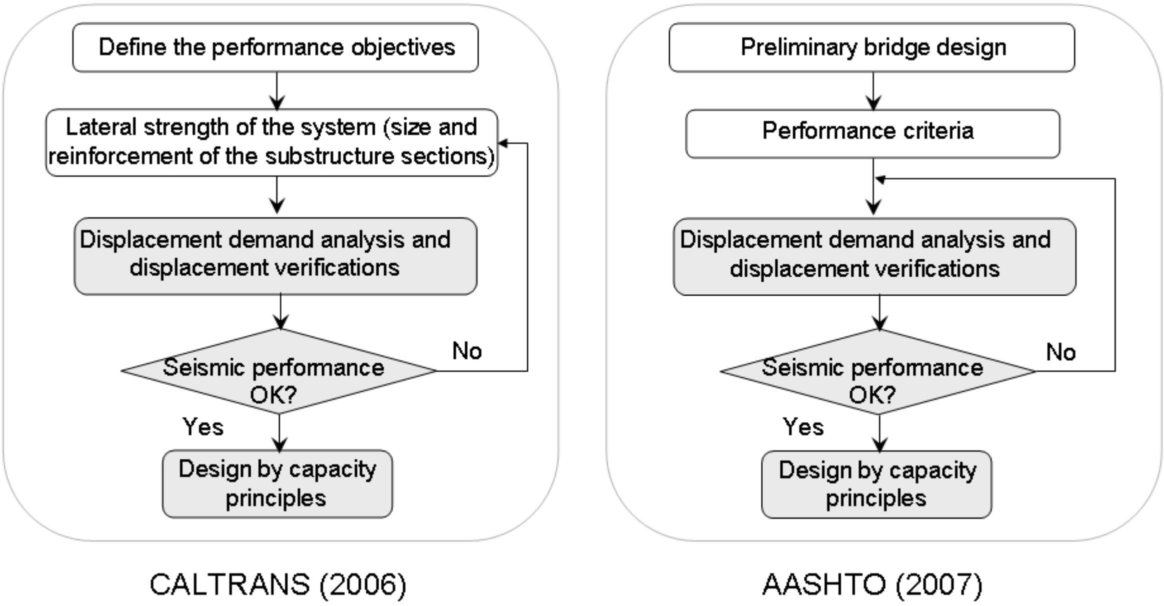

Figure 1.7 Comparison of CALTRANS and AASHTO DBD approaches

Apart of the research already presented in design Codes, some research has been conducted to extend the results from Building Codes to bridges. For instance, Fu and Al Ayed (2002) extended to bridges the Displacement Coefficient Method developed for buildings by BSSC (1997).

In Europe, although there is no an explicit code for bridges, the unified design guidelines Eurocode 8 (1998), included the displacement spectra explicitly developed for a wide range of periods. In a more recent work, Priestley *et al.* (2007) issued one of the first drafts of displacement-based code for buildings.

In Japan, after the Hyogoken-nanbu Earthquake occurred on January 17 of 1995, the Japan Road Association (2002) issued the modified Japanese Specification for Highway Bridges. In these guidelines, seismic performance levels, design forces and performance-based methods were newly introdu.ced (Unjoh *et al.* 2005). However, the Japanese specifications do not consider the displacement-based design as alternative yet.

Tables 1.1 and 1.2 show the Seismic Performance Criteria and the current Design Methods for the Japanese Specifications, respectively.

In Asia, one of the first attempts to outline the performance-based seismic design of buildings was presented by Xue *et al*. (2008). It is worthwhile to mention that these drafts of building codes are important since they can motivate the corresponding specifications for bridges.

Summarizing, the current status of DBD may be described as follows:

- Well established provisions for conventional bridges and buildings.
- Extensive research on buildings with supplemental dampers.
- Some research on isolated bridges.
- Lack of methodologies for isolated bridges with seismic dampers.

Seismic Performance Criteria

Seismic performance criteria	**Safety**	**Serviceability**	**Reparability**	
			Short-term	Long-term
Seismic performance 1 -Functional/Operational- (Predominantly elastic behavior)	Secure safety against collapse	Secure pre-earthquake function	Need no repair for restoration of function	Need minor repair
Seismic performance 2 –Operational/Life Safety (Inelastic behavior)	Secure safety against collapse	Secure rapid restoration of function	Emergency repair enables restoration of function	Possible to perform permanent repair easily
Seismic performance 3 –Near Collapse-	Secure safety against collapse	–	–	–

Table 1.2 Seismic Performance Criteria in the Japanese Specifications

<table>
<tr><th colspan="2" rowspan="2">Types of design ground motions</th><th colspan="2">Importance of bridges</th><th colspan="2">Design Methods</th></tr>
<tr><td>Type-A
(Standard bridges)</td><td>Type-B
(Important bridges)</td><td>Equivalent static lateral force methods</td><td>Dynamic Analysis</td></tr>
<tr><td colspan="2">Ground motions with high probability to occur</td><td colspan="2">Prevent damage</td><td>Seismic Coefficient Method</td><td rowspan="3">Step by Step Analysis
or
Response Spectrum Analysis</td></tr>
<tr><td rowspan="2">Ground motions with low probability to occur</td><td>Type-I
(Plate boundary earthquakes)</td><td rowspan="2">Prevent critical damage</td><td rowspan="2">Limited damage</td><td rowspan="2">Ductility Design Method</td></tr>
<tr><td>Type-II
(Inland earthquakes)</td></tr>
</table>

Table 1.3 Design method for bridges in the Japanese Specifications

1.5 MOTIVATION AND RESEARCH OBJECTIVES

In bridges, in order to ensure seismic performance required, seismic isolation is often used to reduce the forces induced into the structural elements by the earthquake. However, some types of seismic isolation often induce large structural displacements. In structural design, controlling of damage and limiting displacements are crucial to maintain the adequate performance of the bridge. Then, for isolated bridges, various types of dampers are occasionally used to limit the displacements under allowable values. Among others, the most recurrent devices are those working by the compression of a viscous fluid, namely viscous dampers. These dampers generally have small values of stiffness so that the structural period of the bridge remains approximately the same after their inclusion into the bridge.

On the other hand, design methodologies that cover the limitations of the current force-based design have been developed. Among them, the most promising seems to be the displacement-based design (DBD) approach. In the literature, there is a large amount of DBD methodologies for buildings, bridges, piles, and retaining walls. Although some of them were modified to consider seismic isolated systems or systems with supplemental dampers, in spite of its importance, a methodology that considers the combined effects of seismic isolation and viscous dampers in bridges with elastic or inelastic piers has not yet been issued. Moreover, although a large number of real bridges are skewed, most of the displacement-based design methodologies are applicable to straight and regular bridges.

Another important aspect to consider is the computational resources used to design isolated bridges with viscous dampers with the current force-based design. Time-consuming iterative analyses are required to accurately calculate the coefficients of viscous dampers. On the contrary, the displacement-based design seems to be a more efficient tool to fasten these calculations with minimum computational resources.

Therefore, in order to contribute to a better understanding of the displacement-based design of bridges with viscous dampers, and to generate tools to contribute to minimize the computational resources in the calculation of the dampers coefficients, the general objectives of this study are: a) to develop equivalent linearization equations to estimate the maximum inelastic displacements of a single-degree-of-freedom system, b) to develop a displacement-based design methodology for straight isolated bridges with viscous dampers, in such a way that the coefficients of the dampers can straightforwardly be calculated to limit the displacement under predefined values, and c) to develop a displacement-based methodology for design of isolated skewed piers with viscous dampers considering the earthquake bidirectional effects.

1.6 ORGANIZATION OF THE DISSERTATION

Chapter 1. The present chapter presents a general introduction to the design of structures subjected to earthquakes. The methods based on forces and displacements are introduced within the framework of the performance-based seismic engineering. A general review of the current force-based method is presented and its limitations are described. An extensive literature review on displacement-based design methodologies is presented. Additionally, the current seismic design specifications for bridges in which the displacement-based methodologies have been adopted are listed. The research objectives and motivation of the research are presented. This chapter concludes with a description of the organization of the dissertation.

Chapter 2. This chapter introduces the fundamental concepts that are used through the dissertation. The fundamental aspects of the base isolation and viscous dampers used in this research, such as modeling, equivalent damping and hysteretic behavior, are described based on a simplified 2-degree-of-freedom (2DOF) model for isolated piers with viscous dampers. The relevant aspects of the Seismic Design Specifications adopted for this research, such as types of earthquakes, classification of soils, and elastic displacement spectra are presented.

Chapter 3. In this chapter, new equations for the optimal pair of equivalent properties are derived using statistical procedures on equivalent linearization and defined in terms of the ductility ratio and initial period of vibration. The modified Clough hysteretic model and 30 artificial accelerograms, compatible with the acceleration spectra for firm and soft soils and defined by the Japanese Design Specifications for Highway Bridges, are used in the analysis. The results obtained with the proposed equations are verified and their limitations discussed. These equations are particularly useful to account for the inelastic behavior of piers and bridges modeled as a single-degree-of-freedom system.

Chapter 4. This chapter introduces a new displacement-based design procedure for RC bridges on hysteretic isolated devices with viscous dampers. For new bridges, the limit state considered in this study is such that the piers and the deck remain elastic while the isolated devices are allowed to behave inelastically. For existing bridges, the displacement of the pier is modified by a ductility factor of 1.5 to achieve the desired limit state. In the proposed DBD methodology, the dampers can either be linear or nonlinear. The proposed design method has two advantages: the direct calculation of the design forces on the piers, and the fast calculation of the damping coefficient of the viscous dampers to limit the maximum displacement of the structural elements under the target value. The application of the proposed methodology is presented and their results are validated by nonlinear time history analysis.

Chapter 5. In this chapter, an extensive literature review on methods to account for the bidirectional structural response is presented and the problems associated with bidirectional components of earthquakes on skewed piers are described. To solve this type of design, a new methodology is presented for the isolated skewed piers with viscous dampers. Finally, the application of the proposed methodology is presented and the results verified and discussed.

Chapter 6. In this chapter the conclusions and final comments of the research are presented.

The overview of the dissertation is shown in Figure 1.8

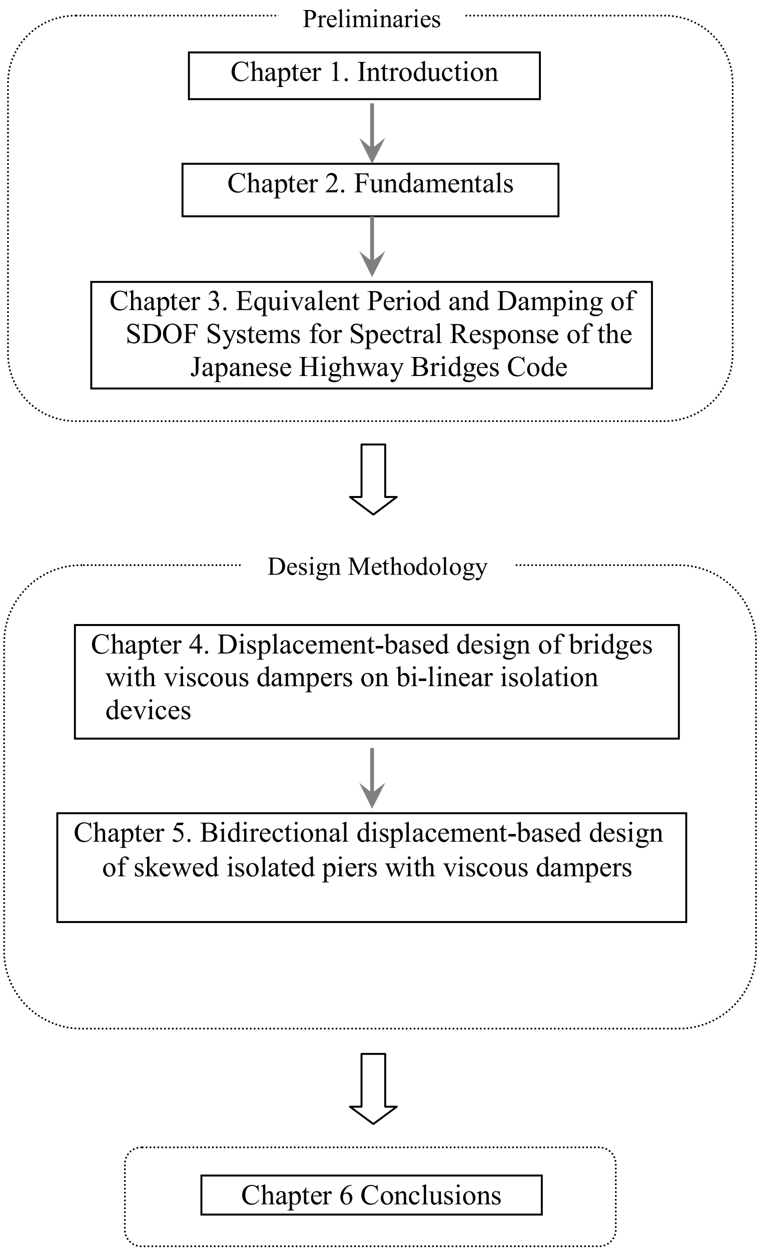

Figure 1.8 Organization of the dissertation

REFERENCES

American Association of State Highway and Transportation Officials (AASHTO), (2002), AASHTO/AWS D1.5M/D1.5 Bridge Welding Code.

AASHTO, (2004), LRFD Bridge design specifications, fourth edition, American Association of State Highway and Transportation Officials, Washington, D.C.

American Technology Council (ATC), (1996), " ATC-32, Improved Seismic Design Criteria for California Bridges: Provisional Recommendations", Seismic Safety Commission, Report No. SSC 96-01, Redwood City, California.

ATC, (1998), NCHRP 12-49, *Comprehensive Specification for Seismic Design of Bridges*, ATC/MCEER.

ATC, (2003), NCHRP 12-49 *Recommended LRFD Guidelines for the Seismic Design of Highway Bridges*. ATC/MCEER.

Bertero R. D. and Bertero V. V. (2002), "Performance-based seismic engineering: the need for a reliable conceptual comprehensive approach", *Earthquake Engineering & Structural Dynamics*, **31**(3): 627–652.

Building Seismic Safety Council (BSSC), (1997), "NEHRP Guidelines for the Seismic Rehabilitation of Buildings," Report FEMA 273/274, Federal Emergency management Agency, Washington, D.C.

BSSC, (2000), "Prestandard and Commentary for the Seismic Rehabilitation of Buildings", Federal Emergency Management Agency, Washington, D.C.

Caltrans, (2006), Seismic Design Criteria, California Department of Transportation, Sacramento, CA.

Cardone D., Dolce M. and Palermo G. (2009), "Direct displacement-based design of seismically isolated bridges", *Bull. Earthquake Eng*. 7:391–410.

Chandler A.M. and Lam N.T.K. (2001), "Performance-based design in earthquake engineering: a multidisciplinary review", *Engineering Structures*, 23: 1525–1543.

Chopra A. K. and Goel R. K. (2001), "Direct Displacement-Based Design: Use of Inelastic vs. Elastic Design Spectra", *Earthquake Spectra*, 17(1): 47-64.

Eurocode 8, (1998), “Design provisions for earthquake resistance of structures”, ENV 1998, 1-1/3, *CEN*, Brussels.

Fu C.C. and Alayed H., (2003), "Seismic Analysis of Bridges Using Displacement-Based Approach", *Transportation Research Board*, (03-3175), January 12-16, Washington, D.C.

Jacobsen L. S. (1930), “Steady forced vibrations as influenced by damping”, *ASME*, *Transactions*, 52(1): 169-181.

Japan Road Association (JRA), (2002), Seismic Design Specifications for Highway Bridges (in Japanese)

Jara M. and Casas J. R. (2006), “A direct displacement-based method for the seismic design of bridges on bi-linear isolation devices”, *Engineering Structures*, 28: 869–879.

Kim J., Choi H. and Min K. (2006), “Displacement-Based Design of Supplemental Dampers for Seismic Retrofit of a Framed Structure”, *Journal of Structural Engineering*, 132(6): 873-883.

Kim J. and Choi H. (2003), “Performance-based design of added viscous dampers using capacity spectrum method”, *Journal of Earthquake Engineering*, (7)1: 1-24.

Lin Y. Y., Chang K. C. and Chen C. Y. (2008), “Direct displacement-based design for seismic retrofit of existing buildings using nonlinear viscous dampers”, *Bull. Earthquake Eng.* 6(3): 535–552.

Lin Y.Y. and Chen C.Y. (2008), “Shaking table study on displacement-based design for seismic retrofit of existing buildings using nonlinear viscous dampers”, *Proceedings of the 14th World Conference on Earthquake Engineering*, Beijing, China, October.

Lin Y.Y., Tsai M.H., Hwang J.S., Chang K.C. (2003), “Direct displacement-based design for building with passive energy dissipation systems”, *Engineering Structures*, 25: 25–37.

Medhekar M. S. and Kennedy D. J. L. (2000), “Displacement-based seismic design of buildings—theory”, *Engineering Structures*, 22(3): 201–209

Moehle J. P. (1992), “Displacement-based design of R/C structures subjected to earthquakes”, *Earthquake Spectra*, 8(3): 403-427.

Moehle, J.P., Eberhard, M.O. (2000), "Earthquake Damage to Bridges", *Bridge Engineering Handbook,* Ed. Wai-Fah Chen and Lian Duan Boca Raton: CRC Press.

Oguzmert, M. (2006), "Displacement-based seismic design of structures using equivalent linear system parameters", *Civil and Environmental Engineering - Dissertations and Theses.* Paper 5. http://surface.syr.edu/cie_etd/5

Panagiotakos T. B. and Fardis M.N. (2001), “A Displacement-based Seismic Design Procedure of RC Buildings and Comparison with EC8”, *Journal of Earthquake Engineering and Structural Dynamics*, 30(10): 1439-1462.

Pang W. and Rosowsky D. (2007), “Direct displacement procedure for performance-based seismic design of multistory woodframe structures”, NESSWOOW Report NW-02

Pietra D., Calvi G. M. and Pinho R. (2008), *Displacement-based seismic design of isolated bridges*, Research Report No. ROSE 2008/01. IUSS Press.

Priestley, M.J.N. (1993) “Myths and Fallacies in Earthquake Engineering - Conflicts between Design and Reality”, *Bull. NZNSEE*, 26(3): 329-341.

Priestley, M.J.N. and Kowalsky, M.J. (2000), “Direct Displacement-Based Design of Concrete Buildings”, Bulletin of the New Zealand National Society for Earthquake Engineering, Vol. 33, No. 4, pp. 421-444.

Priestley M. J. N., Calvi G. M. and Kowalsky M. J. (2007), *Displacement-based seismic design of structures*, IUSS Press, Pavia, Italy.

SEAOC (1995), “Performance-based seismic engineering”, Vision 2000 Committee, Structural Engineers Association of California, Sacramento, CA.

SEAOC (1999) “Guidelines for performance-based seismic engineering”, SEAOC Blue Book - draft of Appendix I.

Shibata A. and Sozen M.A. (1976), “Substitute-structure method for seismic design in R/C”, *Journal of Structural Engineering,* ASCE, 102(ST1): 1-18.

Shinde J. K., Symans M. D., Pang W. C. and Rosowsky D. V. (2008), “Displacement-based design of woodframed structures with linear viscous fluid dampers”, *Proceedings of the 14th World Conference on Earthquake Engineering*, Beijing, China, October.

Terán-Gilmore A. y Virto Cambray N. (2009), “Preliminary design of low-rise buildings stiffened with buckling restrained braces by a displacement-based approach”, *Earthquake Spectra*, 25(1), 185-211.

United States Geological Survey’s (USGS), (2011), *Historic World Earthquakes*, http://earthquake.usgs.gov/earthquakes/world/historical.php

Unjoh S., Nakatani S., Tamura K., Fukui J. and Hoshikuma J. (2002), "Seismic design specifications for highway bridges", *Wind and Seismic Effects, Proceedings of the 34th Joint Panel Meeting, Gaithersburg*, Maryland, 13-15 May, National Institute of Standards and Technology.

Wada A, Huang Y. and Iwata M. (2000), "Passive damping technology for buildings in Japan", *Prog. Struct. Engng Mater*, 2: 335-350.

Wallace J. W. (1995a), "Seismic design of RC structural walls. Part I: new code format", *Journal of Structural Engineering*, ASCE, 121(1): 75–87.

Wallace J. W. (1995b), "Seismic design of RC structural walls. Part II: applications", *Journal of Structural Engineering*, ASCE, 121(1): 88–100.

Xue Q, Wu C., Chen C. and Chen K. (2008), "The draft code for performance-based seismic design of buildings in Taiwan", *Engineering Structures*, (30)6: 1535-1547.

CHAPTER 2

FUNDAMENTALS

2.1 GENERAL REMARKS

In Japan, the seismic isolation bridges using elastomeric bearings as lead rubber bearings and high damping rubber bearings have been specified from 1996 in the design provisions from the Japan Road Association, and have been particularly constructed after the Hyogoken-nanbu Earthquake occurred on January 17 of 1995. Figure 2.1 schematically illustrates the concept of seismic isolation. Seismic isolation increases the original vibration period of the structure (green point) reducing the seismic forces into the elements (red point). Seismic isolation with elastomeric bearings, however, has limitations on applicable sites, structural configurations, soil conditions (including liquefaction effects), natural periods, and others. Moreover, devices such as lead rubber bearings (LRB) are used assuming relatively large displacements sometimes costly to accommodate. In contrast, seismic dampers are primarily used for retrofit of existing bridges due their capability of reducing the resulting displacements. In order to enhance the seismic demand in course of retrofit; combination of replacement of the bearings with elastomeric type, and the application of the seismic damper is a typical option.

In this chapter, in order to introduce the concepts that are used hereafter, the fundamentals of seismic isolation, viscous dampers and the design spectra given by the Japanese Specifications are presented and placed into the context of this research.

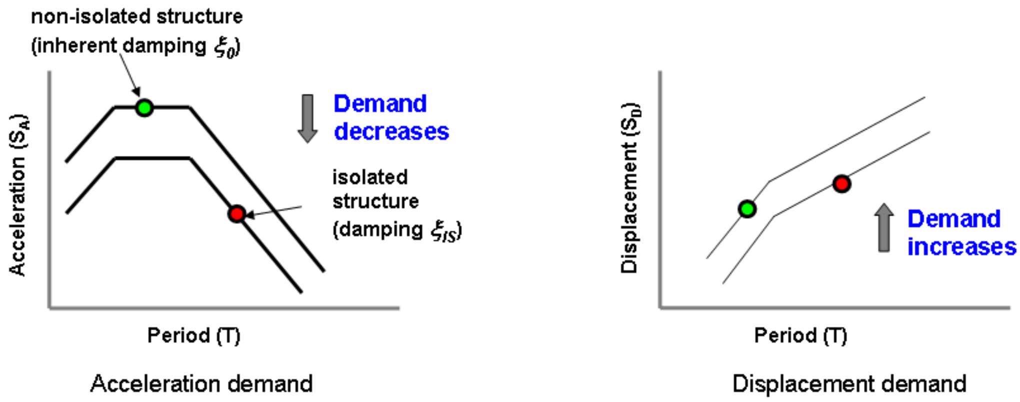

Figure 2.1 Acceleration and displacement response of an isolated bridge

2.2 SEISMIC ISOLATION

2.2.1 MODELING

The objective of seismic isolation systems is to prevent the structure from being subjected to the earthquake energy by decoupling the structure from the damaging components of the earthquake. The other purpose of the isolation system is to provide additional means of energy dissipation, thereby reducing the induced displacement of the superstructure. A variety of isolation devices including elastomeric bearings (with and without lead core), frictional/sliding bearings, roller bearings, etc. have been developed and used practically for aseismic design of structures in all over the world. The inclusion of isolators has several advantages for bridges. A description of these advantages and a detailed review of works on base isolation systems had been widely reported (Kelly 1986, Skinner *et al*. 1993, Kunde and Jangid 2003, Vasant *et al*. 2006).

In isolated bridges, the superstructure is usually supported on isolators whose dynamic characteristics are chosen to uncouple the ground motion, and in some cases they also provide substantial damping. The displacement and yielding are concentrated at the level of the isolation devices, and the superstructure behaves almost as a rigid body. Therefore, the established capacity design principle for isolated bridges is that hysteretic energy dissipation should be restricted to the isolation system.

In bridges with viscous dampers, the most commonly used isolation systems are lead rubber bearings (LRB) (Figure 2.2). The cyclic behavior of a LRB is considered to be well represented by a bilinear hysteretic model characterized by the elastic stiffness, yielding strength, the ratio of the elastic stiffness to the inelastic stiffness, and the ductility ratio. The hysteretic model and the corresponding modeling parameters are shown in Figure 2.3.

Seismic isolation has limitations on applicable sites and structural configurations (depending on soil conditions including liquefaction effect), natural periods of the structure and soil, etc. Moreover, due its inherent characteristics, the lead rubber bearings absorb relatively large displacement increasing the period of vibration of the structure reducing the seismic forces in the elements and increasing the resulting displacements. Then, the designs of deck gap, expansion joints and the isolators themselves become relevant points in the isolation design. The addition of seismic dampers to a set of elastomeric base isolation pads greatly enhances their performance. The first and most significant effect is to cut down on dynamic displacement, possibly by as much as 50%. There is an associated reduction in base shear by the same amount, which means lower forces and accelerations in the isolated structure. A secondary advantage from the addition of dampers is that the subsequent reduction in displacement and base shear reduces the tendency for uplift and even if it occurs, the damping force on viscous dampers is not affected. A third and most significant advantage of using damping elements in conjunction with LRB is that the pads can be made from natural rubber or other low damping material.

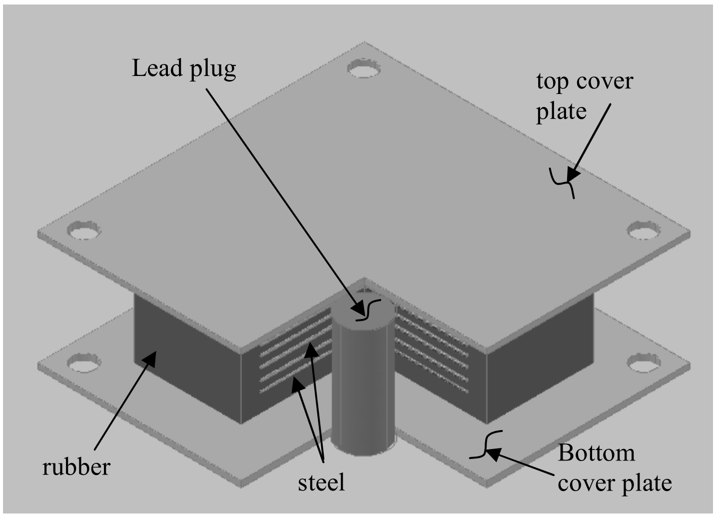

Figure 2.2 Lead Rubber bearings

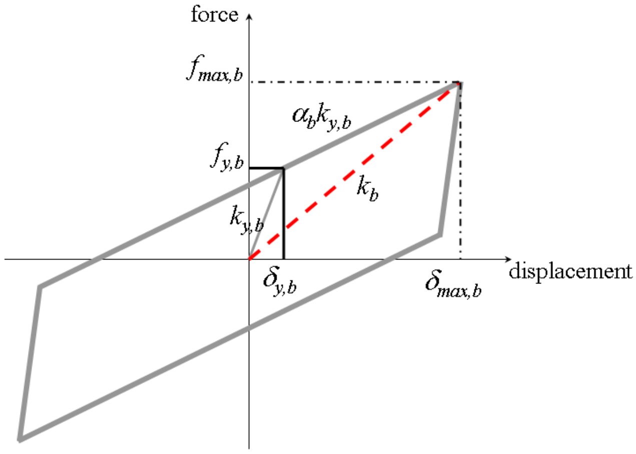

Figure 2.3 Bilinear modeling of rubber and lead rubber bearings

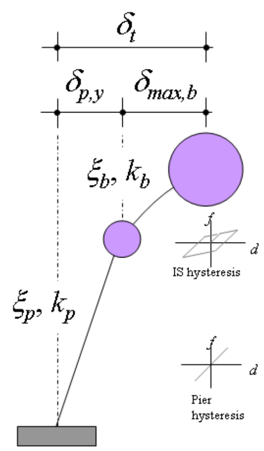

Figure 2.4 Single substructure for base-isolated bridge pier

2.2.2 EQUIVALENT STIFFNESS AND DAMPING

The equivalent stiffness (k_b) is defined as the diagonal slope of the simplified maximum response shown in Figure 2.3 as

$$k_b = \frac{f_{\max,b}}{\delta_{\max,b}} \tag{2.1}$$

Traditionally, the equivalent damping has been calculated by relating the maximum bilinear loop area (W) to the loop area of a velocity-damped isolator with stiffness k_b at the displacement $\delta_{max,b}$ as

$$\xi_b = \frac{W}{2\pi k_b (\delta_{\max,b})^2} \tag{2.2}$$

However, Equation 2.2 does not account for all the hysteretic cycles experienced by the isolator in a real case. Therefore, in this work the following more accurate expression to calculate the equivalent damping of bilinear isolators will be used (Jara and Jara, 2006):

$$\xi_b = 0.05 + 0.05\ln(\mu_b) \tag{2.3}$$

The first term of the is the inherent damping of the structure and μ_b is the ductility ratio of the bearing defined as the following ratio:

$$\mu_b = \frac{\delta_{\max,b}}{\delta_{y,b}} \tag{2.4}$$

The proposed design methodology considers this damping in such a way that the inherent damping of the structure is not duplicated. Figure 2.4 shows the typical substructure modeling for base-isolated piers.

2.3 VISCOUS DAMPERS

2.3.1 MODELING

Viscous dampers were originally developed for applications in the military and heavy industry. However, due their inherent characteristics (Soon and Constantinou, 1994), they have been extensively used in the seismic protection of structures (Whittaker and Constantinou, 2000). Viscous dampers reduce structural displacements and dissipate seismic energy enhancing the seismic performance.

Figure 2.5 shows a typical viscous damper. It consists of a stainless steel piston with an orifice head, the chambers are filled with a viscous fluid such as silicon oil. The damping force is given by the difference of the pressure between each side of the piston head. The damping constant of the damper is determined by adjusting the configuration of the piston head. For a pure viscous behavior, the damper force and the velocity should remain in phase. It has been observed, however, that some restoring force may occur at high frequency motions.

Several analytical models for representing viscous dampers have been proposed (H. B. Yun, *et al.* 2006). In this study, the velocity exponent model (Maxwell model with null damper stiffness) is used since it captures the frequency dependence of the damping observed in the fluid orifice dampers, especially at higher frequencies of deformation (Singh *et al*. 2003).

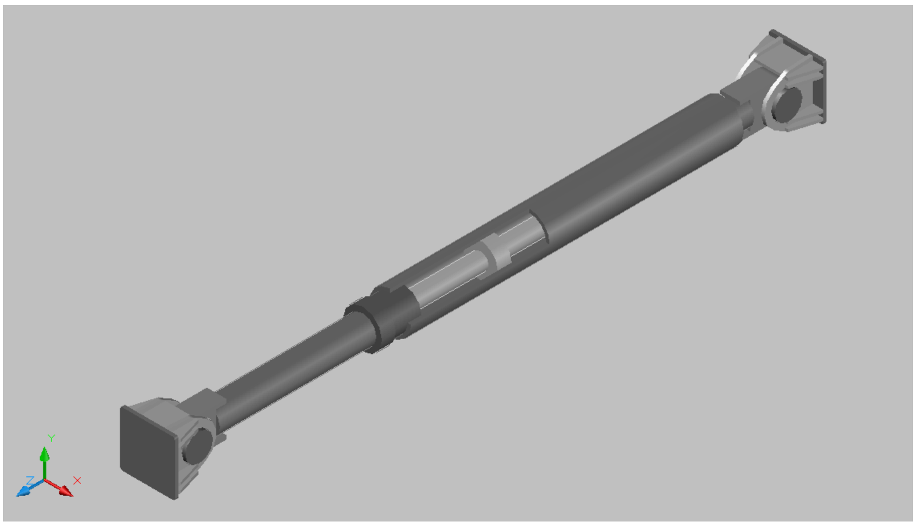

Figure 2.5 Typical viscous damper

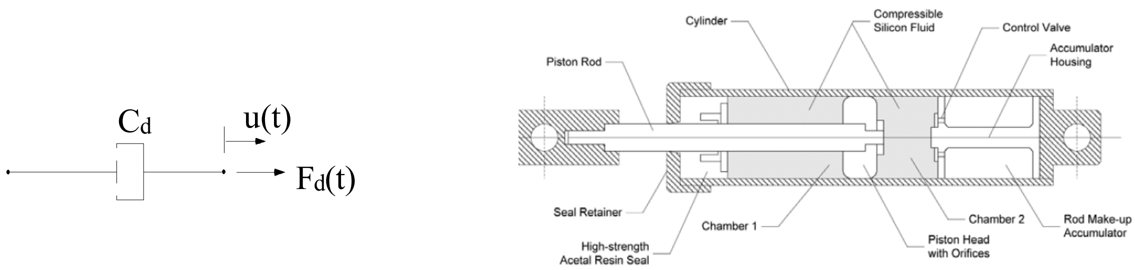

Figure 2.6 Modeling and components of a typical viscous damper (Soong and Dargus, 1997)

In the velocity exponent model (Figure 2.6) the force developed by a viscous damper is defined based on the velocity of the system according to the following relationship:

$$F_d = C_d |\dot{u}|^{\alpha} \operatorname{sgn}(\dot{u}) \tag{2.5}$$

where C_d is the damping coefficient, $\dot{u}$ is the relative velocity between the ends of the damper, α represents the damping exponent and sgn is the signum function, which satisfy sgn($\dot{u}$) = 1 if $\dot{u} \geq 0$ and sgn($\dot{u}$) = -1 if $\dot{u} < 0$.

The constants C_d and α are specific properties for each damper. It can be observed that when α=1, the relationship given by Equation 2.5 is linear, otherwise, the relationship is nonlinear. The relationships between the damping force with the velocity and displacement are shown schematically in Figure 2.7. For low velocities, the nonlinear dampers (α<1) develop more damping force than the linear viscous and nonlinear (α>1) dampers. When the relative velocities become larger, linear dampers (or nonlinear devices with α>1) provide more damping force than the nonlinear dampers (α<1).

Figure 2.8 illustrates the force-velocity relationship of a typical viscous damper subjected to one cycle of sinusoidal excitation. Figures 2.9 shows the basic relationship and the hysteresis loop of pure viscous dampers for several values of α.

Due to the absence of storage stiffness, the natural period of the structure after the incorporation of dampers is assumed to remain unchanged.

The typical modeling of a pier column with base isolation and viscous dampers is shown in Figure 2.10.

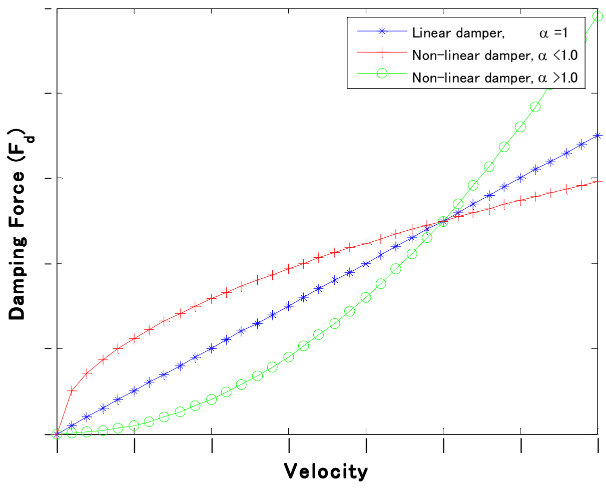

Figure 2.7 Force-velocity relationship of viscous damper

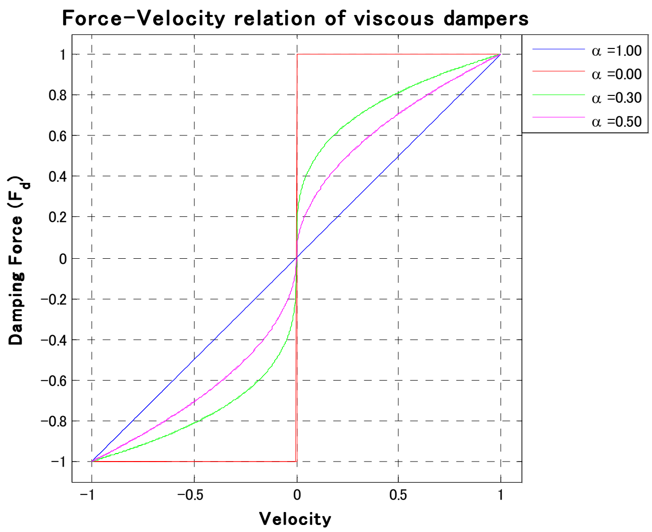

Figure 2.8 Force-velocity relationship of viscous damper (Harmonic excitation)

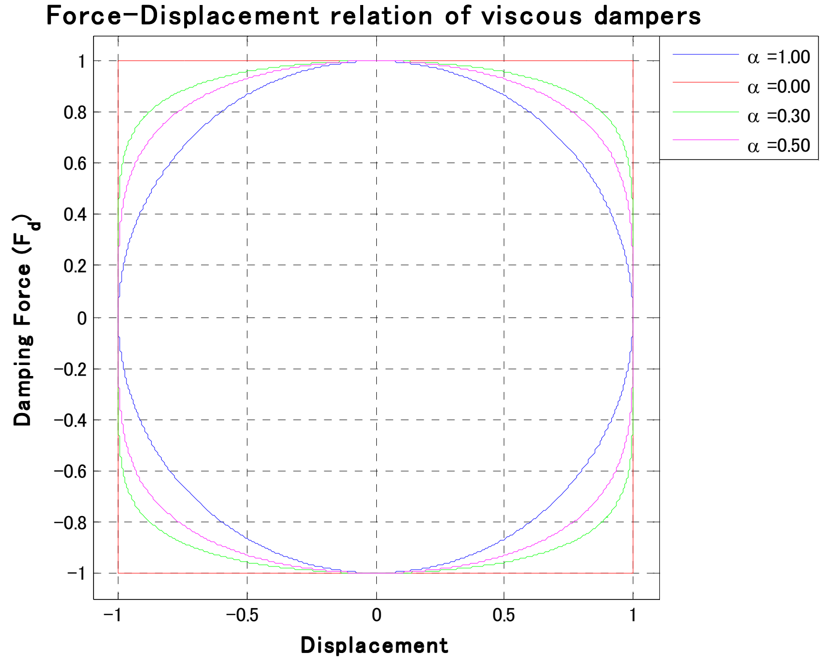

Figure 2.9 Force-displacement relationship of viscous damper

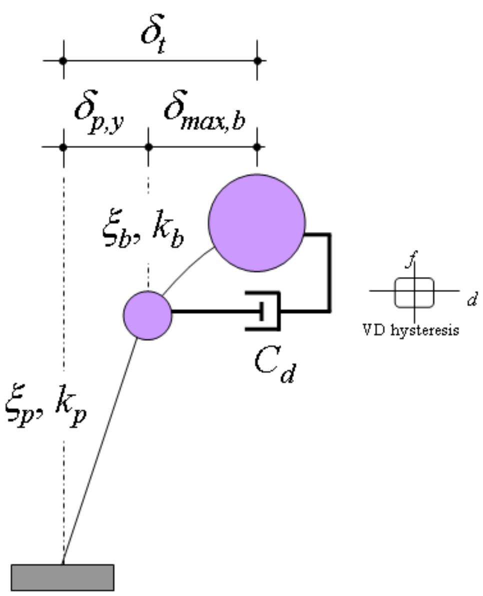

Figure 2.10 Single substructure for base-isolated bridge pier with viscous damper

2.3.2 DAMPING PROVIDED BY VISCOUS DAMPERS

2.3.2.1 LINEAR DAMPERS

For buildings with viscous dampers, the total damping of the system is given by the sum of the inherent structural damping, ξ_0, and the damping provided by the added dampers, ξ_d, (FEMA 356, Ramirez *et al*. 2000):

$$\xi_{eq} = \xi_0 + \xi_d \tag{2.6}$$

Equation 2.6, can also be used for bridges due to the separation of the damping terms: the inherent damping that considers all of the damping sources of the structure regardless of their nature and the damping provided by the supplemental damping.

For common structures, ξ_0 is usually assumed to be 5% and ξ_d is calculated with equivalent linearization concepts, based on the equal energy dissipation (Seleemah and Constantinou, 1997) and the equal average consumption (Pekcan *et al*. 1999).

For SDOF systems subjected to one cycle of harmonic vibration, the damping ratio (ξ_d) provided by linear viscous dampers is (Chopra 2003, ATC 1993)

$$\xi_d = \frac{W_D}{4\pi W_S} \tag{2.7}$$

where W_D is the energy dissipated by the damper during one cycle of harmonic excitation and W_S is the strain energy.

For SDOF systems, the quantities W_D and W_S can be straightforwardly calculated. However, for MDOF systems a distinction should be made depending on the type of structure. For buildings, due to the large number of degrees of freedom, W_D and W_S are calculated with the following expressions (Jenn-Shin, 2004)

$$W_D = \sum_j W_{Dj} = \sum_j \pi C_{dj} \left(\frac{2\pi}{T_0}\right)(u_t \phi_{mr,j} \cos\theta_j)^2 \tag{2.8}$$

$$W_S = \frac{2\pi^2}{T^2} \sum_i m_i (u_t \phi_{mi})^2 \tag{2.9}$$

where W_{Dj} is the energy dissipated by the j linear damper in one complete loading cycle, C_{dj} represents the damping coefficient of the linear damper j, T_0 is the fundamental period of vibration of the structure, u_t denotes the maximum displacement, $\phi_{mr,j}$ is the relative modal displacement of the fundamental mode between the ends of the damper j along its longitudinal axis, θ_j is the angle of the damper j respect to the horizontal, m_i represents the mass of the DOF i, and ϕ_{mi} is the modal displacement of the fundamental mode of the DOF i. The damping ratio provided by the linear viscous dampers can be obtained by substitution of Equations 2.8 and 2.9 into Equation 2.7, and the resulting expression is given by FEMA-356 as

$$\xi_d = \frac{T_0 \sum_j C_{d\,j} \phi_{mr,j}^2 \cos^2 \theta_j}{4\pi \sum_i m_i \phi_{mi}^2} \tag{2.10}$$

For bridges with base isolation, the number of degrees of freedom decrease in comparison with the case of buildings. Usually, the pier-IS-VD-deck system can be modeled as a 2DOF system characterized by the tributary mass of the pier m_p, the tributary mass of the girder-deck system m_g, the equivalent damping and stiffness of the pier denoted by ξ_p and k_p, respectively, and the equivalent damping and stiffness of the isolators denoted by ξ_b and k_b, respectively, as shown in Figure 2.11.

For this type of simplified system, the damping provided by the IS-VD system at a pier location can be derived with a similar procedure used in the derivation of Equation 2.10. In the 2DOF system, the damping provided by the IS-VD system $\xi_{(d+b)}$ can be calculated with the following equation (Jenn-Shin and Yi-Shane, 2005)

$$\xi_{(d+b)} = \frac{\xi_{eq}\sqrt{\alpha_1[(1-\gamma)+(1-\alpha_1)\gamma]} - \xi_p\sqrt{[(1-\gamma)/R_p](1-\alpha_1)^2}}{\alpha_1{}^2(1-\gamma)} \tag{2.11}$$

where

$$\alpha_1 = \omega_1{}^2 / \omega_b{}^2 \tag{2.12}$$

$$\omega_b^2 = k_b / m_b \tag{2.13}$$

$$\gamma = m_p / (m_p + m_b) \tag{2.14}$$

$$R_p = k_b / k_p \tag{2.15}$$

and

$$\omega_{1,2}{}^{2} = \frac{(1-\gamma)}{R_p} \frac{[1+R_p/(1-\gamma)] \pm \{[1+R_p/(1-\gamma)]^2 - 4\gamma R_p/(1-\gamma)\}^{1/2}}{2\gamma} \omega_b{}^{2} \tag{2.16}$$

The damping coefficient C_d of the linear viscous damper corresponding to a desired equivalent damping ratio ξ_{eq} is given by

$$C_d = 2m_b\omega_b \left(\frac{\xi_e\sqrt{\alpha_1}[(1-\gamma)+(1-\alpha_1)^2\gamma] - \xi_p\sqrt{((1-\gamma)/R_p)}(1-\alpha_1)^2}{\alpha_1{}^2(1-\gamma)} - \xi_b \right) \tag{2.17}$$

The damping ratio of the dampers ξ_d is then given by

$$\xi_d = \frac{C_d}{2m_b\omega_b} \tag{2.18}$$

2.3.2.2 NONLINEAR DAMPERS

Similar to the linear case, the nonlinear viscous dampers are assumed to follow the force relationship given by Equation 2.5. To simplify the nonlinear solution of the system, the nonlinear dampers are commonly modeled as their linear equivalents with the same damping. For this purpose two approaches are generally used. The first is based on the equal energy dissipation of the corresponding linear and nonlinear cases (Seleemah and Constantinou 1997, Ramirez *et al*. 2000). The second is based on the equal average of the dissipated energy for linear and non-linear dampers (Peckan *et al*. 1999, Lin *et al*. 2008). The former approach gives smaller, and thus conservative, values of equivalent damping compared with those obtained with the latter. In any case, the second method can be used as an alternative to estimate the equivalent linear damping (Lin *et al*. 2008).

Following the equal energy dissipation approach, Jenn-Shin and Yi-Shane (2005) derived the damping coefficient of the equivalent linear viscous damper for the pier-IS-VD system (Figure 2.11) as

$$\xi_d = \frac{C_d\omega_b{}^{\alpha}(x_b - x_p)^{1+\alpha}\lambda}{2\pi m_b} \tag{2.19}$$

where

$$\lambda = 2^{2+\alpha}\left(\frac{\Gamma^2\left(1+\dfrac{\alpha}{2}\right)}{\Gamma(2+\alpha)}\right) \tag{2.20}$$

where Γ is the gamma function.

The damping constant C_{dN} for the dampers is calculated with the following equation

$$C_{dN} = \frac{2\pi m_b (1+R_p)^{\alpha-1}}{\omega_b^{\alpha-2} D^{\alpha-1}\lambda}\left(\frac{\xi_e\sqrt{\alpha_1}[(1-\gamma)+(1-\alpha_1)^2\gamma]-\xi_p\sqrt{((1-\gamma)/R_p)}(1-\alpha_1)^2}{\alpha_1^{\;2}(1-\gamma)}-\xi_b\right) \tag{2.21}$$

where the factor D is defined in terms of the isolator displacements x_b and the pier displacement x_p as

$$D = (x_b - x_p) \tag{2.22}$$

It is important to mention that the Equations 2.12 and 2.21 were developed for elastic systems. To ensure the consistency, the effective stiffness of the isolators (Equation 2.1) should be used.

2.4 DISPLACEMENT SPECTRA FROM THE JAPANESE DESIGN SPECIFICATIONS

2.4.1 ACCELERATION SPECTRA

In this work, the acceleration spectra given by the design Specifications of the Japan Road Association (2002) are considered for the derivation of the displacement spectra.

After the Nihonkai-chubu earthquake occurred on January 17, 1995, the Japanese Specifications were modified and the design ground motions were classified into two categories:

a) Level 1 Earthquakes. This category defines the moderate earthquakes with a high probability to occur (not considered in this study).

b) Level 2 Earthquakes. This category defines the earthquakes with less probability to occur but strong enough to cause critical damage. Under this category, two types of ground motion are defined: Type I, denoted by S_{I0}, the interplate-type earthquakes with a magnitude around 8, and Type II, denoted by S_{II0}, near fault earthquakes of magnitude around 7.

The soils are classified into three types based on the depth of the stratus and the velocity of the wave propagation given defined by the following coefficient:

$$T_G = 4\sum_{i=1}^{n} \frac{H_i}{V_{si}} \tag{2.23}$$

where H is the height and V_S is the horizontal elastic velocity of the wave of the i^{th} soil layer. Firm soils correspond to type I, transition soils correspond to type II, and soft soils correspond to type III. Table 2.1 shows the classification of soils as a function of the coefficient T_g.

Classification of soils	
Soil type	Characteristics
I	Firm soil (TG<0.2)
II	Transition soil (0.2<=TG<0.6)
III	Soft soil (0.6<=TG)

Table 2.1 Classification of soils

Transition soils are not included in this study, therefore the results are limited to soil types I and III. The design acceleration spectra $S_A(T_0)$ for level 2 earthquakes (ξ=5%) are shown in Figures 2.11 and 2.12.

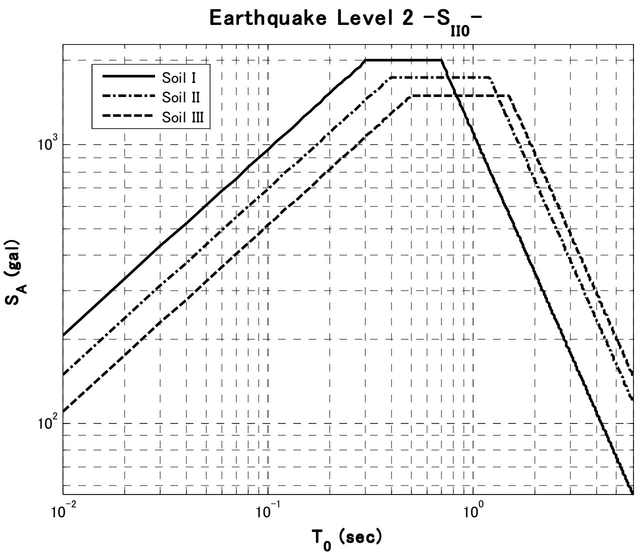

Figure 2.11 Acceleration spectra –Earthquake S_{IO}–

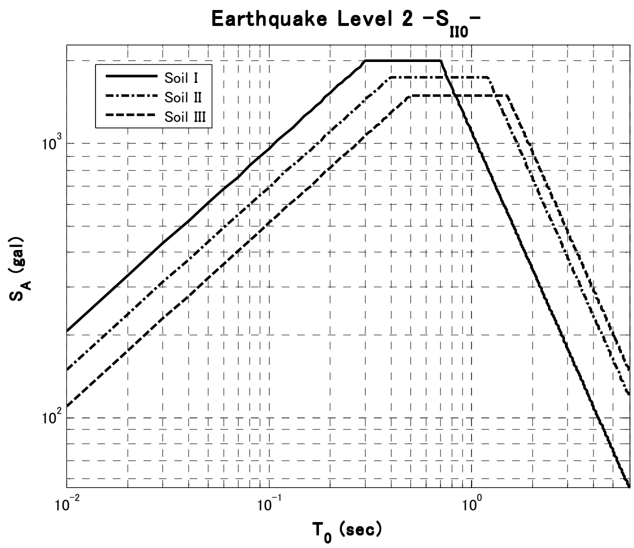

Figure 2.12 Acceleration spectra –Earthquake S_{IIO}–

2.4.2 ARTIFICIAL EARTHQUAKES COMPATIBLE WITH THE ACCELEROGRAMS

Level 1 earthquakes have been extensively recorded with high quality throughout the years. For level 2 earthquakes, however, the number of recorded motions is quite limited. In fact, Hamada (2000) documented only five earthquakes with magnitude equal or greater than 8 from 1889 to 1995, and 14 with magnitude greater than or equal to 7 in the same period. From these, only 9 are considered type 2 and most of them occurred in the first half of the past century. Therefore, due to the lack of available records for level 2 earthquakes, a family of 30 artificial accelerograms was generated for each type of earthquake for firm and soft soils.

The earthquakes were generated to be compatible with both the acceleration $S_A(T_0)$ and the displacement spectra $S_D(T_0)$.

In the Japanese specifications, the displacement spectrum is not explicitly included. However, for elastic systems and for small or intermediate periods, it can be calculated from the acceleration spectrum by the following relationship:

$$S_D(T_0) = S_A(T_0)\left(\frac{T_0}{2\pi}\right)^2 \tag{2.24}$$

For long periods, the displacements obtained in this manner increase indefinitely giving unrealistic predictions. Then, some adjustments to calculate consistent acceleration-displacement spectra should be done (Boomer *et al*. 2000). However, in this work for the generation of artificial earthquakes, the displacement spectra is assumed to be constant beyond the corner period regardless the type of soil and type of earthquake. The corner period is assumed to be (Priestley *et al*. 2007):

$$T_c = 1 + 2.5(M_w - 5.7) \text{ (sec)} \tag{2.25}$$

where M_w is the earthquake magnitude.

Figure 2.13 shows the procedure to generate the artificial motions. The detailed explanation and notation used in Figure 2.13 can be found in Clough and Penzien (2003). Their duration was obtained from the ground motion samples in the seismic code, and the parameters are shown in Table 2.2.

Type of Earthquake	**Type of Soil**	**Magnitude**	**T_C [sec]**	**Duration [sec]**	**Earthquakes generated**
S_{I0} (S_{II0})	I	8.0 (7.0)	6.75 (4.25)	30 (30)	30 (30)
S_{I0} (S_{II0})	III	8.0 (7.0)	6.75 (4.25)	60 (30)	30 (30)
				Total	120

Table 2.2. Parameters used in the artificial earthquakes generation

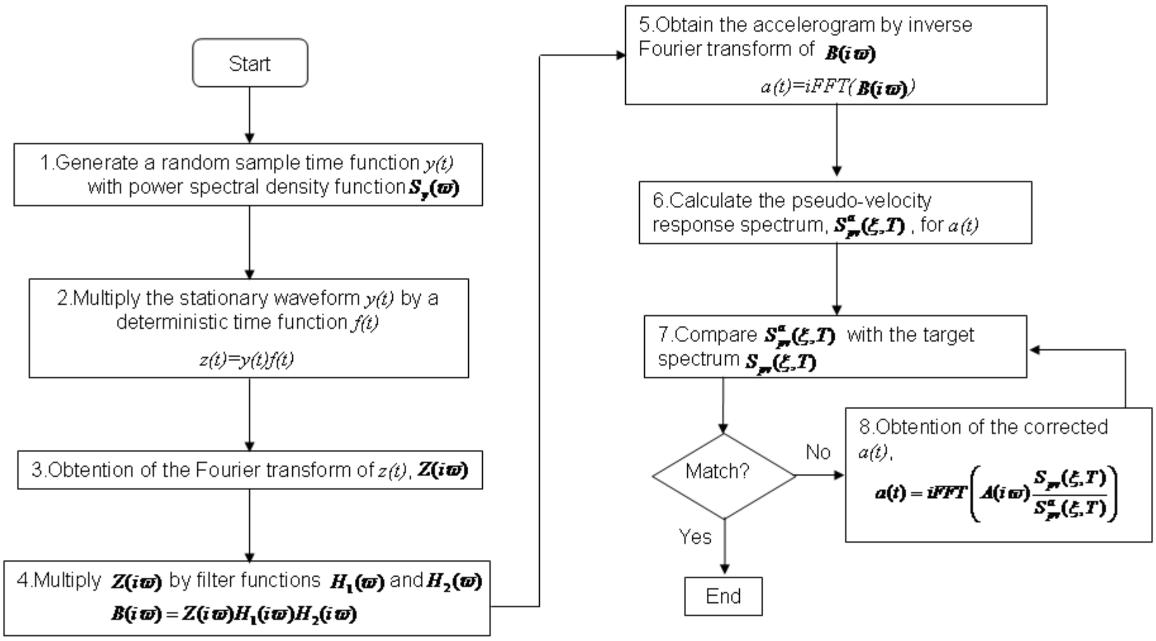

Figure 2.13 Procedure to generate artificial earthquakes

2.4.3 ELASTIC DISPLACEMENT SPECTRA

The elastic displacement design spectrum (S_D) can be obtained in a straightforward manner from the elastic design acceleration spectra, S_A, given by the design specifications with the following equation

$$S_D(T_0,\xi)=\left(\frac{T_0}{2\pi}\right)^2\eta(\xi)S_A(T_0,\xi_0=5\%) \tag{2.26}$$

where T_0 and ξ_0 are the natural period and damping coefficient respectively, S_D represents the displacement design spectra, and $\eta(\xi)$ is the reduction factor for damping ξ defined in the Japanese specifications as

$$\eta(\xi)=\frac{1.5}{40\xi+1}+0.5 \tag{2.27}$$

The variation of the reduction factor is shown in Figure 2.14. It can be observed the reduction of the damping is less significant when ξ>60 %.

In order to identify some error sources, a comparison of Equation 2.27 with other approaches to calculate the reduction factor is shown in Figure 2.15. There is a great variation in the behavior of the reduction factor due the type of earthquakes considered in each derivation. Equation 2.27 adopted in the Japanese Specifications was developed explicitly for the typical earthquakes in Japan. For this reason, it is strongly suggested to follow only one design code during the design process in order to limit the cumulative error.

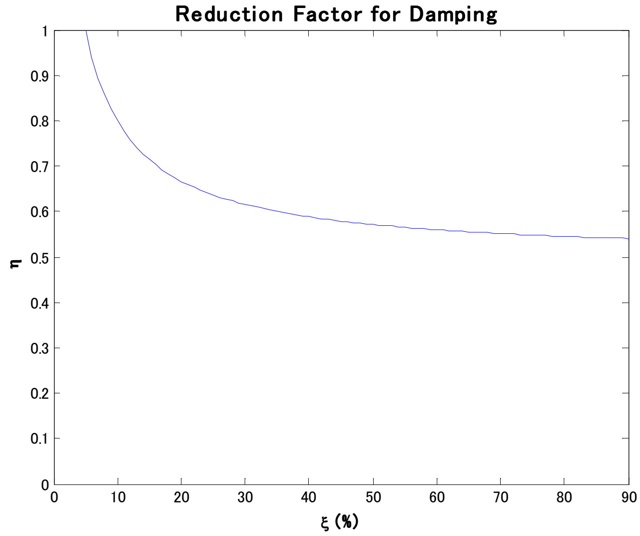

Figure 2.14 Reduction factor for damping

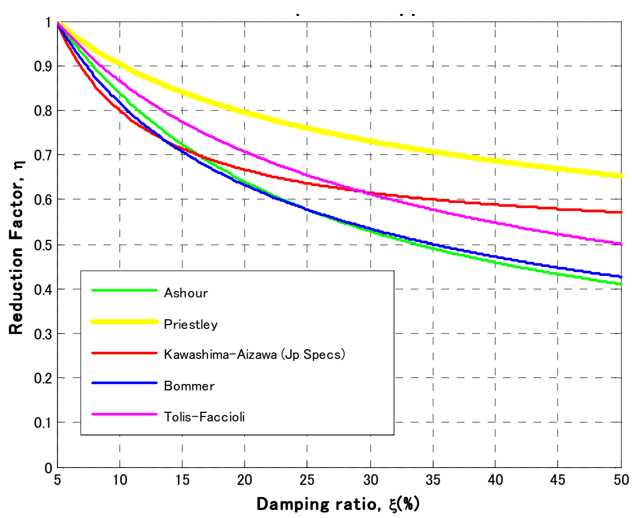

Figure 2.15 Comparison of reduction factors

Figures 2.16 and 2.17 show the corresponding displacement spectra in the range of periods considered. Figures 2.18 and 2.19 show the typical earthquakes obtained.

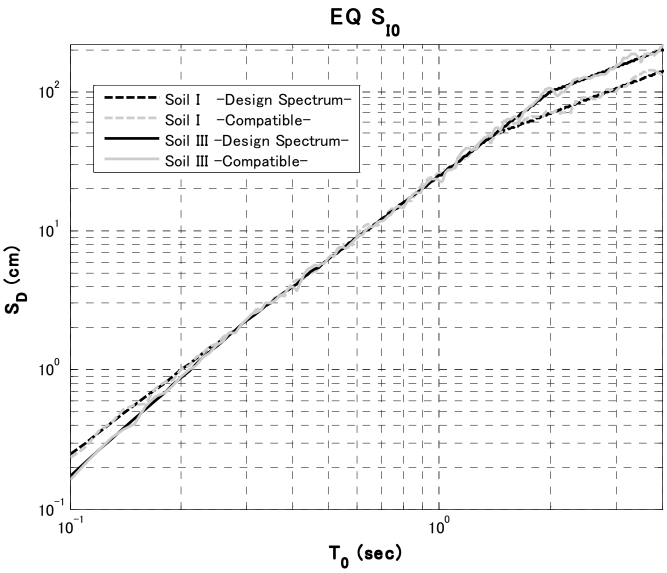

Figure 2.16 Displacement spectra EQ S_{IO}

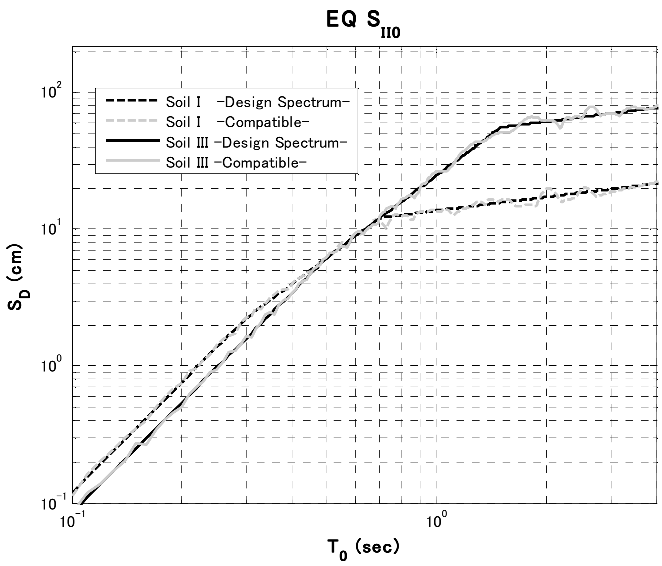

Figure 2.17 Displacement spectra EQ S_{IIO}

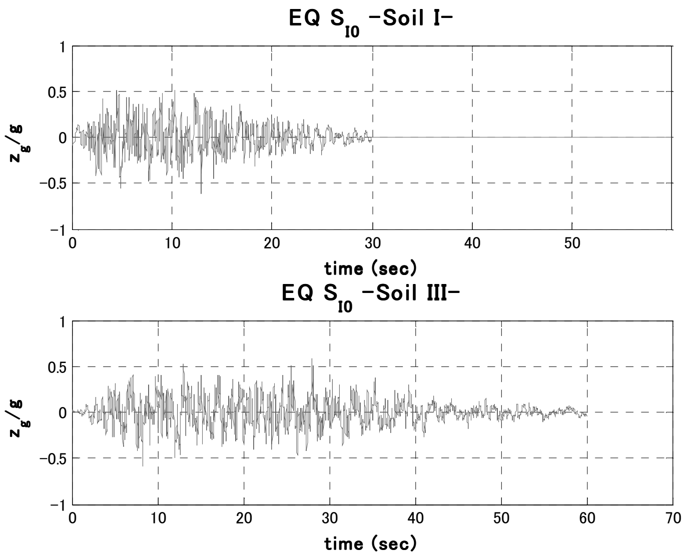

Figure 2.18 Earthquakes generated -Sample EQ S_{IO}-

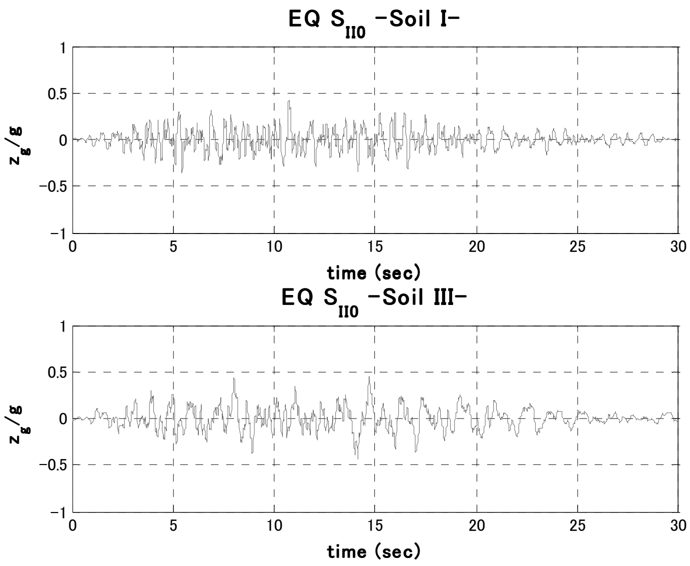

Figure 2.19 Earthquakes generated -Sample EQ S_{IIO}-

2.4.4 INELASTIC DISPLACEMENT SPECTRA

Like in the linear case, the maximum inelastic displacement demand, S_{DNL}, can be obtained from the design acceleration spectra, S_A. To this end, two approaches have been proposed. The first uses suitable expressions for the equivalent period, T_{eq}, and damping, ξ_{eq}, (Priestley *et al*. 2007) (these equations will be derived and presented in Chapter 3). The second one is based on the following equation and steps:

$$S_{DNL}(T_{eq,p},\xi_{eq,p}) = \left(\frac{T_{eq,p}}{2\pi}\right)^2 \eta(\xi) S_A(T_{eq,p},\xi = 5\%) \tag{2.28}$$

where $T_{eq,p}$ and $\xi_{eq,p}$ are the equivalent properties of the system calculated with the Equations presented in Chapter 3.

To obtain the inelastic response:

- Set the ductility level of the structure (μ).
- Calculate the equivalent period ($T_{eq,p}$) and damping ($\xi_{eq,p}$) for the initial period, T_0.
- Calculate the reduction damping factor η.
- Determine the acceleration value for the elastic acceleration spectrum S_A (T_{eq}, ξ=5%).
- Finally, compute the maximum response with Equation 2.28

2.5 SUMMARY

In this Chapter, the fundamental concepts that are used throughout this study were introduced. The concepts of seismic isolation and additional damping through viscous dampers were presented and their mechanical modeling and dynamic characteristics such as stiffness and damping were described. Additionally, the elastic design displacement spectra derived from the Japanese Design Specifications for Highway Bridges were presented. Finally, a method to calculate the inelastic displacement demand from the elastic spectra was described.

REFERENCES

ATC (1993), ATC-17-1, *Proceedings of seminar on seismic isolation, passive energy dissipation and active control*, Applied Technology Council, Redwood City, CA.

Bommer, J. J., Elnashai, A. S. and Weir, A. G. (2000), "Compatible acceleration and displacement spectra for seismic codes", *Proceedings of the 12th World Conference on Earthquake Engineering*, Auckland, New Zealand, February.

Chopra A. K. (2003), Dynamics of Structures: Theory and Applications to Earthquake Engineering, 1st edn, Prentice-Hall, Englewood.

Clough, R.W. and Penzien, J. (2003), *Dynamics of Structures*, Computer and Structures, Inc.

FEMA, (2000). NEHRP Prestandard and Commentary for the Seismic Rehabilitation of Building, No. 356.

Hamada, M. (2000), "Key concepts for earthquake resistant design of civil engineering structures after the 1995 Hyogoken-nanbu earthquake", *Earthquake Resistant Design Codes in Japan*, JSCE.

Japan Road Association (JRA), (2002), *Seismic Design Specifications for Highway Bridges* (in Japanese).

Jara M. and Casas J. R. (2006), "A direct displacement-based method for the seismic design of bridges on bi-linear isolation devices", *Engineering Structures*, 28: 869–879.

Jenn-Shin H. and Yi-Shane T., (2005), "Design formulations for supplemental viscous dampers to highway bridges", *Earthquake Engng Struct. Dyn.*, **34**:1627‑1642.

Kelly, J.M., (1986). "Aseismic base isolation: A review and bibliography", *Soil Dynamics and Earthquake Engineering*, (5):202-216.

Kunde M.C. and Jangid R.S. (2003), "Seismic behavior of isolated bridges: A-state-of-the-art review", *Electronic Journal of Structural Engineering* (3):140-170.

Lin Y. Y., Chang K. C. and Chen C. Y. (2008), "Direct displacement-based design for seismic retrofit of existing buildings using nonlinear viscous dampers", *Bull Earthquake Eng.* 6(3):535–552.

Pekcan G., Mander J.B. and Chen S.S. (1999), "Fundamental considerations for the design of non-linear viscous dampers", *Earthquake Engng. Struct. Dyn.*, 28: 1405-1425.

Ramirez O. M., Constantinou M. C., Kircher A., Whittaker A. S., Johnson M. W. and Gomez J. D. (2000), *Development and evaluation of simplified procedures for analysis and design of buildings with passive energy dissipation systems*, Report No. MCEER-00-0010, Multidisciplinary Center Earthquake Engineering Research, Buffalo, New York.

Seleemah A. A. and Constantinou M. C. (1997), *Investigation of seismic response of buildings with linear and nonlinear fluid viscous dampers*, Report No. NCEER-97-0004, National Center for Earthquake Engineering Research, Buffalo, New York.

Singh M. P., Verma N. P. and Moreschi L. M. (2003), “Seismic analysis and design with Maxwell dampers”, *Journal of Structural Engineering*, **129**(3):273-282.

Skinner R. I., Robinson W. H. and McVerry G. H. (1993), *An introduction to Seismic Isolation*, John Wiley and Sons Ltd, England.

Soong T.T. and Constantinou M. C. (1994), *Passive and Active Structural Vibration Control in Civil Engineering*, Springer-Verlag, New York.

Soong T.T. and Dargush, G.F. (1997), *Passive Energy Dissipation Systems in Structural Engineering*, John Wiley & Sons.

Vasant A. Matsagar and R. S. Jangid (2006), “Seismic Response of Simply Supported Base-Isolated Bridge with Different Isolators”, *International Journal of Applied Science and Engineering*, (4)1: 53-69.

Whittaker A. and Constantinou M. C. (2000), “Fluid viscous dampers for building construction”, *First International Symposium on Passive Control*, 132-142, Tokyo Institute of Technology, Tokyo, Japan.

Yun H. B., and Tasbighoo F., Masri S. F., Caffrey J. P., Wolfe R. W., Markis N. and Black C. (2006), “Comparison of modeling approaches for full scale nonlinear viscous dampers”, *Journal of Vibration and Control*, 14:51-76

CHAPTER 3

EQUIVALENT PERIOD AND DAMPING OF SDOF SYSTEMS FOR SPECTRAL RESPONSE OF THE JAPANESE HIGHWAY BRIDGE CODE

3.1 GENERAL REMARKS

Since performance-based design was proposed, several seismic design and assessment methodologies have been developed to fulfill its requirements. One of the most promising approaches is based on the control of displacements under the assumption that the damage can be managed if the deformations are controlled. In this approach, known as displacement-based design (DBD), the structure is simplified into an equivalent linear system to estimate the seismic deformation of an inelastic single-degree-of-freedom (SDOF) system, representing the first (elastic) mode of vibration (Fig. 3.1). Considerable work has been carried out in the past to determine the equivalent elastic properties (period and damping) of the inelastic SDOF system. Most of the proposed equations are only defined in terms of the ductility and the initial damping of the real structure. Exceptions are the works of Kwan and Billington (2003), Blandon and Priestley (2005), and Guyader and Iwan (2006). These researchers define the equivalent damping in terms of both the ductility and the initial natural period of the oscillator. However for the equivalent damping, Guyader and Iwan (2006) limited this dependency for ductility values greater than 6.5. Blandon and Priestley (2005) do not present equations for explicit calculations of the equivalent period. Nevertheless, the equivalent period is obtained iteratively within the displacement design method. On the other side, Kwan and Billington (2003) limited the range of periods between 0.1 and 1.5 sec. In recent works, Lin and Miranda (2008) and Goda and Atkinson (2010) presented equations for the equivalent period and damping of existing structures including the initial period dependency, however, these researchers used the constant strength instead of ductility ratio as the known parameter.

The proposed equations for the equivalent properties have been derived using either of the following procedures: methods based on the harmonic response or methods based on random response. To evaluate the accuracy of the different issued equations, several comparisons of the estimations given by these approaches have been carried out. From these, one of the most remarkable results is that the equivalent period and equivalent damping should be defined in terms of the initial period. Otherwise, the dispersion and scattering of the predictions could be substantial even for relatively small mean errors and especially for large values of ductility (Miranda and Ruiz-Garcia 2002, Blandon and Priestley 2005, Degee *et al*. 2008, Zaharia and Taucer 2008). Moreover, the equivalent properties should be derived for a series of earthquakes of similar characteristics for no more than one hysteretic model (Zaharia and Taucer 2008, Goda and Atkinson 2010). In general, it has been found that, methods based on the harmonic response considerably overestimates the period shift whereas methods based on random response give more realistic results estimations (Chopra and Goel 1999).

In this work, in order to overcome the underlined deficiencies in the estimations of the inelastic displacements, the equations for the equivalent damping and the equivalent period are defined as functions of the ductility and the initial period of vibration and derived by statistical procedures. Originally, the equations are intended to be used for the displacement-based design of bridges with initial period no longer than 4 sec. The estimated displacements obtained with the proposed equations are verified and discussed. Finally, a revision of the scope and limitations of the proposed equations are presented.

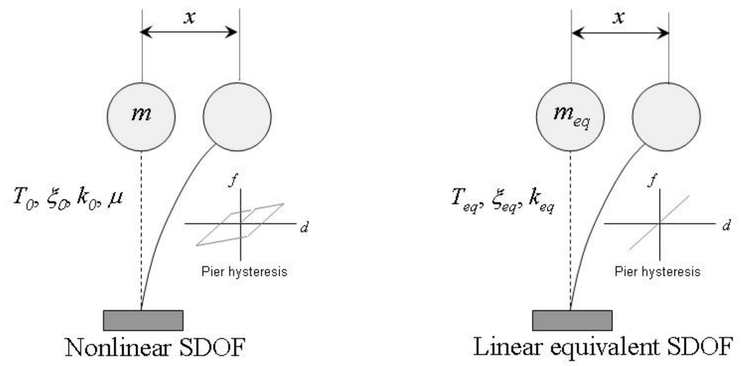

Figure 3.1. Nonlinear SDOF simplified into an equivalent SDOF system

3.2 Preliminary Considerations

3.2.1 Definition of Equivalent Properties

Consider an inelastic single degree of freedom (SDOF) system with structural response described by the following equation of motion:

$$\ddot{x} + 2\xi_0\omega_0\dot{x} + \frac{R_F(x)}{m} = -\ddot{z}_g \tag{3.1}$$

In the above equation, m, ξ_0, and $R_F(x)$ are the mass, damping coefficient and the restoring force of the system, respectively, $\ddot{z}_g$ is the ground acceleration, x is the displacement of the mass relative to the ground, and by convention a single dot denotes the first derivative with respect to time, and a double dot indicates the second derivative with respect to time. The natural frequency of vibration, ω_0, is defined in terms of the initial stiffness, k_0, and the period of vibration of the system, T_0, by

$$\omega_0 = \sqrt{\frac{k_0}{m}} = \frac{2\pi}{T_0} \tag{3.2}$$

By substitution of the Eq. (3.2) into the Eq. (3.1), the inelastic response of the oscillator may be written in a more convenient form as

$$\ddot{x} + \left(\frac{4\pi}{T_0}\right)\xi_0 \dot{x} + \frac{R_F(x)}{m} = -\ddot{z}_g \tag{3.3}$$

The inelastic SDOF system is capable of undergoing a maximum inelastic deformation characterized by the ductility ratio, μ, which is defined as the ratio between the maximum inelastic displacement and the yielding displacement.

The maximum inelastic displacement can be exactly calculated using a nonlinear analysis of Eq. (3.3) or can be approximated by either of the following methods: (a) those based on a displacement modification factor (Newmark and Hall 1982, Miranda 2000), and (b) those based on equivalent linearization. Only the latter will be considered in this study.

In the equivalent linearization method, the maximum inelastic displacement (Eq. 3.3) can be estimated from the equivalent linear model represented by

$$\ddot{x}_{eq} + \left(\frac{4\pi}{T_{eq}}\right)\xi_{eq} \dot{x}_{eq} + \left(\frac{2\pi}{T_{eq}}\right)^2 x_{eq} = -\ddot{z}_g \tag{3.4}$$

where T_{eq} and ξ_{eq} are the equivalent period and equivalent damping respectively, such that max $|x(T_0,\xi)|$ = max$|x(T_{eq},\xi_{eq})|$. In the ideal case, the equivalent displacement x_{eq} should match the inelastic displacement x. However, due to the approximated nature of equivalent linearization this will occur only when Equations 2.3 and 2.4 represent exactly the same system which is when μ=1. For other values of μ, the equivalent and real displacements will only match for a few cases although sufficiently accurate approximations, for engineering purposes, can be obtained.

As it will be clarified in the next section, the equivalent period can be defined in terms of the original period modified by a shifted constant C as

$$T_{eq} = CT_0 \tag{3.5}$$

Due to the energy dissipated by the hysteretic behavior in nonlinear systems, it can be expected that T_{eq} will be longer than T_o and ξ_{eq} will be greater than ξ_0. In this study, the optimal equivalent damping and period are the combinations of T_{eq} and ξ_{eq}, which gives the best approximated value for the maximum inelastic displacement obtained from Eq. 3.3.

3.2.2 REVIEW OF PREVIOUS STUDIES

Since the first approach of equivalent linearization made by Jacobsen (1930, 1960) and the equivalent-substructure formulation made by Gulkan and Sozen (1974), extensive research has been done on expressions for the suitable equations for the equivalent properties T_{eq} and ξ_{eq}. Miranda and Ruiz Garcia (2002) presented a review of the most significant approximate methods to estimate maximum inelastic displacement demands based on equivalent linearization such as those from Rosenblueth and Herrera (1964), Gulkan and Sozen (1974), Iwan (1980) and Kowalski *et al.* (1994). In this section, from the large amount of information available in the literature, only more recent references relevant to this study will be described.

Kwan and Billington (2003) used Iwan's method and 20 ground motion records, to derive the following equations (valid for periods between 0.1-1.5 sec):

$$T_{eq} = 0.8T_0\mu^{C_1} \tag{3.6a}$$

$$\xi_{eq} = \frac{2C_2}{\pi}\left(\frac{T_{eq}}{T_0}\right)^2 \frac{\mu-1}{\mu^2} + 0.55\left(\frac{T_{eq}}{T_0}\right)^2 \xi_0 \tag{3.6b}$$

where the coefficients C_1 and C_2 varies according with the hysteretic system: Elastoplastic (EP), Slightly/Moderately degrading (DG), Slip (SL), Origin oriented (OO), and Bilinear elastic (BE). For instance, for EP and DG systems C_1=0.5 and C_2=0.56.

Blandon and Priestley (2005) presented the following equation for the equivalent damping derived from iterative analysis with six synthetic accelerograms:

$$\xi_{eq} = \frac{a}{\pi}\left(1-\frac{1}{\mu^b}\right)\left(1+\frac{1}{(T_{eq}+c)^d}\right)\cdot\frac{1}{N} \tag{3.7}$$

where N is a normalizing factor and a, b, c, and d are constants which consider the hysteretic model: Takeda thin (TH), Takeda fat (TF), Bilinear inelastic (BI), EP, Ramberg Osgood (RO) and Ring Spring (RS). In this case, the effective period T_{eq} is determined by an iterative procedure during the design process. To illustrate this equation the coefficients for the TH model are considered (a=95, b=0.5, c=0.85 and d=4).

Guyader and Iwan (2006) derived equations from statistical studies, in which the mean and the standard deviation of the error in the estimation were minimized, using an ensemble of 28 far-field ground motions (varying in earthquake magnitude, soil conditions and epicentral distance). In this case, the equivalent properties are defined by

$$\xi_{eq} = \xi_0 + A_G(\mu-1)^2 + B_G(\mu-1)^3 \quad \text{for } \mu < 4.0 \tag{3.8a}$$

$$T_{eq} = T_0[1 + G_G(\mu-1)^2 - H_G(\mu-1)^3] \quad \text{for } \mu < 4.0 \tag{3.8c}$$

$$\xi_{eq} = \xi_0 + C_G + D_G(\mu-1) \quad \text{for } 4.0 \le \mu \le 6.5 \tag{3.8b}$$

$$T_{eq} = T_0[1 + I_G + J_G(\mu-1)] \quad \text{for } 4.0 \le \mu \le 6.5 \tag{3.8d}$$

$$\xi_{eq} = \xi_0 + E_G\left[\frac{F_G(\mu-1)-1}{F_G(\mu-1)^2}\right]\left(\frac{T_{eq}}{T_0}\right)^2 \quad \text{for } \mu > 6.5 \tag{3.8e}$$

$$T_{eq} = T_0\left[1 + K_G\left(\sqrt{\frac{\mu-1}{1+L_G(\mu-1)-1}} - 1\right)\right] \quad \text{for } \mu > 6.5 \tag{3.8f}$$

In the above equations, the variables associated with the subscript G depends on the hysteretic model (BI, DG, Pinching). For the DG case, for instance: A_G=5.6420, B_G=-1.2962, C_G=10.182, D_G=1.8661, E_G=19.51, F_G=0.38, G_G=0.1809, H_G=-0.0366, I_G=0.17472, J_G=0.1640, K_G=0.92, and L_G=0.05.

Dwairi *et al*. (2007), by using a variation of the Jacobsen's approach derived the following equations to be used in the direct displacement-based design:

$$\xi_{eq} = \xi_0 + C^h\left(\frac{\mu-1}{\mu\pi}\right) \tag{3.9}$$

where C^h is a function which varies depending on the hysteretic model considered (RS, TH, TF and EP). For instance, for the TF pattern C^h=65+50(1-T_{eq}) if T_{eq} < 1 sec, and C^h=65 if $T_{eq} \geq$ 1 sec. The equivalent period is obtained during the design procedure by using displacement spectrum. More recently, Zaharia and Taucer (2008) derived new coefficients for the Iwan's equations (for BI and RS systems), with a series of 30 synthetic earthquakes compatible with the Eurocode 8 spectra. The equivalent properties are defined by:

$$T_{eq} = T_0[1 + A(\mu - 1)^a] \tag{3.10a}$$

$$\xi_{eq} = \xi_0 + B(\mu - 1)^b \tag{3.10b}$$

where A, a, B, and b are constants which consider the hysteretic model and the type of spectra. For bilinear systems and spectra type 1 the coefficients are A=0.153, a=1.02, B= 2.14 and b=1.02.

For existing structures, where the strength ratio, R (elastic lateral strength/yield lateral strength), is generally known rather than the ductility ratio, Lin and Miranda (2008) derived the following equations for bilinear hysteretic systems subjected to 72 ground motions:

$$T_{eq} = T_0\left[1 + \frac{m_1}{T_0^{m_2}}(R^{1.8} - 1)\right] \tag{3.11a}$$

$$\xi_{eq} = \xi_0 + \frac{n_1}{T_0^{n_2}}(R - 1) \tag{3.11b}$$

Where m_1, n_1, m_2 and n_2 are constants which value depends on the postyield stiffness ratio.

Goda and Atkinson (2010) proposed the following form of equations to estimate the maximum displacements demands of existing structures based on 70 earthquakes from Japan and 172 from California:

$$T_{eq} = 1 + f(T_0, R; a) \tag{3.12a}$$

$$\xi_{eq} = 0.05 + f(T_0, R; a) \tag{3.12a}$$

with $f(T_0, R; a) = \exp(a_1 \min(T_0, 0.2) + a_2 T_0^{a_3} + a_4(R - 0.5)^{a_5} + a_6 T_0)$, where the vector a contains six model coefficients a_i. Equations 2.13 can be used for various hysteretic characteristics with different post-yield-to-initial stiffness ratios and degradation/pinching behavior.

Excepting the method from Rosenblueth and Herrera (1964), based on the steady-state harmonic response, Figures 3.2 and 3.3 shows the variation of the ratio T_{eq} /T_0 and ξ_{eq} respectively for the described equivalent linearization models.

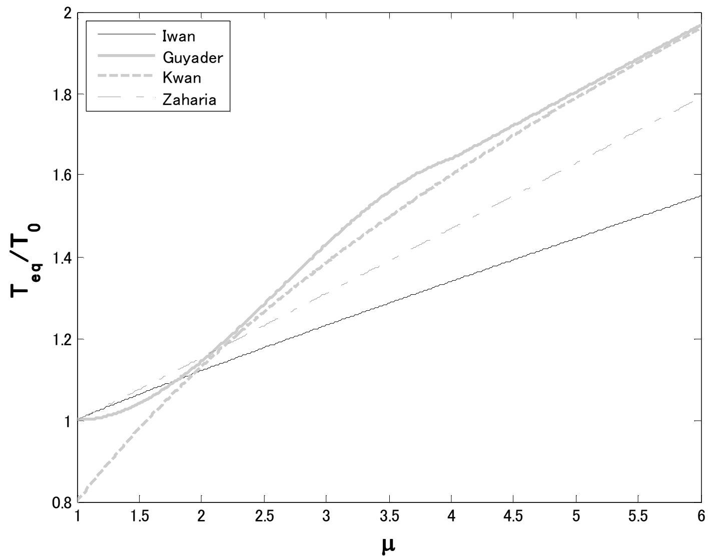

Figure 3.2. Comparison of T_{eq} /T_0 for different equivalent linearization models

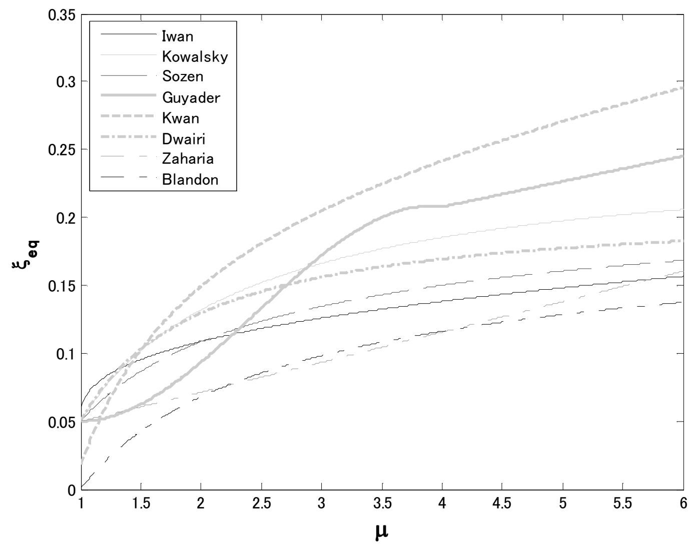

Figure 3.3. Comparison of ξ_{eq} for different equivalent linearization models

3.3 EQUIVALENT PERIOD AND DAMPING INCLUDING INITIAL PERIOD DEPENDENCY

3.3.1 FORM OF THE EQUATIONS

As suggested by the most recent studies on equivalent linearization, the equivalent period and the equivalent damping should be defined in terms of the ductility ratio and initial periods of vibration. Then, hereafter the conceptual scope can be outlined as follows:

- Formulate a single expression for the equivalent period, T_{eq}, and another for the equivalent damping, ξ_{eq}, with variable coefficients that consider the type of earthquake and the class of soil.
- The equation for T_{eq} will be formulated as a function of μ and T_O as $T_{eq}= T_{eq}(\mu, T_0)$.
- The equation for ξ_{eq} will be formulated as a function of ξ_0, μ, and T_0 as $\xi_{eq}=\xi_{eq}(\xi_0, \mu, T_0)$.
- The equations will be generated from accelerograms compatible with the acceleration spectra for strong earthquakes specified in the adopted design guidelines.

From the large number of mathematical expressions that fit the curve, a compact form that incorporates both the conceptual scope and the period dependency of the equivalent damping found in the regression analysis (also pointed out by Guyader and Iwan, 2006 and Lin and Miranda, 2008) is required. The following specific set of equations is proposed

$$T_{eq} = T_0[1 + A{T_0}^B(\mu^C - 1)] \tag{3.13a}$$

$$\xi_{eq} = \xi_0 + a{T_0}^b(\mu^c - 1)] \tag{3.13b}$$

where the A, B, C, a, b and c are constants calculated by regression analysis explained in the following section.

This form of expressions are suggested for its concise and simple form. Moreover, as will be shown later, these equations are sufficiently accurate and easy to implement for practical purposes.

3.3.2 REGRESSION ANALYSIS PROCEDURE

In one of the most recurrent empirical approaches to obtain the equivalent properties (Iwan 1980, Kwan and Billington 2003, Zaharia and Taucer 2008), the values of T_{eq} and ξ_{eq} are the couple which minimizes the root-mean-square error, $\bar{\varepsilon}$, of the ratio between the averaged inelastic exact displacement and the averaged equivalent elastic displacement throughout the range of periods, i, given by

$$\bar{\varepsilon}(\varepsilon_{eq},T_{eq}) = \sqrt{\sum_{i=1}^{N}\frac{\varepsilon_i^{\,2}}{N}} \tag{3.14}$$

with

$$\varepsilon(\xi_{eq},T_{eq})_i = \frac{SD_e(T_{eq}(T_0,\mu),\xi_{eq})_i}{SD_{nl}(\mu,T_0,\xi_0)_i} - 1 \tag{3.15}$$

where N is the number of periods.

This approach assumes that the equivalent linear spectrum closely represents the behavior of the inelastic spectra in all the range of periods. However, this is not necessarily true. In this study, since all the earthquakes have similar characteristics, a different approach that would work better is adopted: the root-mean-square error is calculated for each period for all of the earthquakes considered (Lin and Miranda 2008, Sánchez-Flores and Igarashi, 2010).

According to this and considering the objectives previously mentioned, the method consists of the following steps:

1. Set the minimum and maximum values of the equivalent damping coefficient.
2. Select the interval of periods.
3. Obtain the elastic equivalent (shifted) displacement response spectra $(SD_e)_k$, for all of the damping values throughout the range of periods, for all the artificial earthquakes, k, in terms of the equivalent and original period, and the equivalent damping as

$$\left(SD_e\right)_k = SD_e(T_{eq}(\mu,T_0),\xi_{eq}(\xi_0,\mu,T_0))_k \tag{3.16}$$

4. Set the range of ductility values and the hysteretic model for the nonlinear analysis.

5. Calculate the inelastic displacement response spectra $(SD_{nl})_k$, in terms of the original period, damping, and ductility ratio for all of the artificial earthquakes as

$$\left(SD_{nl}\right)_k = SD_{nl}(T_0, \xi_0, \mu)_k \tag{3.17}$$

6. Calculate the difference, ε, between the inelastic and the shifted elastic spectra in the i^{th} period for each earthquake

$$\varepsilon(\xi_{eq}, T_{eq})_{ik} = \frac{SD_e(T_{eq}(T_0, \mu), \xi_{eq})_{ik}}{SD_{nl}(T_0, \xi_0, \mu)_{ik}} - 1 \tag{3.18}$$

7. Calculate the root-mean-square (RMS) error, ($\bar{\varepsilon}_i$), of the ratio between the inelastic and the elastic shifted spectra for the total number of earthquakes for the i^{th} period

$$\bar{\varepsilon}(\varepsilon_{eq}, T_{eq})_i = \sqrt{\sum_{k=1}^{N_k} \frac{{\varepsilon_{ik}}^2}{N_k}} \tag{3.19}$$

where N_k is the total number of earthquakes.

8. Find the optimum combination of of $T_{eq}(\mu, T_0)$ and $\xi_{eq}(\xi_0, \mu, T_0)$, which gives the minimum RMS error. The optimal values are then substituted into the Eq. (3.4) to calculate the equivalent linear spectrum.

   To verify if the optimal values were properly calculated, the mean ratio between the displacements calculated by the equivalent linear system (with T_{eq} and ξ_{eq}) and those computed by the exact inelastic analysis are calculated in each period, i, with

$$\bar{E}(T_0, \mu, \xi_{eq}, T_{eq})_i = \frac{1}{N_k} \sum_{k=1}^{N_k} \frac{SD_e(T_{eq}(T_0, \mu), \xi_{eq})_{ik}}{SD_{nl}(T_0, \xi_0, \mu)_{ik}} \tag{3.20}$$

   If the optimal parameters are good estimations, the mean ratio in the above equation should be very close to the unity throughout the range of periods for all ductility values.

9. Perform nonlinear regression analyses to fit a curve which closely represents T_{eq} and ξ_{eq}. To this end, in this work, techniques of two-stage nonlinear regression analysis for two variables (Bevington and Robinson, 1992) were carried out.
10. Verification of the results obtained by mean of statistical procedures.

All of the procedures previously described are summarized in Fig. 3.4.

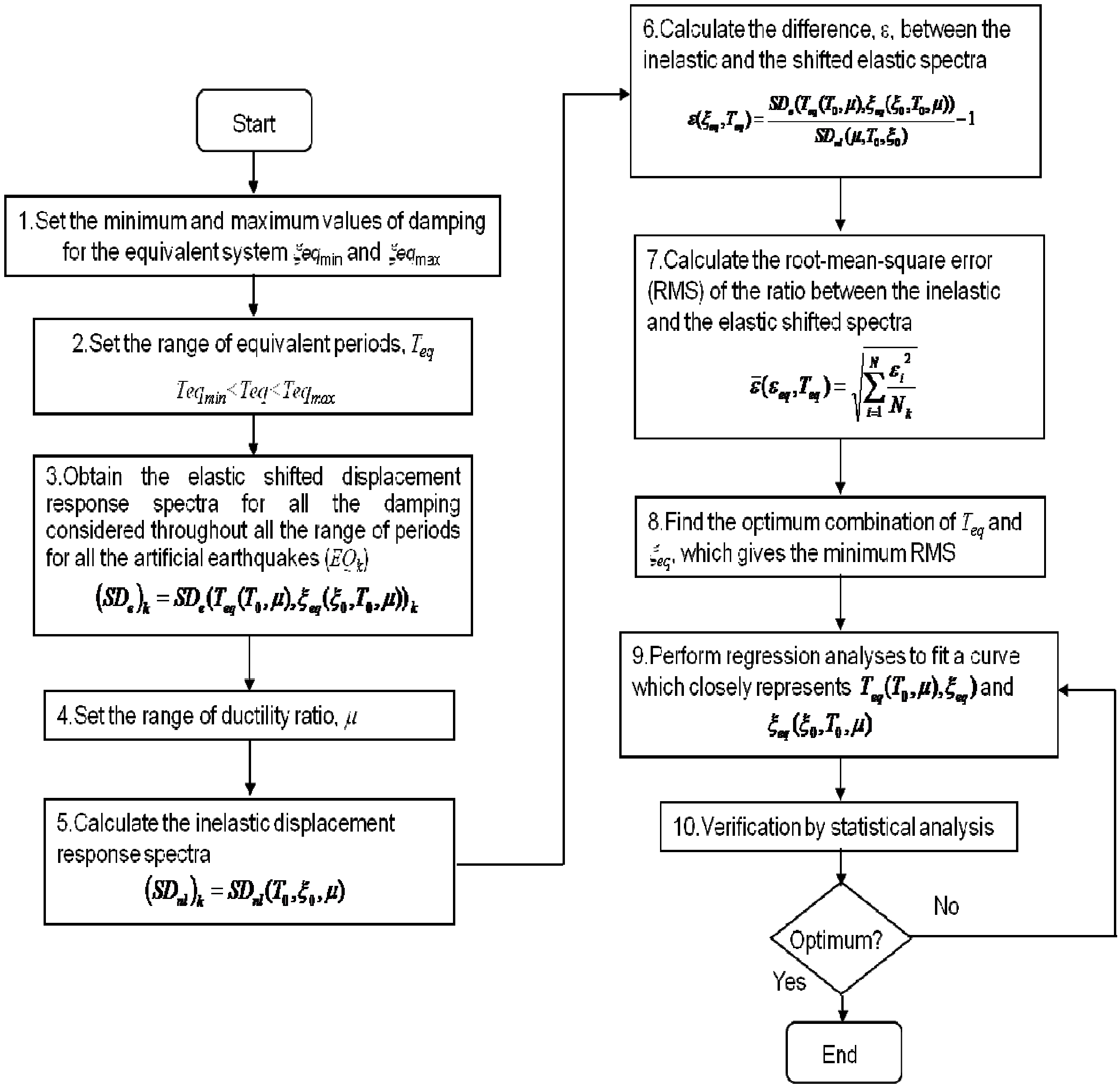

Figure 3.4. Procedure to derive expressions for the equivalent properties

3.3.3 NUMERICAL SCOPE

The aspects considered for the time history analysis are described as follows.

For nonlinear analysis:

- Seven ductility values are evaluated: 1, 1.5, 2, 3, 4, 5, and 6.
  In general, ductility values beyond 6 are not common in conventional bridges. Moreover, for performance based-design where the damage should be controlled, additional damping devices are usually included. Therefore, the ductility is reduced and the damping becomes the most significant source of energy dissipation.
- The equations for equivalent properties may have different coefficients depending on the hysteretic pattern used in their derivation. Even if a single hysteretic pattern is used, the coefficients may change depending on the parameters required on its definition as reported by Lin and Miranda (2008) for a bilinear case. Therefore, an in-depth study on the influence of the hysteretic pattern in equivalent linearization falls beyond the scope of this work. Thus, the time history analyses are limited to the modified Clough hysteretic behavior (Otani, 1981). This model can be used to represent concrete structures that exhibit stiffness degradation under seismic loads when the behavior is primarily flexural as is expected in bridge piers. The post-yielding stiffness is set to 0.05 times the corresponding elastic stiffness.
- The initial damping coefficient ξ_0 is set to 5% to be compatible with the design guideline.
- The period range, T_0, is set from 0.1 sec to 4 sec at intervals of 0.02 sec, due to the resulting equations which are intended to be used in the design of bridges with intermediate periods. Moreover, to be consistent with the displacement spectra the initial period is set lower than that calculated with Equation 2.28.

For the shifted analysis:

- Values of ξ_{eq} varying from 5% to 50% at intervals of 1% are considered.
- The range of the shifted ratio, T_{eq}/T_0, varies from 0.5 to 4 at intervals of 0.01. The maximum value is set after preliminary simulations with the largest value of ductility using Eq. 3.6. The minimum value is given by the ratio T_{eq}/T_0=1.

3.4 RESULTS

All of the steps listed in the regression analysis procedure (Section 3.3.2) can be computed in a straightforward manner. Therefore, only the estimations of the displacements obtained for the compatible earthquakes are illustrated in this Section 3.2.2 (Steps 7-8).

The relevant aspect is the calculation of the root-mean-square (RMS) error of the ratio between the inelastic and the elastic shifted spectra for the total number of earthquakes for each single period T_i. A matrix of RMS errors with a different period shift and equivalent damping can be computed on the basis of Eq. (3.19). The pair of T_{eq} and ξ_{eq} is the couple for which the error is minimal. To illustrate this, consider the elastic case and the corresponding inelastic one with μ=1 at T_0 =1, subjected to the earthquake S_{I0} -soil I-. Since the maximum displacement should be exactly the same for both cases, the optimal parameters are known beforehand: T_{eq}/T_0=1 and $\xi_{eq} = \xi_0$ = 5%. Therefore, the expected error is $\bar{\varepsilon}$ =0 as illustrated in Figures 3.5 and 3.6

Once the optimal parameters T_{eq}/T_0 and ξ_{eq} are calculated for all the periods and ductility ratios, they can be represented in plots similar to those shown in Figures 3.7 and 3.8. In this figure only ductility ratios of 1.5 and 6 are shown for clarity. When the ductility ratio is 1.5, the equivalent properties are nearly constant throughout the entire range of periods. On the contrary, when the ductility ratio is increased to 6, the optimal properties depend on both initial periods and ductility ratios. For this reason, the equations proposed in section 3.3.1 are defined in terms of these parameters. It can be observed (Figures 3.7. and 3.8.) that in all cases, T_{eq}/T_0 is greater than 1 and ξ_{eq} is greater than ξ_0=5%. This means the period of the equivalent linear system is longer, and the damping ratio of the equivalent linear system is greater than those of the corresponding nonlinear system's initial values.

To quantitatively measure the error in the estimation of the maximum displacement, the range proposed by Guyader and Iwan (2006) is adopted in this work. Then, hereafter the most desirable range of error values will be set between −10% and +20%. This interval considers the general preference to conservative design over unconservative design.

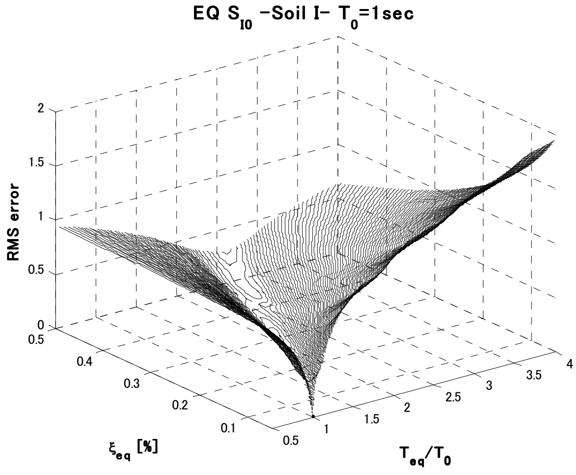

Figure 3.5. Matrix of error in the region RMS error-ξ_{eq}-T_{eq}/T_0

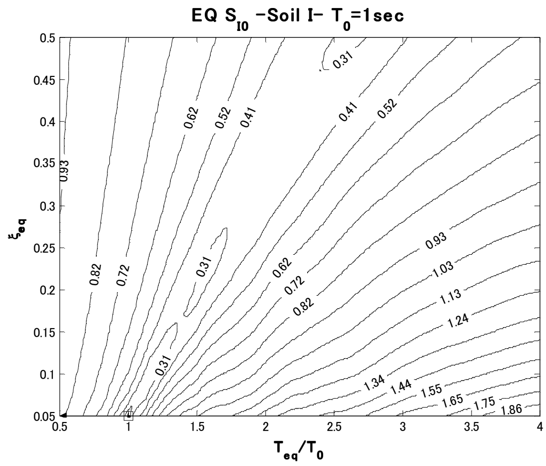

Figure 3.6. Contour of error in the region RMS error-ξ_{eq}-T_{eq}/T_0

With the obtained equivalent properties, the normalized equivalent displacement spectra (S_{DN}), calculated with the ground acceleration normalized by the gravity (g) as $\ddot{z}_g/g$, can be obtained with Eq. (3.4). For comparison, the exact S_{DN} is calculated with Eq. (3.3) for all soils and ductility ratios (Figure 3.9 to Figure 3.12.). From these figures, it can be observed that the linear equivalent spectra closely match the corresponding exact one especially for small periods. Nonetheless, there is a trend to underestimate the displacements for some period intervals. In any case, the error in the estimation is smaller than 5%.

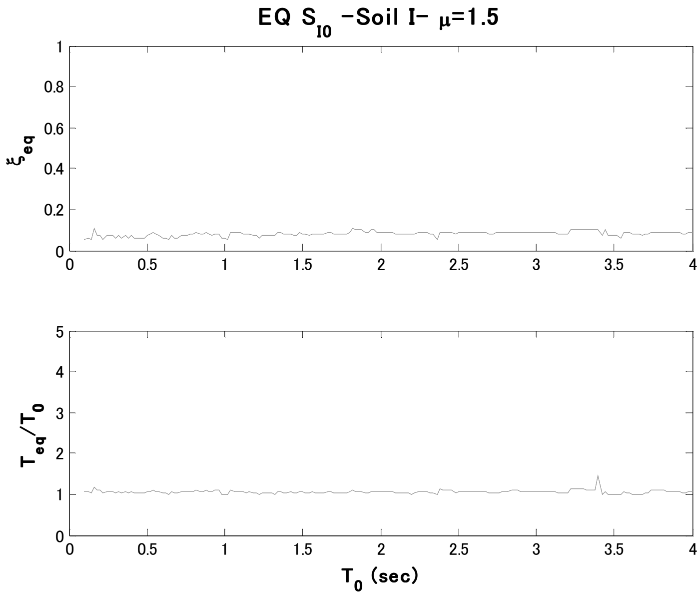

Figure 3.7. Optimal ξ_{eq} and period shift from the minimum RMS error (μ=1.5)

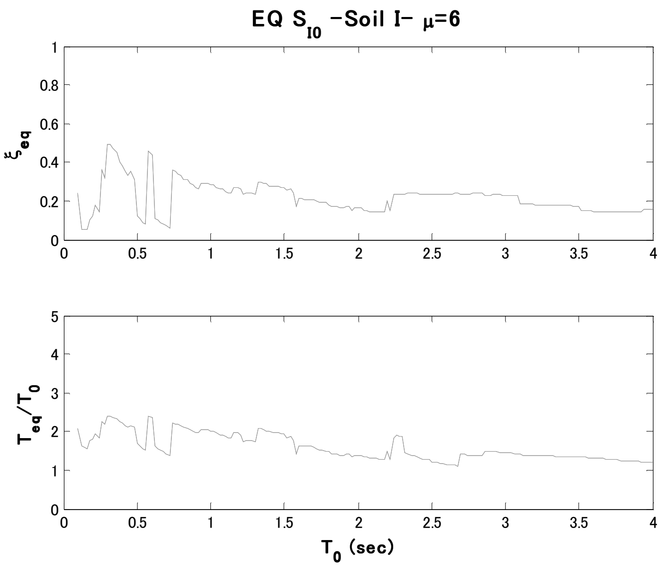

Figure 3.8 Optimal ξ_{eq} and period shift from the minimum RMS error (μ=6)

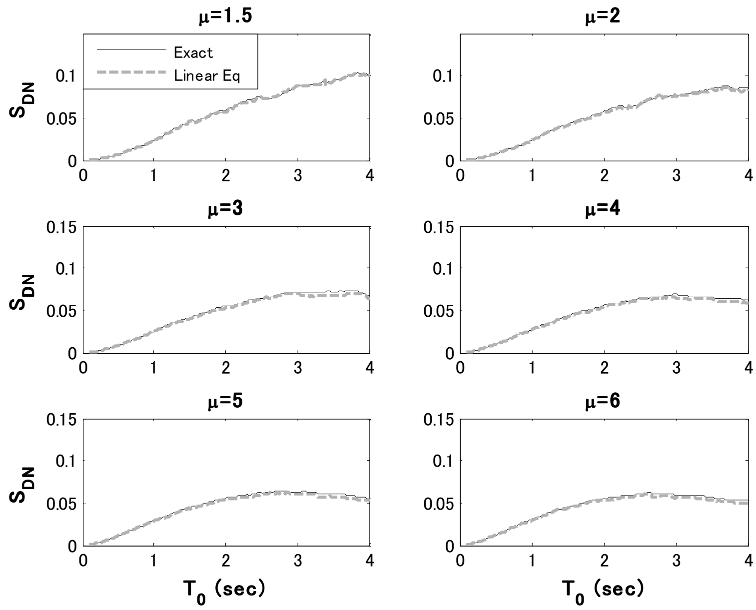

Figure 3.9. Normalized displacement spectra -Earthquake S_{I0}, Soil I-

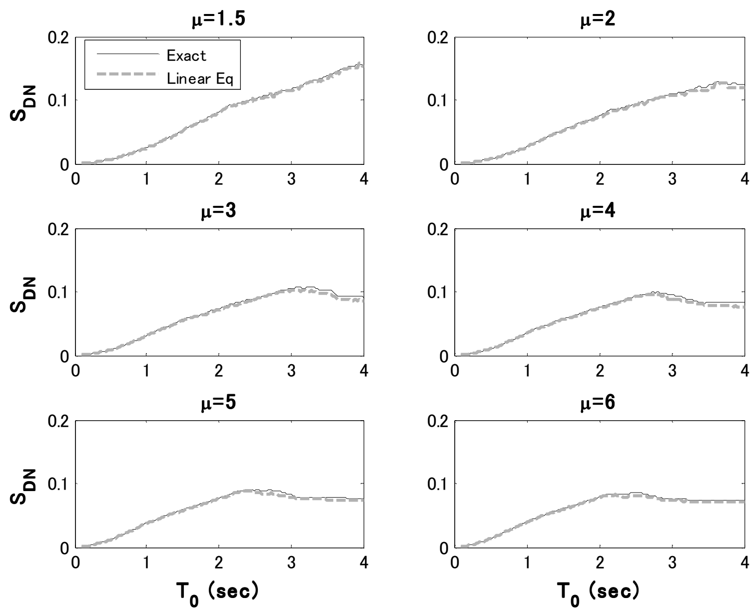

Figure 3.10. Normalized displacement spectra -Earthquake S_{I0}, Soil III-

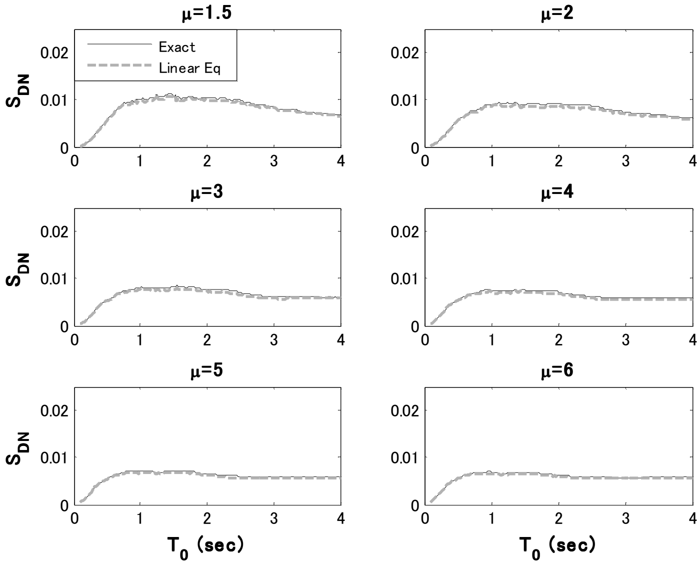

Figure 3.11. Normalized displacement spectra -Earthquake S_{II0}, Soil I-

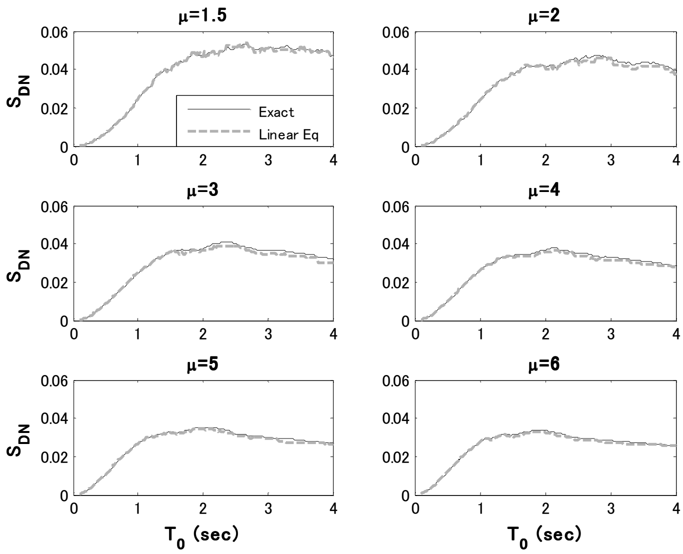

Figure 3.12. Normalized displacement spectra -Earthquake S_{II0}, Soil III-

After the nonlinear regression analysis to fit the curves shown in Figures 3.7. and 3.8., the values of the constants *A*, *B*, *C*, *a*, *b*, and *c* for Equation 3.13 are obtained. The corresponding values are shown in Table 3.1.

Earthquake	Soil Type	A	B	C	a	b	c
S_{IO}	I	0.278	-0.119	0.758	0.350	-0.038	0.210
	III	0.233	-0.102	0.884	0.642	-0.002	0.148
S_{IIO}	I	0.338	-0.462	0.510	5.562	-0.235	0.018
	III	0.199	-0.150	0.897	1.233	-0.087	0.078

Table 3.1. Coefficients for the equations of the equivalent properties

In order to illustrate the main difference of the proposed equations with the others described in Section 3.2.2, a comparison between the ratio T_{eq}/T_0 and ξ_{eq} obtained with the Equations 3.13 and those given by Guyader and Iwan (2006) is presented. For earthquakes S_{I0} in Soils I, the variation is shown in Figure 3.14 and 3.15. It can be observed the ratio T_{eq}/T_0 presents more variation with the initial period than the equivalent damping ξ_{eq}. For other combination of earthquakes and soils, however, the dependency of the initial period in the equivalent damping may be less significant.

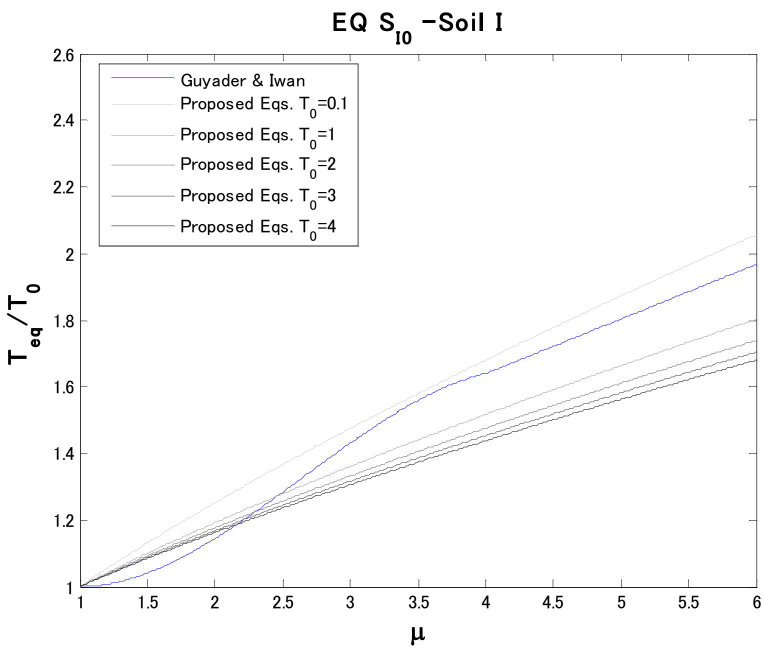

Figure 3.13. Behavior of the proposed T_{eq} /T_0 with other linearization models

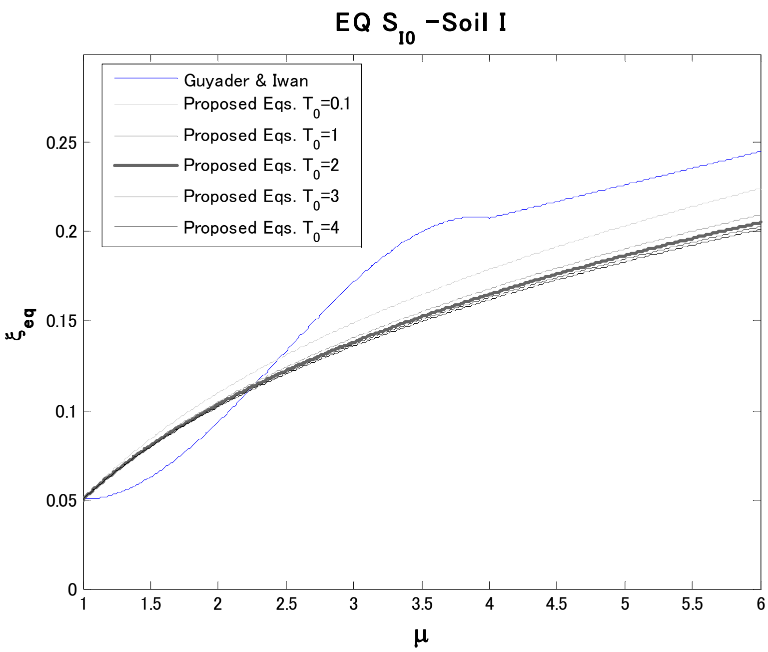

Figure 3.14. Behavior of the proposed ξ_{eq} with other linearization models

3.5 VERIFICATION ANALYSIS AND DISCUSSION

In this section, the accuracy and the dispersion of the results obtained with the proposed equations are investigated.

The accuracy of the estimation is evaluated by the mean error defined by Eq. 3.20, now denoted by E_{mean}, calculated for each earthquake and soil type. Values of E_{mean} close or equal to unity correspond to a good estimation of the maximum displacement, values greater than unity tend to overestimate the maximum displacement, and values smaller than unity tend to underestimate the maximum displacement. The approximate mean to exact displacement ratio is shown in Figures 3.15. and 3.16. for earthquakes type I and in Figures 3.17. and 3.18. for earthquakes type II.

For firm soils, the equations generally tend to overestimate the maximum displacements for periods greater than 0.6 and 0.9 sec for earthquakes type I and II, respectively. For the former earthquakes, the displacements are underestimated for periods smaller than 0.6. For the latter, the displacements are overestimated for all ductility ratios for periods smaller than 0.2 sec and underestimated between 0.2 and 0.5 sec. The maximum error of 20% is obtained when μ=3 at T_0= 3.2 for earthquakes S_{I0}, and when μ=5 at T_0=2.6 for earthquakes S_{II0}.

For soft soils, the displacements are generally overestimated for periods larger than 1.3 for type I earthquakes, and for periods longer than 0.8 sec for type II earthquakes. For short periods, the displacement is underestimated in all cases, with the maximum error of -10% obtained when μ=3.

In all cases, the minimum and maximum errors are kept under the predefined allowable limits of -10% and 20%.

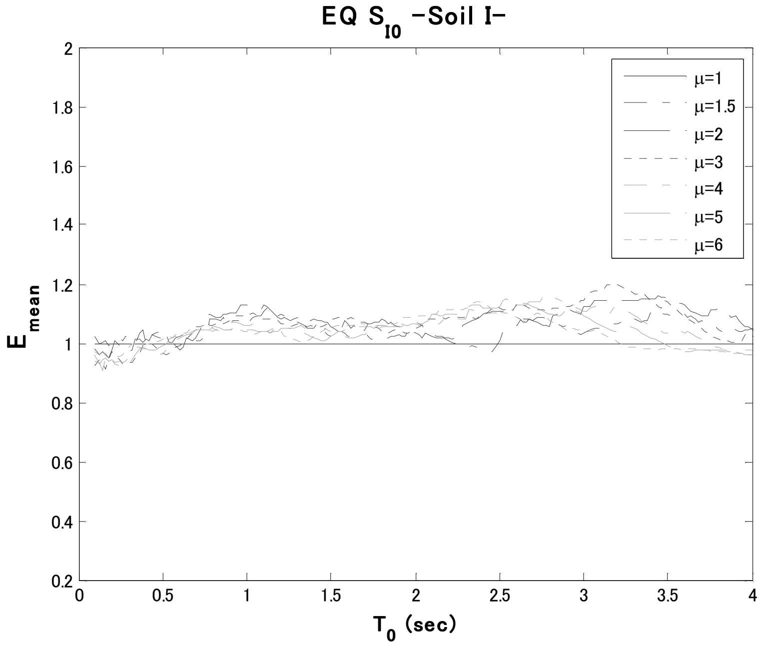

Figure 3.15. Mean approximate to exact displacement ratios -Earthquake S_{I0}- Soil I

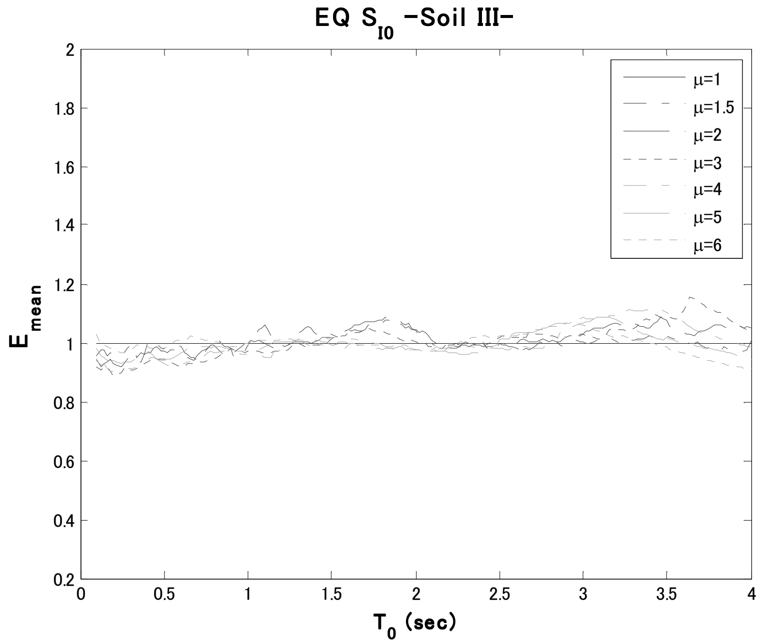

Figure 3.16. Mean approximate to exact displacement ratios -Earthquake S_{I0}- Soil III

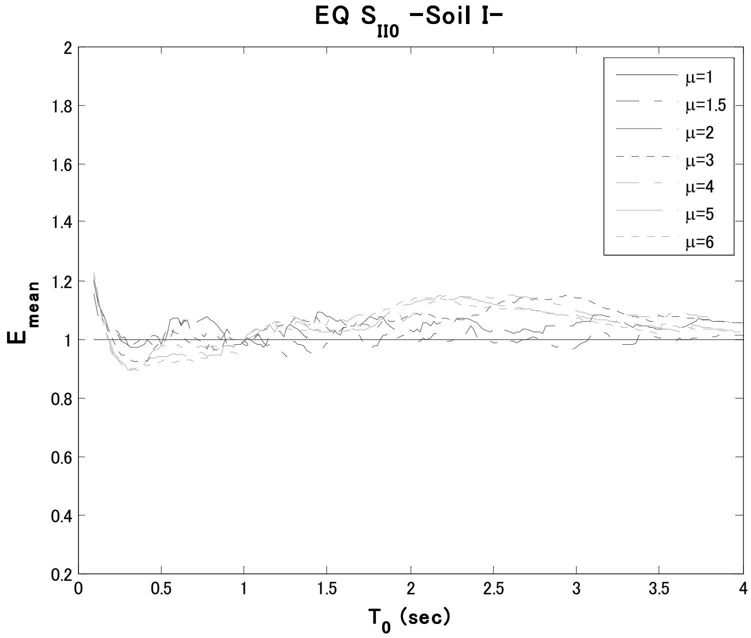

Figure 3.17. Mean approximate to exact displacement ratios -Earthquake S_{II0}- Soil I

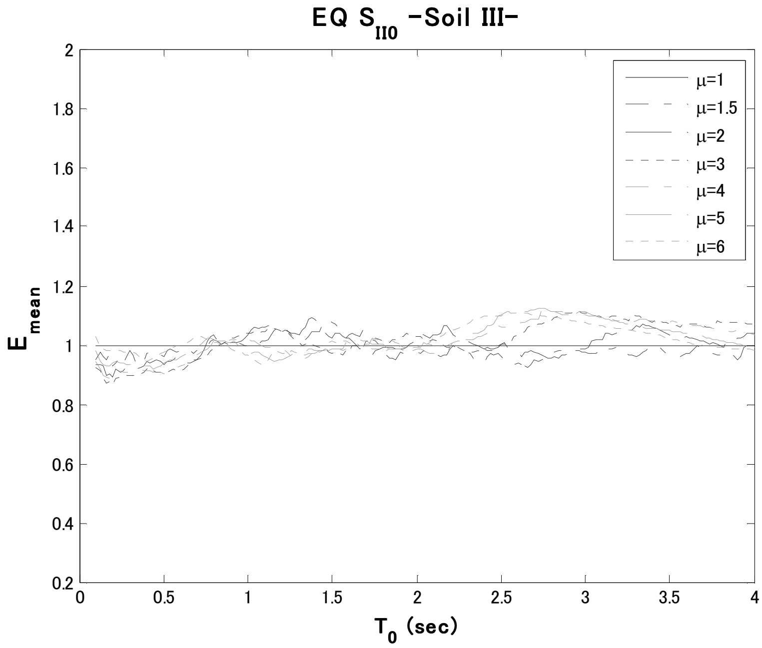

Figure 3.18. Mean approximate to exact displacement ratios -Earthquake S_{II0}- Soil III

Strictly speaking, a raw comparison of the obtained results with those obtained by other methods (Section 3.2.2) would not be accurate. Each set of equations were derived with different number of earthquakes recorded in different types of soils. Furthermore, the hysteretic pattern adopted to model the nonlinear behavior is also different in each case. Therefore, there is no way to obtain an accurate comparison unless the input earthquakes and hysteretic models used are the same in each case. However, in order to illustrate the behavior of the estimation, a comparison between the mean errors obtained with the proposed equations and those obtained with the equations by Guyader and Iwan (2006), for the artificial earthquakes, is presented. The expressions by Guyader and Iwan (2006) cover all of the ranges of periods and ductilities used in this study and are valid for a hysteretic pattern closely related to the modified Clough. The E_{mean} for earthquakes S_{I0} and S_{II0} are presented in Figures 3.19-3.20 and Figures 3.21-3.22, respectively, where the error limits (0.9 and 1.2) are also shown throughout the range of periods (0.1-4 sec). As an additional comparison, the estimations for two real earthquakes were obtained with both approaches and the errors calculated as shown in Figures 3.23 and 3.24.

The following trends were observed:

a) For the family of artificial earthquakes used in this study and for low ductilities (μ=1.5 and μ=2), the proposed equations give better estimations than those by Guyader and Iwan (2006).

b) Except the Iwan and Guyader method for S_{II0} –Soil I- (where the estimation is predominately overestimated), both methods give close estimations for periods until around 2 sec and μ>2. For larger periods, however, the Guyader and Iwan's method tend to underestimate the displacements while the proposed equations tend to overestimate the displacements.

c) For case S_{II0} –Soil I-, for T_0>1.1 sec and μ>2, the equations from Iwan and Guyader give absolute errors smaller than those obtained with the proposed method. However, the estimations from Iwan and Guyader underestimate the displacements whereas the proposed equations overestimate the displacement response.

d) In all cases, the proposed equations give a more conservative design than those obtained with the Guyader and Iwan's method. Furthermore, the estimations given by the proposed equations are between the predefined error limits.

e) For the two real records, the proposed equations give better estimations for low ductilities. For the Chi Chi earthquake, the error in the estimations show a similar behavior, however, for El Centro earthquake and dutilities greater than two, the equations from Guyader and Iwan give better estimations than the proposed equations in this study.

The previous observations suggest that the equivalent properties should be derived based on three classifications: the type of earthquake, the type of hysteretic model, and the specific soil conditions.

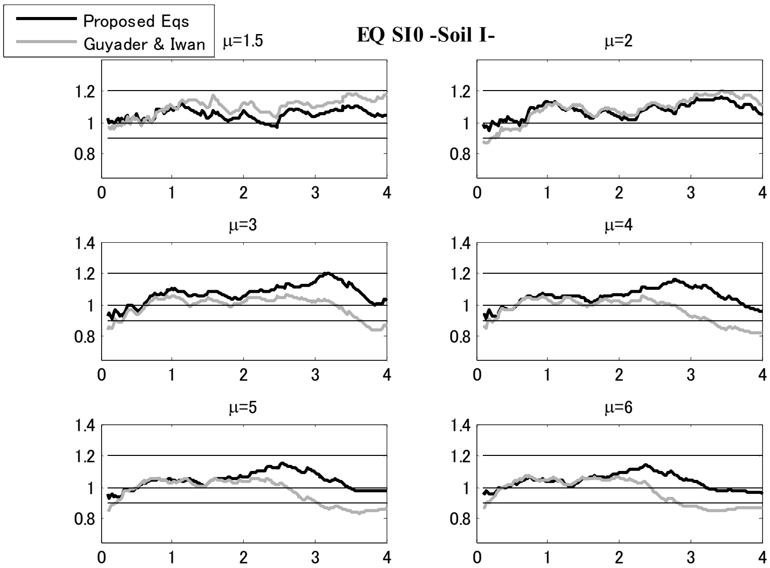

Figure 3.19. Comparison of mean errors -Earthquake S_{I0}- Soil I

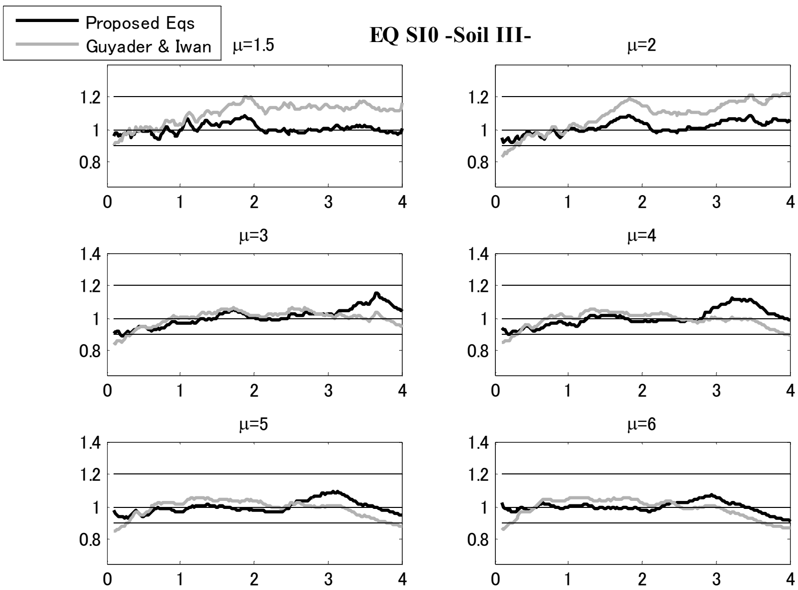

Figure 3.20. Comparison of mean errors -Earthquake S_{I0}- Soil III

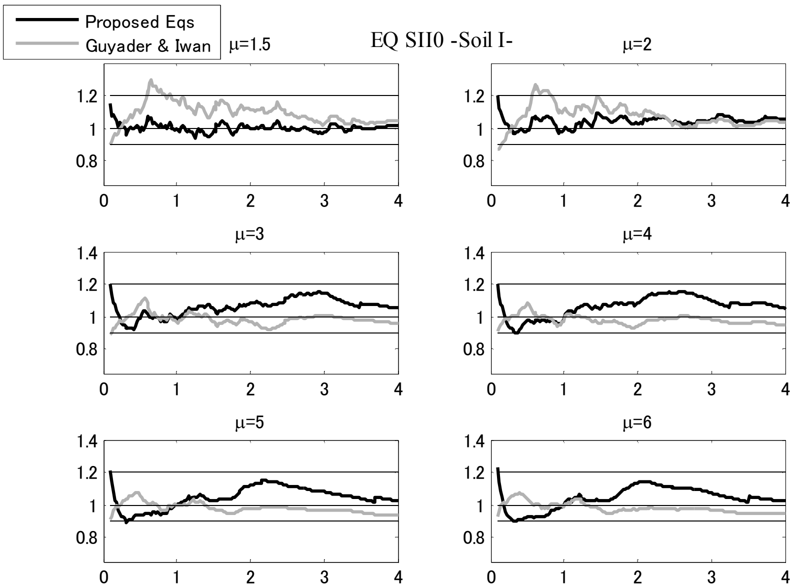

Figure 3.21. Comparison of mean errors -Earthquake S_{II0}- Soil I

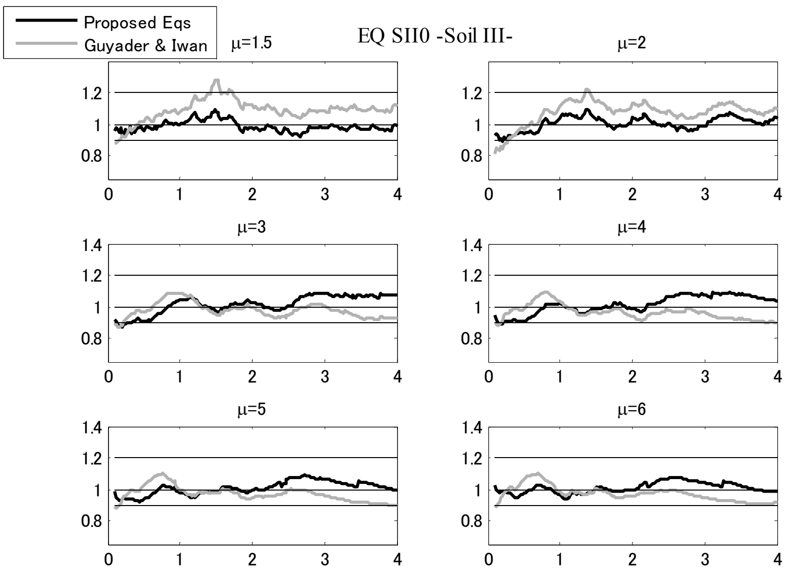

Figure 3.22. Comparison of mean errors -Earthquake S_{I0}- Soil III

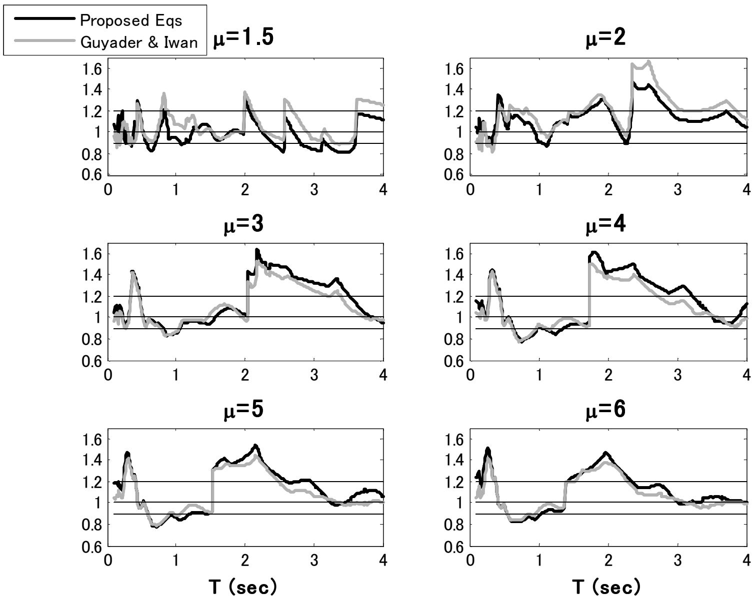

Figure 3.23. Comparison of mean errors –El Centro 1940-

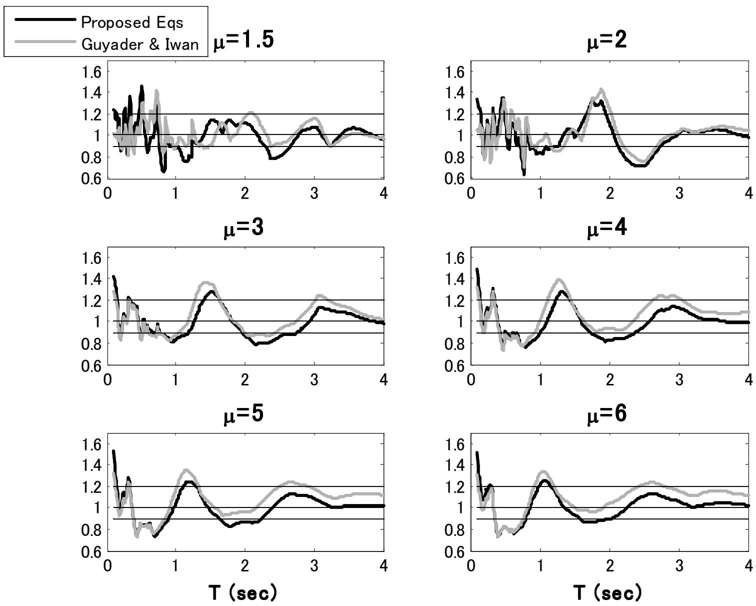

Figure 3.24. Comparison of mean errors –Chi Chi (Taiwan)-

The dispersion of the estimation is evaluated with the standard error defined as

$$\sigma_{S\varepsilon}(\xi_{eq},T_{eq})_i = \sqrt{\frac{1}{N_k-1}\sum_{k=1}^{N_k}\left(\frac{SD_e(T_{eq}(T_0,\mu),\xi_{eq})_{ik}}{SD_{nl}(T_0,\xi_0,\mu)_{ik}}-1\right)^2} \tag{3.21}$$

The results are shown in Figures 3.25. to 3.28. For soil type III (S_{I0} and S_{II0}), the standard errors are generally uniform for small and intermediate periods throughout the range of ductility ratios. For Soil I (S_{I0}), the standard errors increase with the period; the maximum standard error is located at μ=3. For Soil I (S_{II0}), the maximum standard errors are located in the interval $2 \leq T_0 \leq 3$ sec for ductility values greater than 2.

It is interesting to note that in general the standard errors tend to increase for large periods for Soil III (Figure 3.26 and Figure 3.28) whereas the maximum errors for Soil I are located at intermediate periods (Figure 3.25 and Figure 3.27). This confirms the fact that the dispersion of the results depends on the period and the type of soil (Zaharia and Taucer 2008). This behavior also suggests the influence of the earthquakes used in the derivation of the equation. In other words, since a families of artificial earthquakes were used, the influence of the design spectra used to generate the compatible artificial earthquakes is suggested. The artificial earthquakes were derived to be compatible with displacement spectra having corner period, given by Equation 2.25, defined only in terms of the magnitude, regardless the type of earthquake or soil. Possibly, displacements at large shifted periods are underestimated due the corner period is the same for all cases. For this reason, it is recommended that a displacement design spectra compatible with the acceleration spectra are used in the generation of artificial earthquakes, or preferably the use of real records is recommended. In any case, the results suggest that the displacements given by the proposed equations are better estimations than those obtained with the approach of Guyader and Iwan.

Finally, it is important to note that the presented equations were explicitly derived for typical Japanese earthquakes, for systems within a specific range of period and ductilities in firm and soft soils. Therefore, the accuracy of the results may change if a different type of earthquake or soils are used. In this case, additional verifications by comparison with other approaches presented in Section 3.2.2 are strongly recommended.

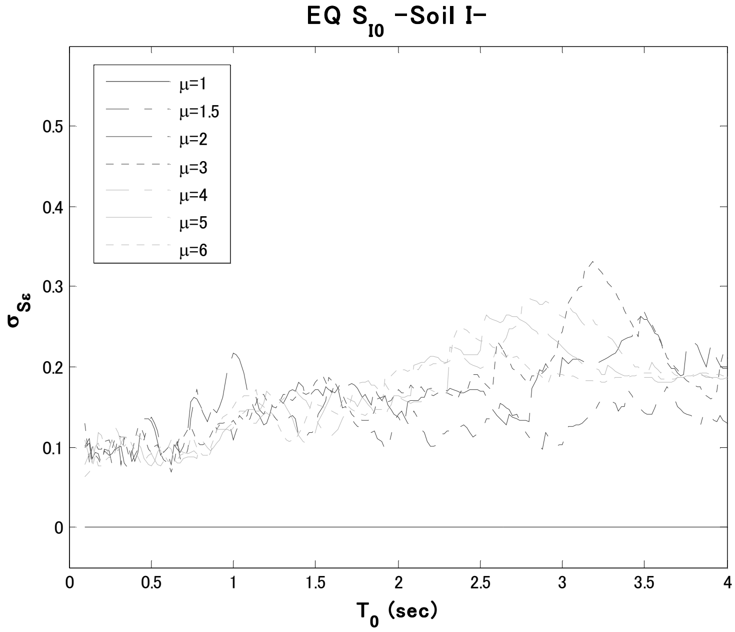

Figure 3.25. Standard errors for Earthquake S_{I0}- Soil I

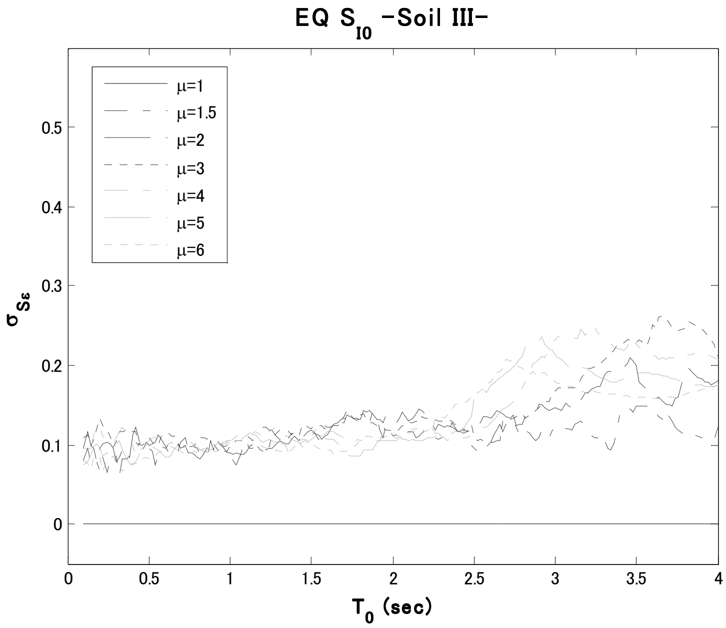

Figure 3.26. Standard errors for Earthquake S_{I0}- Soil III

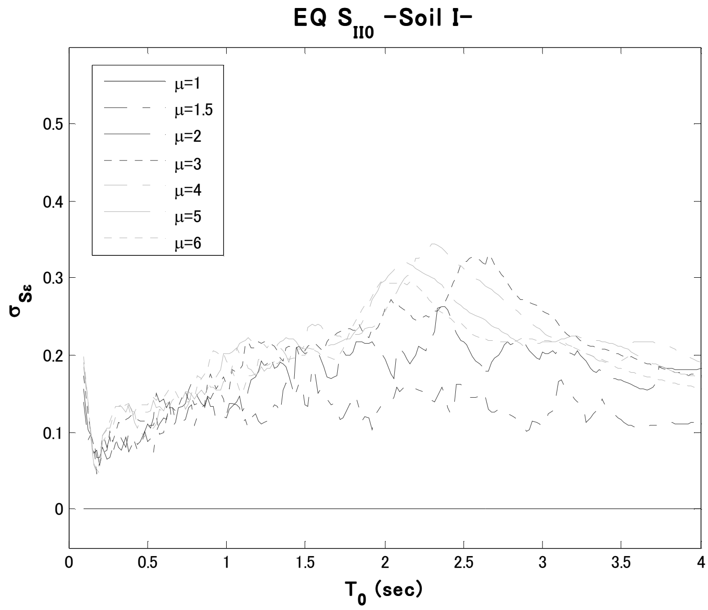

Figure 3.27. Standard errors for Earthquake S_{II0}- Soil I

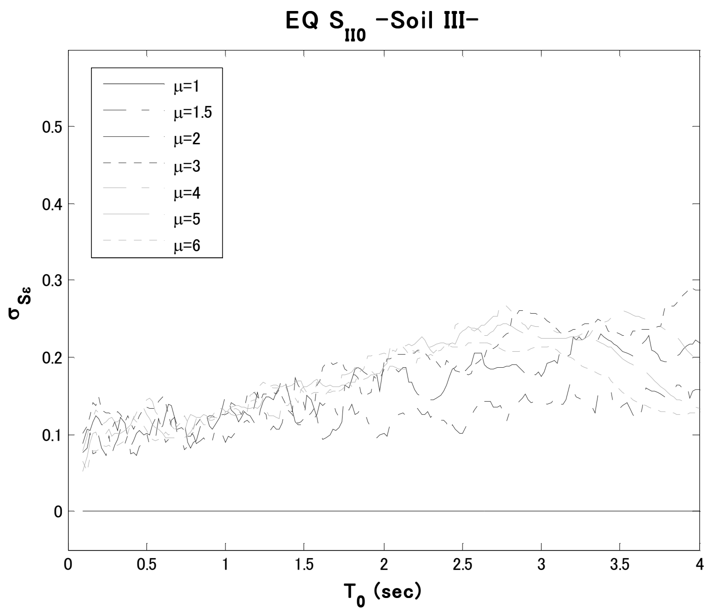

Figure 3.28. Standard errors for Earthquake S_{II0}- Soil III

3.6 SUMMARY

In seismic design and structural assessment using the displacement-based approach, real structures are simplified into equivalent single-degree-of-freedom systems with equivalent properties, namely period and damping. In this Chapter, equations for the optimal pair of equivalent properties were derived using statistical procedures on equivalent linearization and defined in terms of the ductility ratio and initial period of vibration. The modified Clough hysteretic model and 30 artificial accelerograms, compatible with the acceleration spectra for firm and soft soils, defined by the Japanese Design Specifications for Highway Bridges were used in the analysis. The results obtained with the proposed equations were verified and their limitations were discussed.

REFERENCES

Bevington P. R. and Robinson, D. K. (1992), *Data reduction and error analysis for the physical sciences*, McGraw-Hill, New York.

Bommer, J.J., Elnashai, A.S. and Weir, A.G. (2000), "Compatible acceleration and displacement spectra for seismic codes", *Proceedings of the 12th World Conference on Earthquake Engineering*, Auckland, New Zealand, February.

Blandon, C. A. and Priestley, M. J. N. (2005), "Equivalent viscous damping equations for direct displacement based design", *Journal of Earthquake Engineering* **9**(2), 257-278.

Chopra, A. K. and Goel, R. K. (1999), *Capacity-demand diagram methods for estimating seismic deformation of inelastic structures: SDOF systems*, Report PEER-1999/02, Pacific Earthquake Engineering Research Center, University of California, Berkeley, April.

Clough, R.W. and Penzien, J. (2003), *Dynamics of Structures*, Computer and Structures, Inc.

Degee, H., Bento, R. and Massena, B. (2008), "Assessment of existing formulas for equivalent damping to use in direct displacement-based design", *Proceedings of the 14th World Conference on Earthquake Engineering*, Beijing, China, October.

Dwairi, H. M., Kowalski, M. J., and Nau, J. M. (2006), "Equivalent damping in support of direct displacement-based design", *Journal of Earthquake Engineering*, **11**(4), 515-530.

Goda, K. and Atkinson, G. M. (2010), "Non-iterative equivalent linearization of inelastic SDOF systems for earthquakes in Japan and California", *Earthquake Engineering and Structural Dynamics* **39**, 1219-1238.

Gulkan, P. and Sozen, M. (1974), "Inelastic response of reinforced concrete structures to earthquakes motions", ACI Journal, **71**(12), 604–610.

Guyader, A., and Iwan, W. D. (2006), "Determining equivalent linear parameters for use in a capacity spectrum method of analysis", *Journal of Structural Engineering*, **132**(1), 59-67.

Hamada, M. (2000), "Key concepts for earthquake resistant design of civil engineering structures after the 1995 Hyogoken-nanbu earthquake", *Earthquake Resistant Design Codes in Japan*, JSCE.

Iwan, W. D. (1980), "Estimating inelastic response spectra from elastic response spectra", *Earthquake Engineering and Structural Dynamics*, **8**, 375-388.

Jacobsen, L. S. (1930) "Steady forced vibration as influenced by damping", *ASME transactions*, **5**(1), 169-181.

Jacobsen, L. S. (1960), "Damping in composite structures", *Proceedings of the 2nd World Conference on Earthquake Engineering*, Tokyo, Japan **2**, 1029-1044.

Japan Road Association (2002), Seismic design specifications for highway bridges (in Japanese).

Kowalsky, M. J., Priestley, M. J. N. and MacRae, G. (1994), *Displacement-based design. A methodology for seismic design applied to single degree of freedom reinforced concrete structures*, Report SSRP-94/16, Structural Systems Research Project, University of California, San Diego.

Kwan, W. and Billington, S. L. (2003), "Influence of hysteretic behavior on equivalent period and damping of structural systems", *Journal of Structural Engineering*, **129**(5), 576-585.

Lin, Y. Y. and Miranda, E. (2008), "Noniterative equivalent linear method for evaluation of existing structures", *Journal of Structural Engineering*, **134**(11), 1685-1695.

Miranda, E. (2000), "Inelastic displacement ratios for structures on firm sites", *Journal of Structural Engineering*, 126, 1150–1159.

Miranda, E. and Ruiz-Garcia, J. (2002), "Evaluation of approximate methods to estimate maximum inelastic displacement demands", *Earthquake Engineering and Structural Dynamics*, **31**(3), 539-560.

Newmark, N. M. and Hall, W. J. (1982), *Earthquake Spectra and Design*, Earthquake Engineering Research Institute, Berkeley, CA.

Otani, S. (1981), "Hysteresis models of reinforced concrete for earthquake response analysis", *Journal of the Faculty of Engineering*, Tokyo University (B) XXXVI(2), 407-441.

Priestley, M.J.N., Calvi, G.M. and Kowalsky, M.J. (2007), *Displacement-based seismic design of structures*, IUSS Press, Pavia, Italy.

Rosenblueth, E. and Herrera, I. (1964), "On a Kind of Hysteretic Damping", *ASCE Journal of Engineering Mechanics*, **90**(4), 37-48.

Sánchez–Flores, F. and Igarashi, A. (2010), "A new equation for equivalent period and damping of SDOF systems subjected to near source earthquakes", *Proceedings of the Annual Meeting of the JSCE*, Sapporo, Japan, September.

Zaharia, R. and Taucer, F. (2008), *Equivalent period and damping for EC8 spectral response of SDOF ring-spring hysteretic models*, JRC. Scientific and technical Reports EUR 23365 EN–2088.

CHAPTER 4

DISPLACEMENT-BASED DESIGN OF BRIDGES WITH VISCOUS DAMPERS ON BI-LINEAR ISOLATION DEVICES

4.1 GENERAL REMARKS

Through the years, extensive research has been done to enhance the seismic performance of structures with isolators and new seismic energy dissipating devices or damping systems. Currently, these devices are regulated by some of the most well-known major design codes (AASHTO 1999, BSSC 1997, BSSC 2000, JRA 2002). In parallel with research on new technologies, new design methodologies were also developed to fulfill the requirements of the performance-based seismic engineering (SEAOC, 1995). One of the most promising resulting methods is based on the displacement control, namely displacement-based design (DBD).

Conceptually, DBD uses displacement as a parameter to control structural damage. Like other design methods, DBD is an iterative process since the cross-sections of the elements are unknown. The application of displacement-based concepts for assessment or evaluation of existing structures is more straightforward since the characteristics of the structure are known. These characteristics can be used as input for the design methodology. The inelastic displacement and deformation demands can then be computed and compared with the corresponding deformation capacities.

In Chapter 1 a literature review of the proposed design methodologies based on the control of displacement was presented. The aforementioned approaches cover most of the structures currently in use. However, there is not yet a design methodology for isolated bridges with supplemental dampers.

Viscous dampers have shown to be reliable, efficient, and economical devices that protect structures subjected to large earthquakes (Infanti *et al*. 2004). Viscous dampers are usually used in new bridges or in the retrofit of existing ones located in highly seismic areas when the isolators are not able to restrict the large displacements. Due to the lack of stiffness, the viscous dampers do not significantly affect the period of vibration of the structure. A modification in the period can increase either the accelerations or displacements. The viscous damper is still a good option for highway bridges among the large amount of seismic protection devices available.

In this chapter, a new displacement-based design for bridges with seismic isolation and viscous dampers is developed and validated.

The preliminary steps of the method are based on the approach of Priestley *et al*. (2007) and Pietra *et al*. (2008). The rest of the method was developed to: a) maintain the displacement of the structural elements under allowable limits, and b) calculate the damping constant of viscous dampers to control these displacements under a predefined target value. In the proposed method, the bridge is assumed to be fully supported by bilinear hysteretic isolators (IS) with either linear or nonlinear viscous dampers (VD) in all pier-girder locations. For bridges with VDs at only some piers, the method can be applied with a straightforward modification. The target displacement is defined by the maximum displacement of the bearing isolators and the elastic pier deformation. The application of the method is presented by bridge design examples and the results verified by time history analysis.

4.2 DISPLACEMENT-BASED DESIGN

4.2.1 NUMERICAL MODEL FOR CONTINUOUS AND MULTI-SPAN SIMPLY SUPPORTED DECK BRIDGE

The proposed design procedure addresses both continuous and simply supported multi-span deck bridges. It is based on an equivalent linear SDOF model of the bridge obtained from a simplified 2DOF model of each pier-IS-VD-deck system derived as follows:

The tributary mass of the pier (m_p), located on its top, is computed as the sum of its tributary mass and the mass of the pier cap. The tributary mass of the girder-deck system (m_g) is set equal to the mass of half span on the left and half span on the right for continuous bridges. For multi-span bridges in the transverse direction, the tributary mass is similarly computed due to the displacement restrictions imposed by the joints. In the longitudinal direction, two independent IS-girder systems supported by the same pier with different tributary girder-deck masses are considered (Figure 4.1). The 2DOF system includes the equivalent damping and stiffness of the pier (denoted by ξ_p and k_p respectively), and the equivalent damping and stiffness of the isolators (denoted by ξ_b and k_b respectively) as shown in Figure 4.1. In this work, ξ_p is assumed as 5%. It is important to mention that the performance objectives in this study require the pier remain elastic under the seismic action (Section 4.2.2). However, if the pier is allowed to behave inelastically, the stiffness k_p is calculated as the secant stiffness at maximum ductility μ and the equivalent damping ξ_p is calculated with Equation 3.13b and Table 3.1 (Chapter 3).

In both the transverse and longitudinal directions, the maximum displacement of the pier-IS-VD-deck system at the peak seismic response is given by the sum of the corresponding elastic displacement of the pier ($\delta_{y,p}$) and maximum inelastic displacement of the IS ($\delta_{max,b}$). If the displacement of the ground (δ_{gr}) is considered, the total displacement of the i^{th} pier-IS-VD-deck system is given by

$$(\delta_t)_i = (\delta_{y,p} + \delta_{\max,b} + \delta_{gr})_i \tag{4.1}$$

Although the relative displacements of the piers and the isolators may change in each pier-IS-VD-deck system, their sum remains constant equal to δ_t (Figure 4.2.).

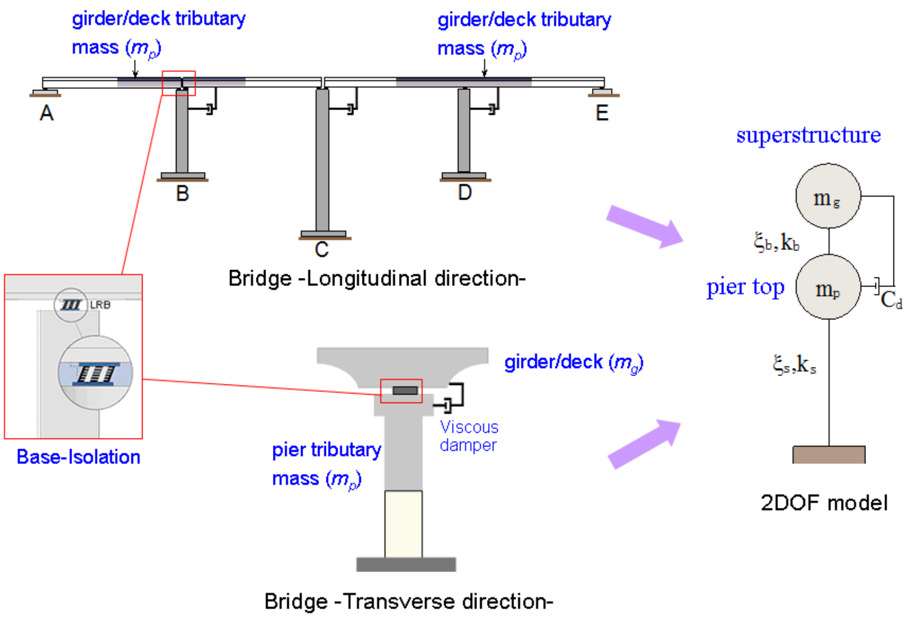

Figure 4.1. Simplified model

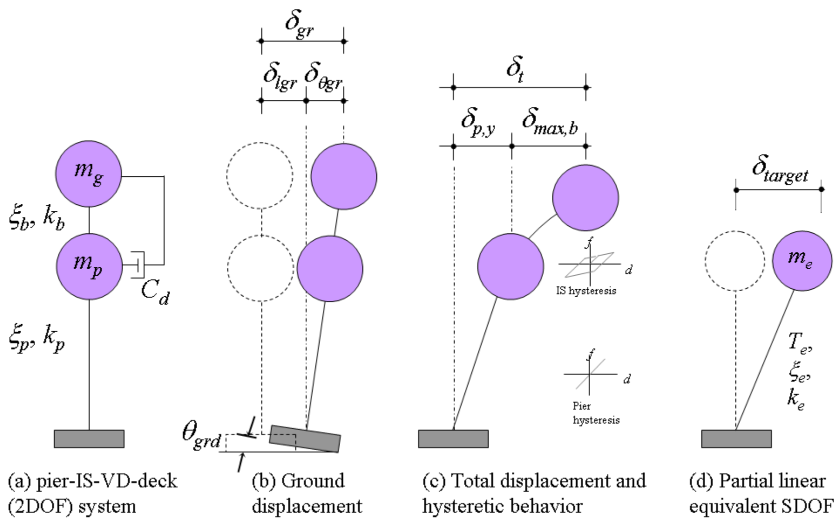

Figure 4.2. Equivalent SDOF system from 2DOF system

4.2.2 DESIGN PERFORMANCE OBJECTIVES

The design philosophy of the proposed methodology is based on the general requirement that the full serviceability of the bridge should be maintained after the design earthquake. Thus, the performance levels of immediate operation (IO) and life safety (LS) should be satisfied. For the former, the system satisfies its structural performance criteria if the piers remain elastic and the isolators develop incipient inelastic behavior. For the latter, the piers must remain elastic for new bridges or inelastically for existing bridges. In either case, the isolators must develop the expected inelastic behavior with the displacement restrictions imposed by the viscous dampers. Therefore, the performance levels can be achieved if the design satisfies the following criteria:

1. The seismic response of the superstructure (girder, deck, movement joints, etc.) and substructure (piers, abutments and foundations) must essentially remain elastic for new bridges (Cardone et al., 2009). For existing bridges, the piers may develop inelastic behavior characterized by low ductility ratio ($1.1<\mu<1.5$).
2. The isolator must be able to sustain the designated maximum design displacement. Adequate clearance satisfying the maximum design displacement should be provided in both the longitudinal and transverse directions, to allow for the movements of joints and to avoid impacts between structural elements. The design displacement of the IS in each direction is assigned based on its physical characteristics. The maximum displacements obtained are verified to keep below allowable limits.
3. The resulting maximum force and stroke of the viscous damper during the design earthquake must be lower than the maximum allowable values.

The seismic isolation in abutments and piers creates a uniform displacement in the transverse direction characterized by a rigid translation of the deck (Figure 4.3). In fact, for regular span bridges, the deformation of the deck in its horizontal plane is negligible compared to the displacements of the pier-IS systems. It is valid for bridges with viscous dampers since their low stiffness does not affect the modal shape of the girder.

The input earthquake is assumed to be uniform at the base of all piers, and the center of stiffness of the pier-IS system coincides with the center of mass of the girder. Therefore, the torsional effects and relative rotations at the joints are neglected as well as the effects of higher modes. Then, the displaced configuration of each pier-IS-VD-deck system is similar to that shown in Figure 4.4.

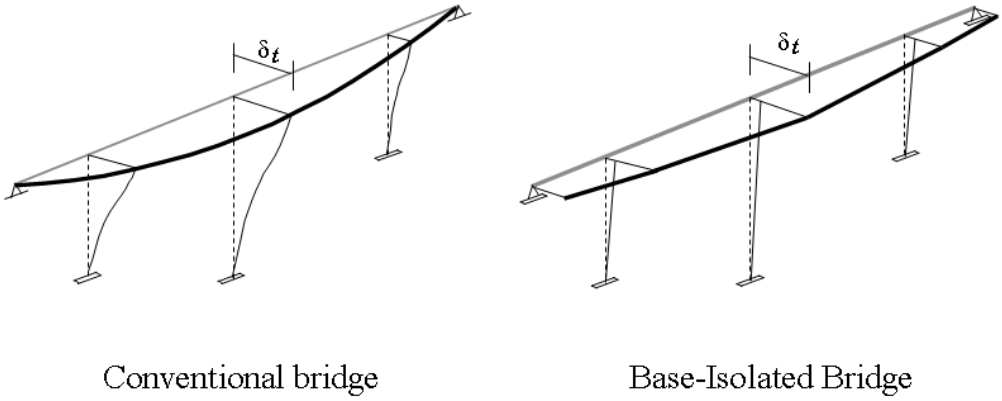

Figure 4.3. Transverse deformation of the bridge

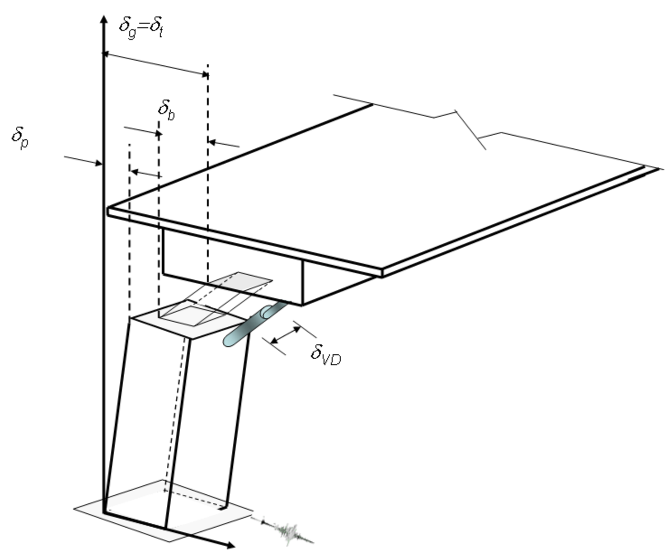

Figure 4.4. Transverse displacements of the bridge

4.2.3 DESIGN OF SINGLE ISOLATED PIERS WITH VISCOUS DAMPERS

4.2.3.1 METHODOLOGY

In order to clarify the method and the modeling considerations presented in section 4.2.1, the design will first be derived for a single pier of the bridge. The proposed methodology consists of the following steps:

i. Selection of the preliminary pier cross section

The geometry of the bridge is limited by either physical restrictions or architectural design. With this information the cross section of the columns is proposed by gravitational analysis, which considers *P-Δ* effects so that the second order effects can be neglected during the design process. The yielding displacement of the piers ($\delta_{y,p}$) can be calculated with the equations from Priestley (2007).

With the obtained cross section, the stiffness of the pier, k_p, and the period of the structure without isolation, T_0, are calculated. To illustrate the advantages of the supplemental damping and the proposed design methodology, the equivalent period of the isolated bridge with viscous dampers T_{0eq} will be set to approximately

$$T_{eq} = \psi T_0 \tag{4.2}$$

where ψ is a constant typically set to 2 as suggested in the Japan Road Association (2002).

ii. Selection of the isolator bearings

The dimensions of the IS bearings can be estimated from preliminary gravitational and seismic static analysis. The damping coefficient is obtained from Equation 2.3, and the total secant stiffness of the j bearings on each pier is given by $k_b=\Sigma k_{b,j}$. It is important to note that the inclusion of the secant stiffness in the 2DOF model validates the use of Equations 2.12 and 2.21 presented in Chapter 2. However, the linear static analysis may not realistically represent the final displacements of bearings. For this reason, it is strongly recommended that 2DOF model considers the nonlinear behavior of the bearings to accelerate the convergence in the solution and at the same time, to obtain more realistic results.

iii. Calculation of the period of the 2DOF system

The period T_e of the pier can be obtained either by modal analysis of the 2DOF system or by using the following well-known expression:

$$T_e = 2\pi\sqrt{\frac{m_e}{k_e}} \tag{4.3}$$

where m_e is the first-mode participating mass of the pier-IS-VD-deck system, and k_e is the equivalent stiffness obtained by the modal stiffness matrix of the 2DOF system or by summing, in parallel, the individual stiffness of the contributing components (k_p and k_b) as

$$k_e = \frac{k_b k_p}{k_b + k_p} \tag{4.4}$$

The periods T_e and T_{eq} are compared, if they differ more than a predefined tolerance ε (in this study equal to 0.01) the selection of the isolators is reviewed until the convergence is achieved.

iv. Target displacement of the pier-IS-deck system

For new bridges, the target displacement is typically given by Equation 4.1 modified by safety factors (not considered in this work for simplification). However, in practical situations (especially for retrofitting of existing bridges or special new ones), the target displacement may be smaller due the restrictions imposed by code updates, new structures built in the neighborhood, or damage in weak structural elements. For this reason, the proposed method is developed for cases where the resulting displacement is larger than that given by Equation 4.1, this condition would assure additional dampers are required. If this condition is not satisfied, the bridge can be either designed with conventional procedures for base-isolated bridges (Jara and Casas 2006, Cardone et al. 2008, Pietra et al. 2008) or the size of the bridge components should be modified (reduced) to justify the supplemental damping.

v. Equivalent damping of the pier-IS system

Since the isolators and the piers form a system connected in series, the algebraic summation of their damping coefficients cannot be assumed. The damping ratio of the pier-IS system can be calculated by the proportional energy damping method as (Roesset *et al.* 1973)

$$(\xi_{eq})_i = \frac{\sum_j^n (\varphi_i^T)_j C_j (\varphi_i)_j}{2\varphi_i^T K_T \varphi_i} \tag{4.5}$$

where $(\xi_{eq})_i$ is the equivalent damping ratio of mode i , $(\varphi_i)_j$ is the mode shape vector of subsystem j corresponding to mode of vibration i , $\boldsymbol{C_j}$ is the damping matrix of the subsystem j, φ_i is the mode shape vector of the overall system of the mode of vibration i, and $\boldsymbol{K_T}$ is the stiffness matrix of the overall system. In this study, the piers and abutments are assumed to be fixed at the base, and the superstructure is assumed to be rigid enough so the displacements are uniform in each span. Therefore, the mode shape vectors for the pier-IS system are given by

$$\varphi_i = \begin{Bmatrix} 1 + \dfrac{(k_b)_j}{(k_p)_j} \\ \dfrac{(k_b)_j}{(k_p)_j} \end{Bmatrix} x_j \tag{4.6}$$

$$\varphi_i = \begin{Bmatrix} 1 \\ \dfrac{(k_b)_j}{(k_p)_j} \end{Bmatrix} x_j \tag{4.7}$$

where x_j is the lateral displacement degree of freedom of the subsystem j. For nonlinear piers, the equivalent stiffness (at the maximum ductility) of the piers should be considered. The stiffness matrix of the 2DOF system is

$$K_T = \begin{bmatrix} (k_b)_j + (k_p)_j & -(k_b)_j \\ -(k_b)_j & (k_b)_j \end{bmatrix}_j \tag{4.8}$$

The damping matrix $\boldsymbol{C_j}$ is given by

$$C_j = C_o + C_b \tag{4.9}$$

where $\boldsymbol{C_o}$ is the proportional damping matrix of the system without IS and $\boldsymbol{C_b}$ the non-proportional damping matrix due to the hysteretic damping provided by the IS. Since the matrix $\boldsymbol{Cj}$ is non-proportional, the product of the numerator in the Equation 4.5 gives a non-diagonal matrix. As a consequence, uncoupling the equations of motion is not possible. However, the influence of the off-diagonal terms on the response can be neglected if the hysteretic damping is less than 30% (Roesset *et al.* 1973). Then, Equation 4.9 is simplified by

$$C_j = \begin{bmatrix} (2\xi_p k_p)_j & 0 \\ 0 & (2\xi_b k_b)_j \end{bmatrix} \tag{4.10}$$

By substituting Eqs. (4.6) - (4.8) and (4.10) into Eq. (4.5), the damping provided by each pier-IS system is obtained as

$$\xi_{IS} = \frac{\left(\xi_b + \xi_p \dfrac{k_b}{k_p}\right)}{\left(1 + \dfrac{k_b}{k_p}\right)} \tag{4.11}$$

where the terms involved were defined in Section 4.2.1. For inelastic piers, the equivalent stiffness and damping have to be calculated with Equations 3.13.

The flexibility and the energy dissipation of the foundation can be taken into account in the previous equation as

$$\xi_{IS} = \frac{\left(\xi_b + \xi_p \dfrac{k_b}{k_p} + \xi_{fh} \dfrac{k_b}{k_{fh}} + \xi_{f\theta} \dfrac{k_b L^2}{k_{f\theta}}\right)}{\left(1 + \dfrac{k_b}{k_p} + \dfrac{k_b L^2}{k_{fh}}\right)} \tag{4.12}$$

where ξ_{fh} is the horizontal equivalent damping of the foundation, $\xi_{f\theta}$ is the rotational damping, k_{fh} and $k_{f\theta}$ are the horizontal and rotational stiffness of the foundation, respectively, and L is the height of the pier.

Due to the objectives of this research, hereafter the effects of the foundation and the ground shall not be considered.

For illustration purposes the variation of Equation 4.11 is plotted in Figure 4.5 for values of ξ_b up to 60%. It can be observed that a suitable combination of the ratio k_b/k_p and ξ_b should be chosen if the viscous dampers will be the main source of damping. In the present study, values of $k_b/k_p \leq 1$ and $\xi_b \leq 15\%$ are adopted so the equivalent damping of the pier-IS system without dampers (ξ_{IS}) will be approximately 25% of the maximum damping of the system (ξ_{max}).

vi. Equivalent damping of the pier-IS-VD system

Since T_{eq} is known, the equivalent damping ξ_{eq} that satisfies the specified target displacement is calculated from the displacement spectra. First, it is verified that $T_{eq\ min} < T_{eq} \leq T_{eq\ max}$, where the periods $T_{eq\ min}$ and $T_{eq\ max}$ are given by the values which satisfy $\delta_T = S_D(T_{eq\ min}, \xi = \xi_{IS})$ and $\delta_T = S_D(T_{eq\ max}, \xi = \xi_{max})$. Secondly, the equivalent damping of the system, ξ_{eq}, is obtained from the spectra as the value which satisfies $\delta_T = S_D(T_{eq}, \xi_{eq})$ as show in Figure 4.6. At this point, the equivalent damping is still unknown, then, it is calculated with the iterative approximation shown in Figure 4.7.

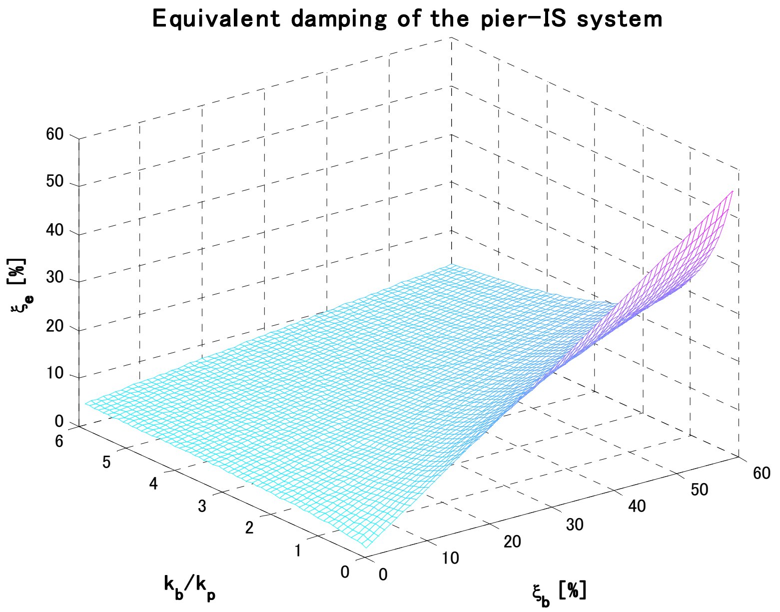

Figure 4.5. Equivalent damping of the pier with isolators

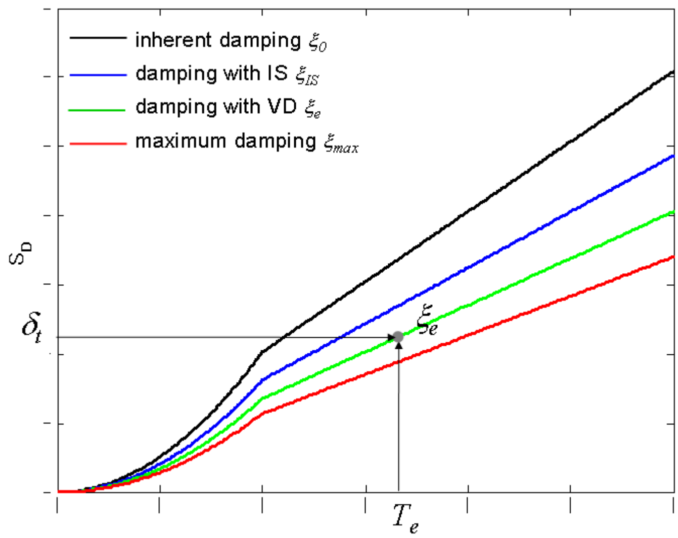

Figure 4.6. Equivalent damping

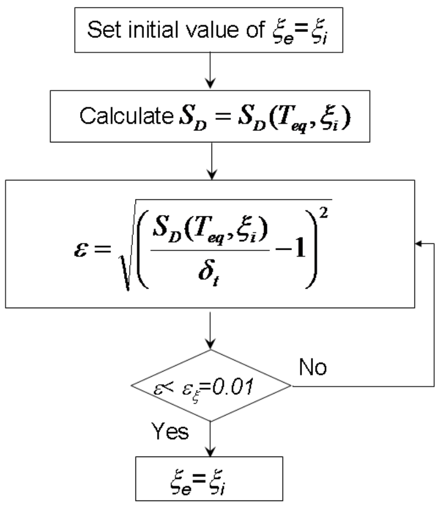

Figure 4.7. Calculation of the equivalent damping

vii. Coefficient of viscous dampers

Once the damping ξ_{eq} is obtained, the parameter C_d of the viscous dampers can be calculated for linear or nonlinear dampers with Equations 2.12 and 2.21, respectively. For the latter, a suitable value of the exponent α should be chosen considering the behavior shown in Figure 2.7. (Chapter 2).

viii. Verification of the displacements

The resulting maximum displacements are verified and must satisfy the following restrictions: $\delta_g \leq \delta_t$, $\delta_p \leq \delta_{y,p}$, and $\delta_b \leq \delta_{max,b}$. If the past relationships are not satisfied, the damping required by the VD can be approximated once more with the displacement ratio δ_g / δ_t.

ix. Capacity design of the structural elements

In this step the piers and foundations are designed by capacity with the following forces:

$$(V_{dg})_i = (k_e \delta_g)_i \tag{4.13}$$

$$(M_{dg})_i = (aV_{dg}H)_i \tag{4.14}$$

where V_{dg} and M_{dg} are the design shear and moment, respectively, and a is a factor defined in terms of the pier ductility demand (Pietra *et al*., 2008).

Additionally, the mechanical characteristics of the IS and VD are fully specified based on the obtained parameters (C_d, ξ_e) and those assumed at the beginning of the analysis (k_b,μ_b).

The procedure is summarized by the diagram in Figure 4.8. (the input are the results of the DBD methodology).

It is important to mention that although the method can be applied at two independent directions (transverse and longitudinal); it cannot be applied in both directions simultaneously except for special cases.

4.2.3.2 ACCURACY OF THE DISPLACEMENT ESTIMATION

The accuracy of the method is evaluated by the mean error between the target displacements and the displacements obtained with the nonlinear time history analysis for the design earthquake, k, as

$$E_{mean} = \frac{1}{k}\sum_{k=1}^{N}\frac{(\xi_{THA})_k}{(\xi_t)_k} \tag{4.15}$$

where k is the number of earthquakes.

If E_{mean}=1, there is a good estimation of the target displacement, if E_{mean}>1 the resulting displacements exceed the target values, and if E_{mean}<1 the target displacement is not exceeded.

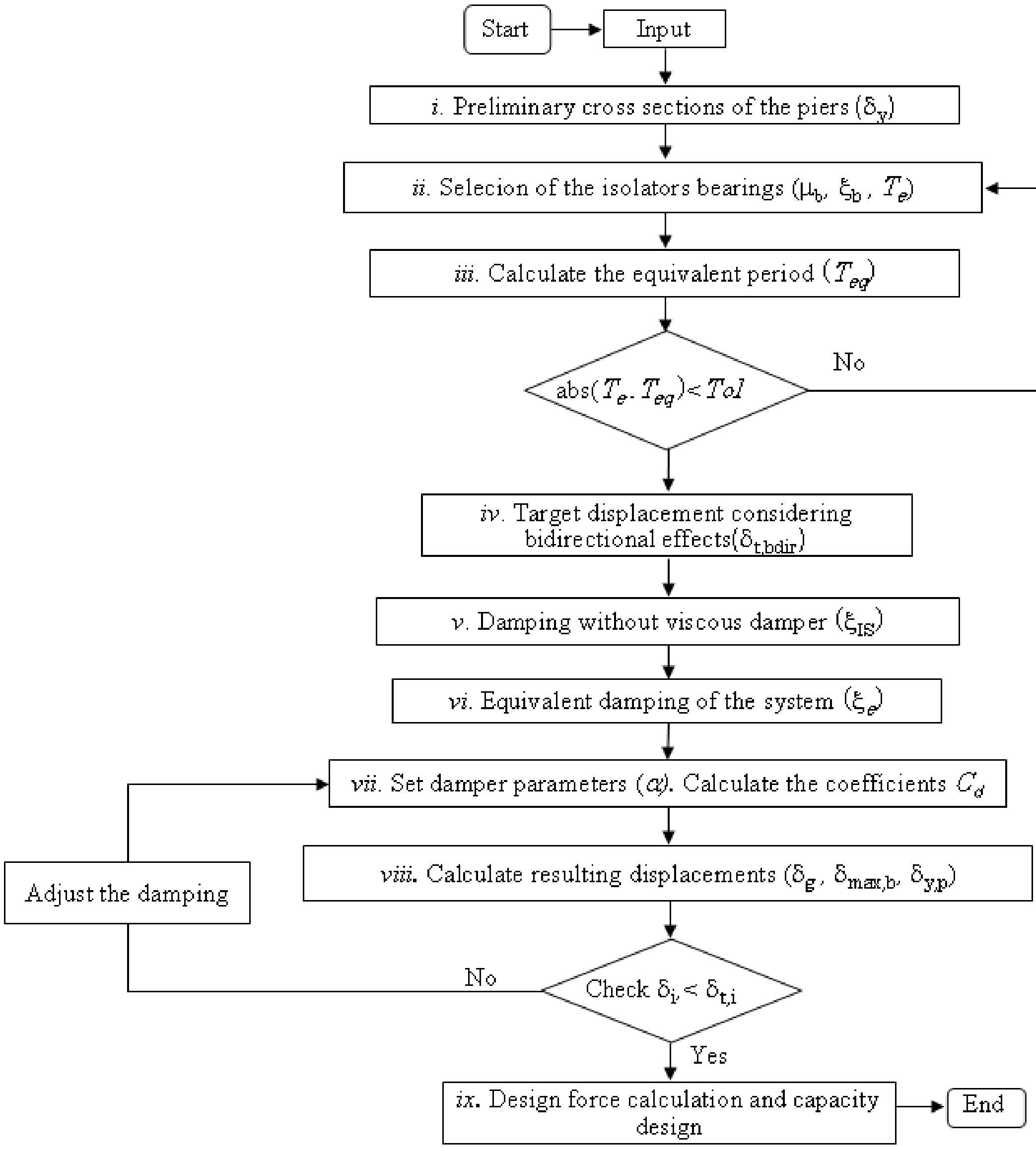

Figure 4.8. Proposed displacement-based design methodology

4.2.3.3 EXAMPLE NO. 1

The bridge considered in the example is more or less similar to that considered in previous studies (Priestley et al. 1996, Cardone et al. 2008). The geometry is kept the same as the original example by Priestley, although some modifications are done on the size of the elements to illustrate the proposed methodology. The bridge consists of four 50 m spans, a deck with a box cross section of 5.25 m^2, a moment of inertia for bending around the vertical axis of 74 m^4 and a weight per unit of length of 200 kN/m. The piers are characterized by rectangular hollow cross sections with the sizes shown in Figure 4.9. All the piers have a cap of 500kN weight. Unlike the example from Priestley et al. (1996), the bridge in this study is assumed to be entirely made of concrete with compressive strength equal to 30 MPa. The period of the bridge without IS and VD is calculated as T_0=0.70. The equivalent period is set to $T_e \approx 2T_0 \approx 1.41$. For simplicity the ground displacements were neglected. The finite element model used in the verification of the design algorithm is shown in Figure 4.10.

To illustrate the method, the design forces and the VD's coefficients for the pier located at section No. 4 will be calculated. The general design is described as follows (with reference to Table 4.1.).

The preliminary stiffness and damping of the pier and bearing isolators are calculated to match T_{eq}=1.41 sec. Then, the maximum displacements of the girder and isolator are calculated as 0.389 m and 0.352 m, respectively, with a pier-IS damping obtained from Equation 4.11. The target displacement of the girder and the bearing are set as 0.30 and 0.25 m, respectively as typical allowable displacement values. In order to limit the displacements, additional dampers are required.

From the displacement spectra in Figure 4.11., the total amount of damping (ξ_e) required to achieve the target displacement of the girder at the selected period is obtained. Then, the coefficient of the dampers is calculated for linear and nonlinear dampers (α=0.3). The resulting damper coefficients are C_d=3664 kN·s/m and C_{dNL}=2515 kN·s/m for linear and nonlinear dampers, respectively as indicated in Table 4.1.

Finally, the displacements are verified. The resulting displacements of the pier without dampers and the pier with linear and nonlinear VD are shown in Figure 4.11. Table 4.1 shows the averaged values of the results obtained by analysis with 30 compatible spectra earthquakes.

In this example, the damper's coefficients that limit the displacements of the structural elements below both, the allowable and target displacements are efficiently obtained (Figure 4.12). The error E_{mean} shows the method gives conservative but accurate predictions (Figure 4.13). The design forces in the pier can then be calculated with Equations 4.13 and 4.14.

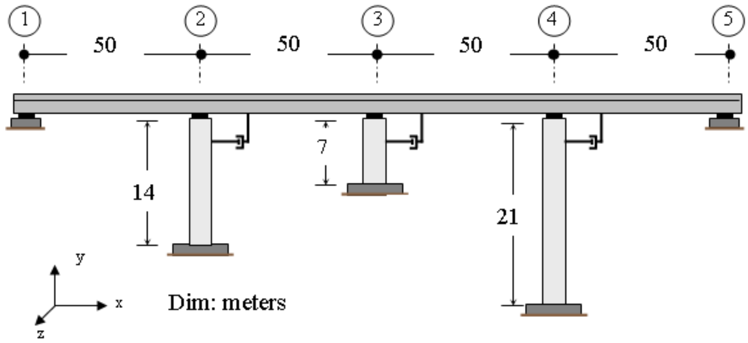

Priestley et al. (1996)

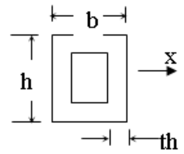

Pier section			
Section	b (m)	h (m)	th (m)
2	2	3	0.4
3	2	2	0.4
4	4	4	0.4

Girder-deck		
Area (m^4)	Ix (m^2)	Wg (kN/m)
5.25	74	200

General			
Materials	Soil	EQ	Period (sec)
fc=30 MPa fy=414 Mpa	III	S_{I0}	T_0=0.70 T_e≈2T_0≈1.41

Figure 4.9. Bridge of Example No.1

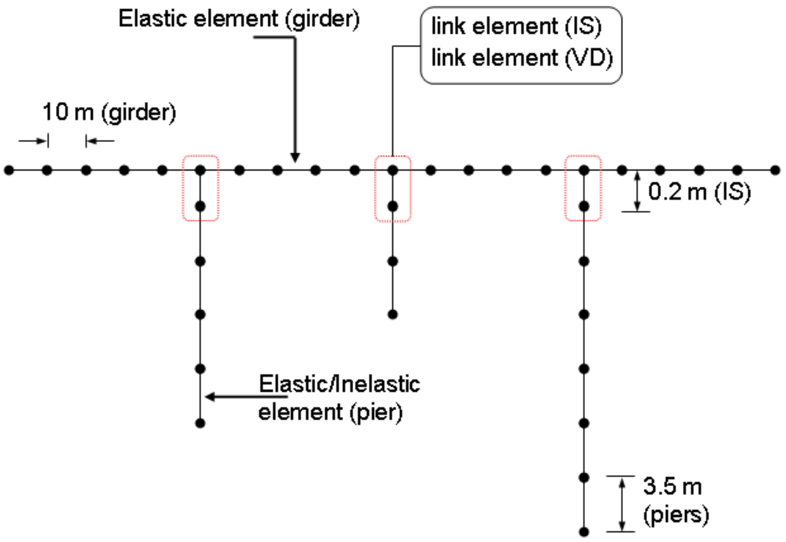

Figure 4.10. Finite element model for the Bridge of Example No.1

Element	k_e (kN/m)	Damping	δ_a (m)	δ_Y (m)	δ_{THA} (m) NL	E_{mean} NL	δ_{THA} (m) LIN	E_{mean} LIN
Pier	292970	ξ_p =5%	0.037	$\delta_{y,p}$ =0.10	0.049	0.49	0.052	0.52
Girder	--	ξ_g =5%	0.389	δ_g =0.30	0.291	0.97	0.289	0.96
IS	25154	ξ_b =14%	0.352	$\delta_{i,b}$ =0.25	0.242	0.97	0.237	0.95
VD linear	--	Cd=3664 kN*s/m	--	Stroke max=0.25	--	--	0.237	0.95
VD nonlinear (α=0.3)	--	Cd_{nl}=2515 kN*s/m	--	Stroke max=0.25	0.242	0.97	--	--

Table 4.1. Pier design - Example 1-

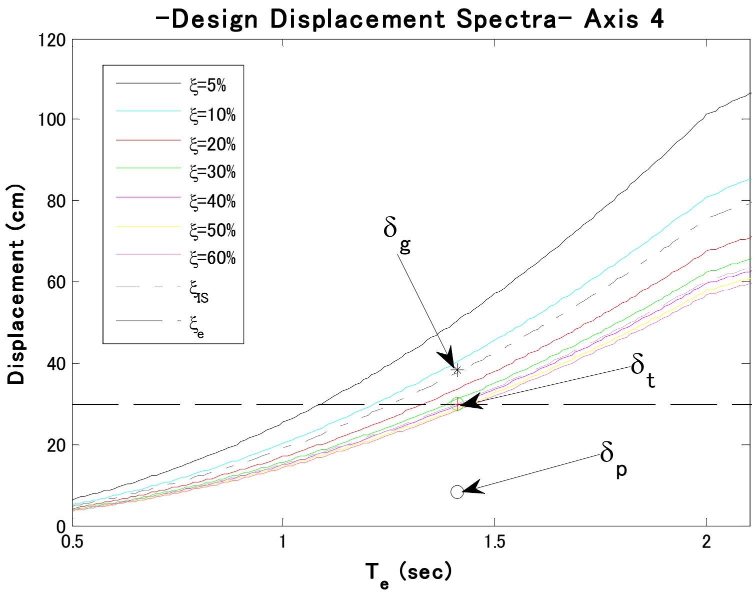

Figure 4.11. Displacement spectra

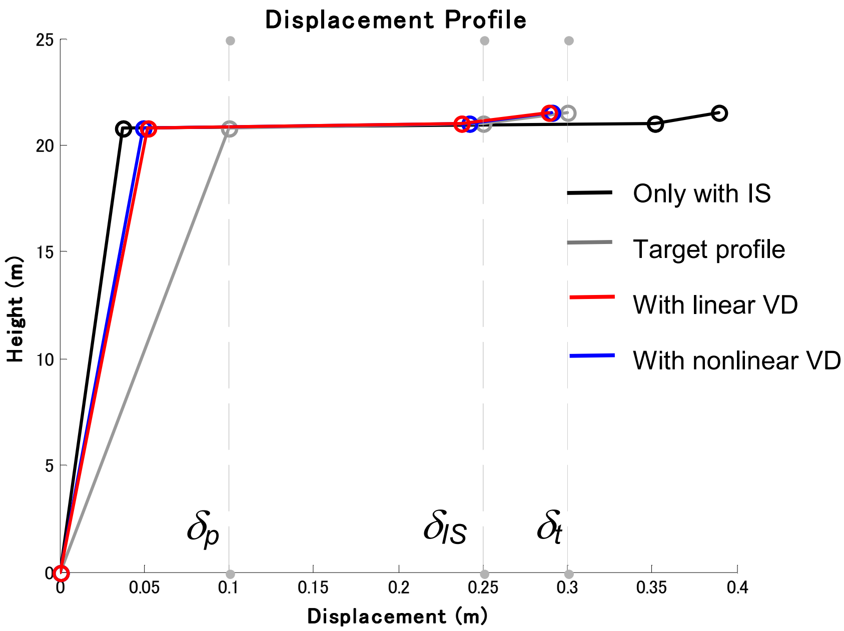

Figure 4.12. Maximum displacement profile –Single pier Section 4-

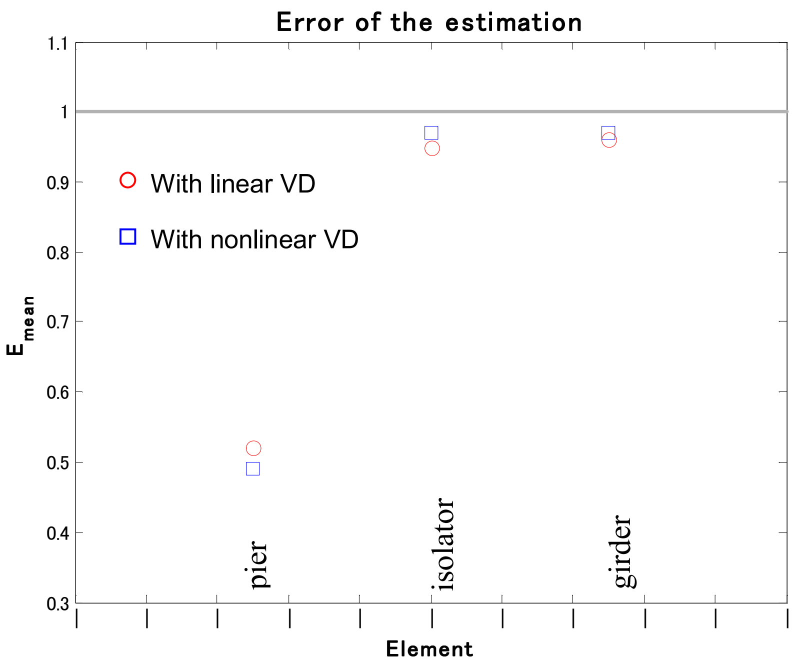

Figure 4.13. Error of the estimation –Single pier Section 4-

4.2.4. DESIGN OF ISOLATED BRIDGES WITH VISCOUS DAMPERS

4.2.4.1 METHODOLOGY

The displacement-based design methodology (Figure 4.8) for single piers is still valid for uniformly straight bridges. However, there are some basic differences: the target displacement and damping of the system, the inclusion of the abutment effects and the distribution of the equivalent damping into each pier. In general, the equivalent SDOF for the whole bridge can be derived from the 2DOF system at each pier location (Figure 4.14) with the method presented in Section 4.2.3.1.

The methodology consists of the following steps:

i. *Selection of the preliminary pier cross section and*

ii. *Selection of the isolator bearings*

Similar to the steps described in section 4.2.3.

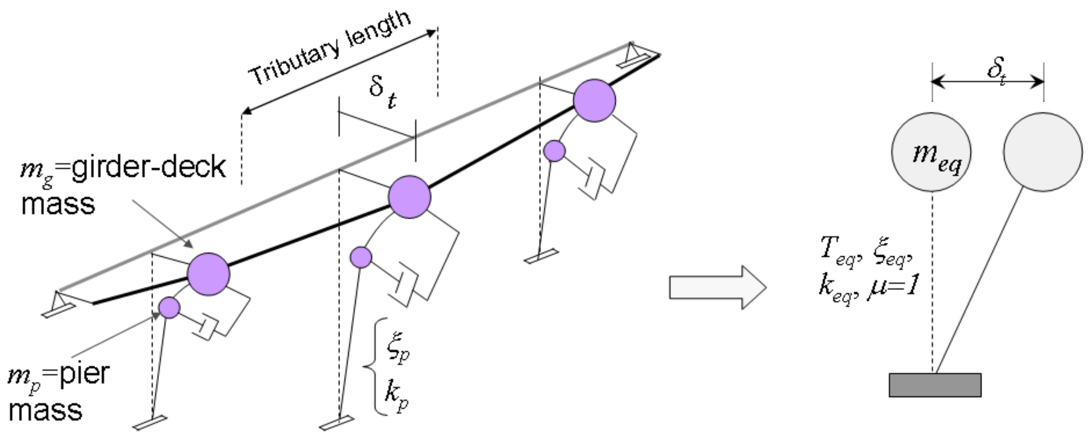

Figure 4.14. SDOF system for the whole bridge

iii. Calculation of the period of the 2DOF systems

The equivalent period of the bridge is given the following equation:

$$T_{eq} = 2\pi\sqrt{\frac{M_{eq}}{K_{eq}}} \tag{4.16}$$

where M_{eq} is the sum of each mass m_i, calculated in Section 4.2.3, and the corresponding mass of the abutments m_{ab}; the equivalent stiffness K_{eq} is given by summing each stiffness k_e and the abutment stiffness k_{ab} as

$$K_{eq} = \sum_i^n (k_e)_i + \sum k_{ab} \tag{4.17}$$

The stiffness of the isolators in the abutments can be calculated either by the procedure due to Priestley (1997) or by matching the value of the equivalent period in regular bridges.

iv. Target displacement of the bridge

The target displacement of the whole bridge (δ_T) is given by the following equation

$$\delta_T = \frac{\sum_{i=1}^{n} m_i \delta_{t,i}^2}{\sum_{i=1}^{n} m_i \delta_{t,i}} \tag{4.18}$$

where m_i is the contributing effective mass for the first mode, the subscript i represents the i^{th} span, and δ_t represents the design target displacement of each pier-IS-VD-deck system calculated with Equation 4.1.

If the displacement of the girder is uniform along the span, the previous equation (Priestley et al., 2007) is reduced to

$$\delta_T = \frac{\sum_{i=1}^{n} (m\delta_t^2)_i}{\sum_{i=1}^{n} (m\delta_t)_i} = \delta_t \tag{4.19}$$

v. Equivalent damping of the pier-IS systems

For the entire bridge, the term ξ_{IS} is the damping of the isolated structure calculated with the following equation (Pietra et al. 2008)

$$\xi_{IS} = \frac{\sum_{i}^{n} (\chi\delta\xi_e)_i + \xi_{deck}\chi_{ab}(\delta_T - \bar{\delta}_{ab})}{\sum_{i}^{n} (\chi\delta)_i + \chi_{ab}(\delta_T - \bar{\delta}_{ab})} \tag{4.20}$$

where χ is the fraction of the total base shear that is carried by each isolator in the pier-IS-VD-deck system, χ_{ab} is the sum of the fraction of shear carried at the two abutments, δ_{ab} is the mean of the displacements from the abutments, and δ_{deck} is the inherent damping of the deck assumed between 3%-5%.

vi. Equivalent damping of the pier-IS-VD systems

Similar step to that described in Section 3 4.2.3.

vii. Coefficient of viscous dampers

Once the equivalent damping of the systems is obtained, it has to be distributed on each pier-IS-VD-deck system. For irregular bridges, the distribution can be done by calculating the exact contribution of each system by the modal strain energy approach in conjunction with a finite element model. For regular bridges, the damping can be distributed, like bridges without damping, according to the tributary mass or to the strength of the isolators (χ) in each pier-IS-deck system as (Pietra et al. 2008):

$$\xi_{eq} = \sum_{i}^{n} \chi \delta_{t,i} \xi_{e,i} / \sum_{i}^{n} \chi \delta_{t,i} \tag{4.21}$$

For regular bridges with equal mass distribution at each pier and uniform displacement, Equation 3.14 is simplified to

$$\xi_{eq} = \delta_{t,i} \tag{4.22}$$

The coefficients for the viscous dampers are then calculated with the damping $\xi_{e,i}$.

viii. *Verification of the target displacement and*

ix. *Capacity design of the structural element.*

Similar to the steps mentioned in Section 4.2.3.

4.2.4.2 EXAMPLE NO. 2

The bridge described in section 4.2.3 will be designed with the proposed methodology in the transverse direction. The target displacement of the girder and isolators are 0.30 and 0.25 m, respectively. This implies the displacements in each pier location should not exceed these values. Due to the mass regularity, the contributing damping at each pier location is equal to the damping system (Equation 4.22) and no iterations for damping distribution are required. The period calculated with the proposed design and with the model used in the nonlinear time history analysis (THA) are T_{eq}=1.408 sec and T_{THA}=1.411 sec, respectively.

The initial data and the results are shown in Table 4.2. For all cases, it can be observed from the E_{mean} column that the obtained displacements are smaller than the allowable limits. This is illustratively confirmed in the results presented in Figures 4.15 to 4.20. In these Figures, the displaced configuration of the piers and the corresponding error obtained for linear and nonlinear dampers are shown. It is important to mention that in the current version of the design method the optimum size of the pier cannot be obtained. However, if some iterations are done the displaced configuration can be approximated as close as the target displacement as shown in Figures 4.17 and 4.18.

It is interesting to note that the displacements obtained for the elements at Section 4, are smaller than those obtained in the Example 1 for the same section. This reduction in the displacements suggests the interaction with the abutment and the deformation of the pier may influence the overall displacement response.

Although the design forces are not shown, they can be straightforwardly calculated with Equations 4.13 and 4.14. About the hysteretic behavior of isolators and dampers, Figures 4.21 and 4.26 show the hysteresis loops for these devices. In general, the more conservative results are obtained with linear viscous dampers.

Section	Element	k_e (kN/m)	Damping	δ_{IS} (m)	δ_T (m)	δ_{THA} (m) NL	E_{mean} NL	δ_{THA} (m) LIN	E_{mean} LIN
1	IS	10250	ξ_b =16%	--	δ_{Lb} =0.250	0.25	1.0	0.240	0.96
2	Pier	111738	ξ_p =5%	0.039	$\delta_{y,p}$ =0.07	0.051	0.73	0.051	0.73
	Girder	--	ξ_g =5%	0.398	δ_t =0.30	0.281	0.94	0.279	0.93
	IS	25154	ξ_b =14%	0.359	δ_{Lb} =0.25	0.230	0.92	0.228	0.91
	VD linear	--	Cd=3316 kN*s/m	--	Stroke max=0.25	--	--	0.228	0.91
	VD nonlinear	--	Cd_{nl}=2281 kN*s/m	--	Stroke max=0.25	0.230	0.92	--	--
3	Pier	277981	ξ_p =5%	0.014	$\delta_{y,p}$ =0.04	0.04	1.00	0.038	0.95
	Girder	--	ξ_g =5%	0.355	δ_t =0.30	0.29	0.97	0.288	0.96
	IS	21935	ξ_b =14%	0.341	δ_{Lb} =0.25	0.25	1.00	0.250	1.0
	VD linear	--	Cd=2520 kN*s/m	--	Stroke max=0.25	--	--	0.250	1.0
	VD nonlinear	--	Cd_{nl}=1724 kN*s/m	--	Stroke max=0.25	0.25	1.00	--	--
4	Pier	277981	ξ_p =5%	0.037	$\delta_{y,p}$ =0.10	0.051	0.51	0.053	0.53
	Girder	--	ξ_g =5%	0.380	δ_t =0.30	0.283	0.94	0.272	0.91
	IS	21935	ξ_b =14%	0.343	δ_{Lb} =0.25	0.232	0.93	0.219	0.88
	VD linear	--	Cd=3664 kN*s/m	--	Stroke max=0.25	--	--	0.219	0.88
	VD nonlinear	--	Cd_{nl}=2515 kN*s/m	--	Stroke max=0.25	0.232	0.93	--	--
5	IS	10250	ξ_b =16%	--	δ_{Lb} =0.250	0.251	1.00	0.231	0.92

Table 4.2. Bridge design Example No. 2

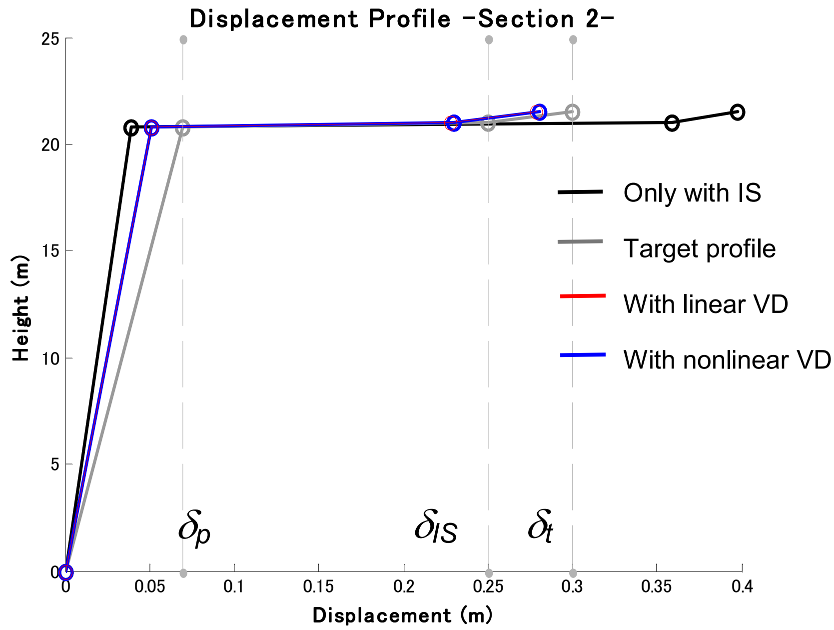

Figure 4.15. Maximum displacement profile –integrated pier section 2-

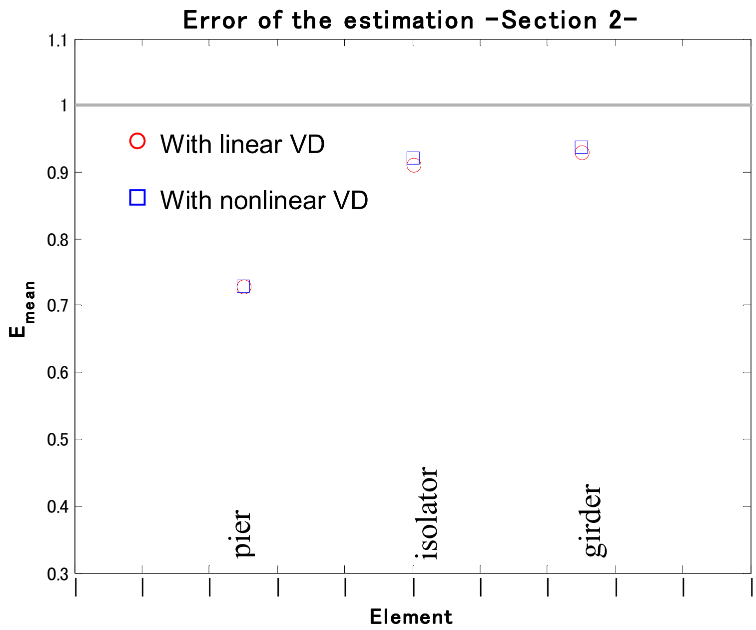

Figure 4.16. Error of the estimation – integrated pier section 2-

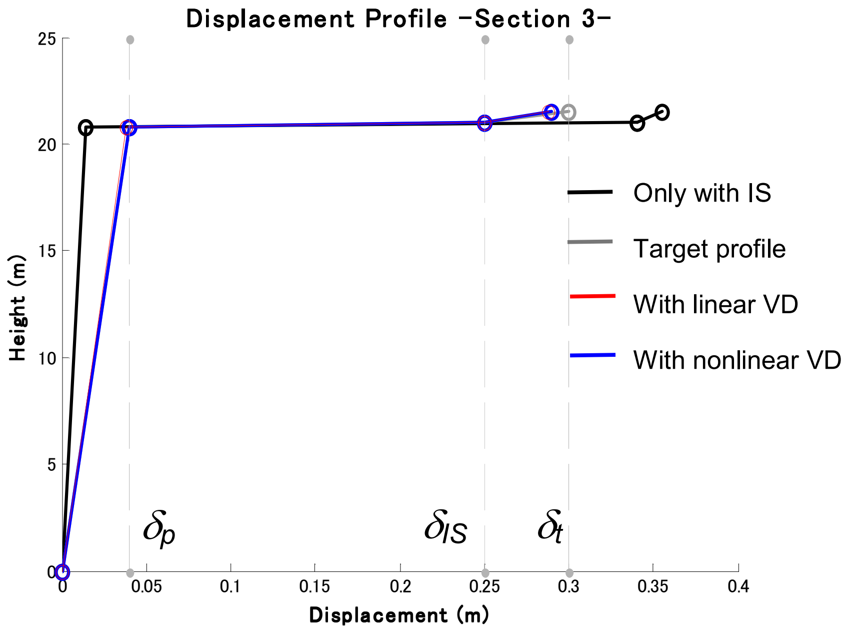

Figure 4.17. Maximum displacement profile –integrated pier section 3-

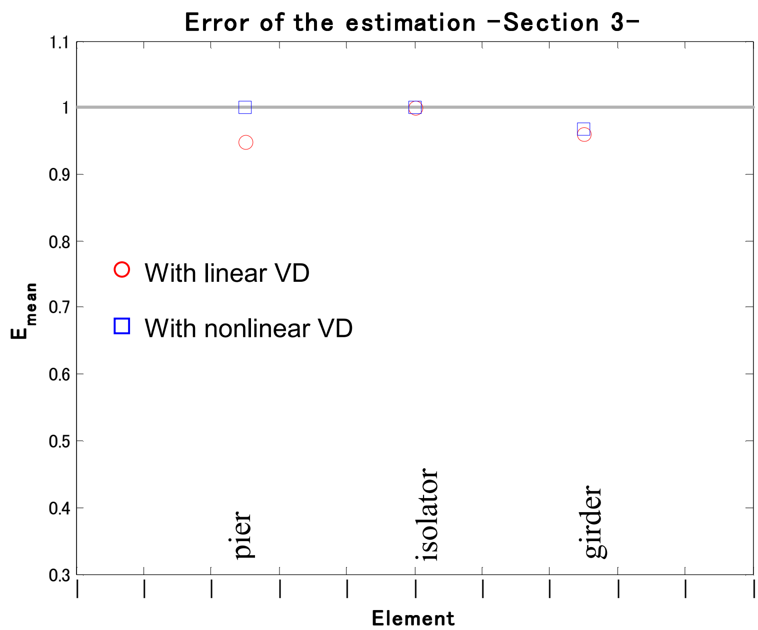

Figure 4.18. Error of the estimation – integrated pier section 2-

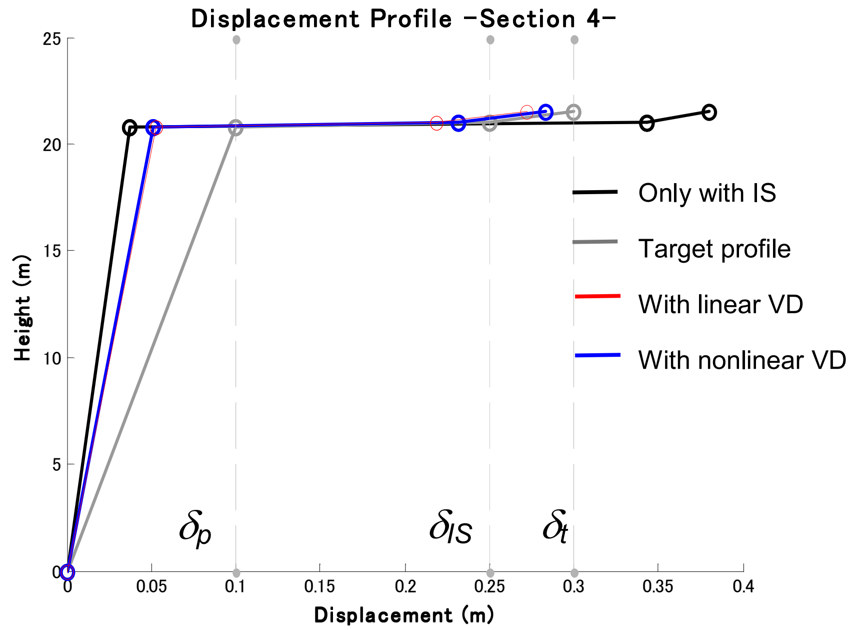

Figure 4.19. Maximum displacement profile –integrated pier section 3-

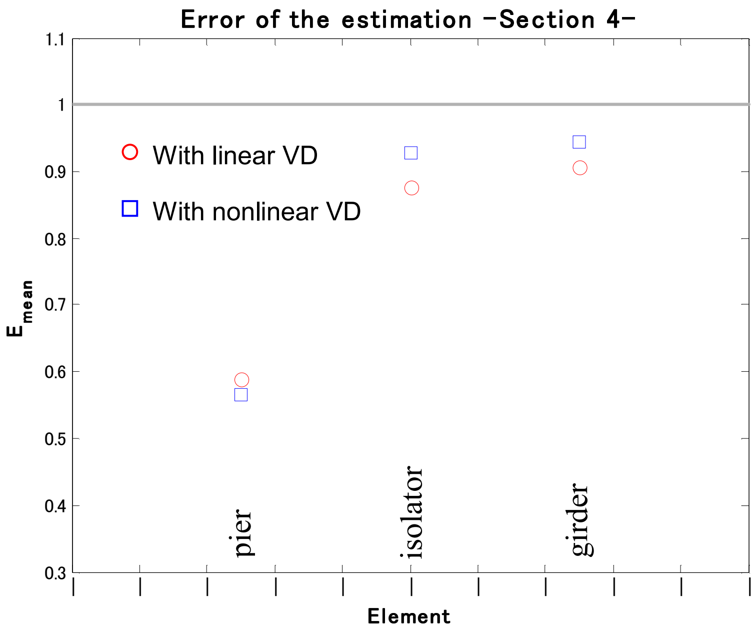

Figure 4.20. Error of the estimation – integrated pier section 2-

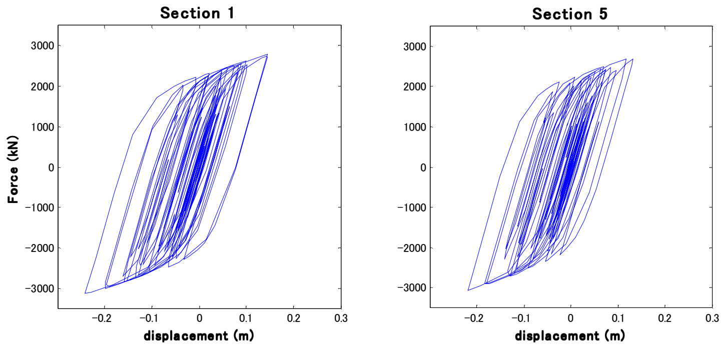

Figure 4.21 Hysteresis of the IS in the abutments –case: Linear VD-

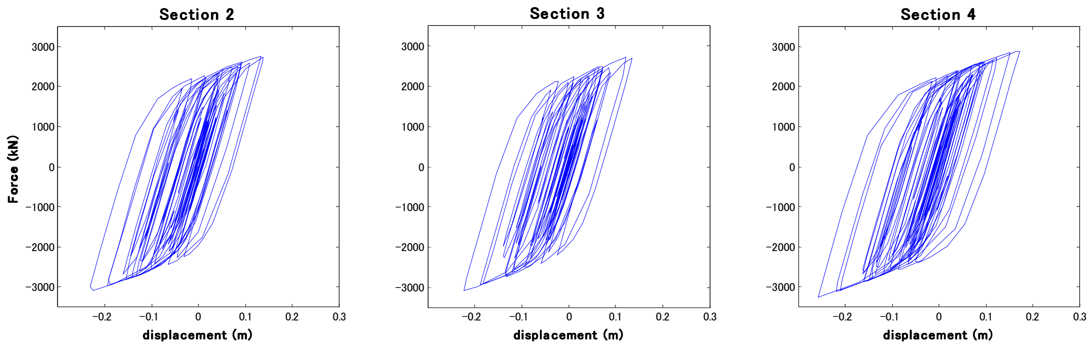

Figure 4.22 Hysteresis of the IS in the piers –case: Linear VD-

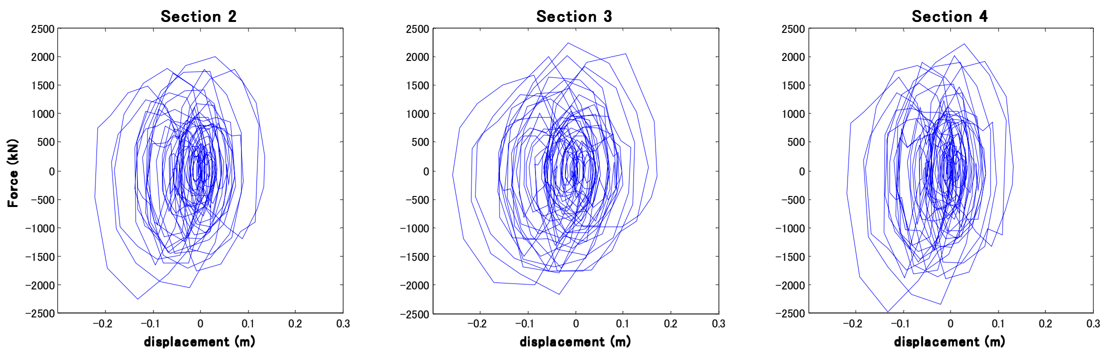

Figure 4.23 Hysteresis of the VD in the piers –case: Linear VD-

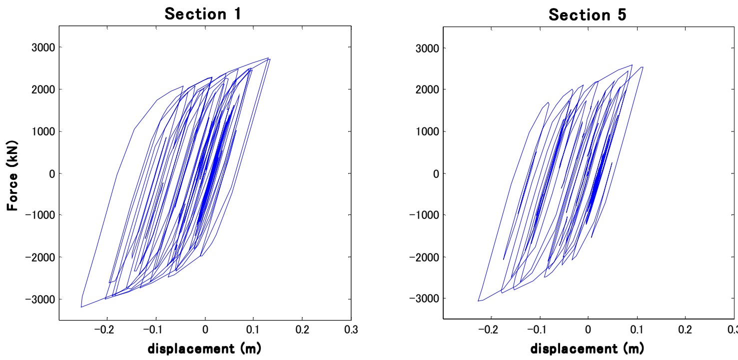

Figure 4.24 Hysteresis of the IS in the abutments –case: Nonlinear VD-

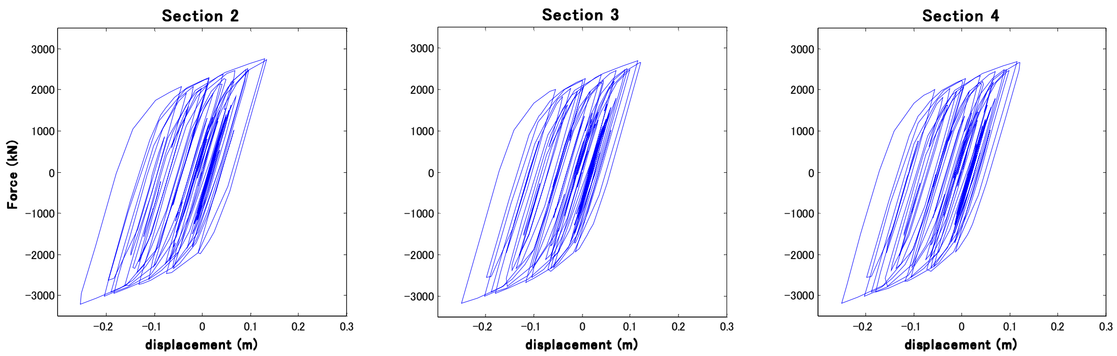

Figure 4.25 Hysteresis of the IS in the piers –case: Nonlinear VD-

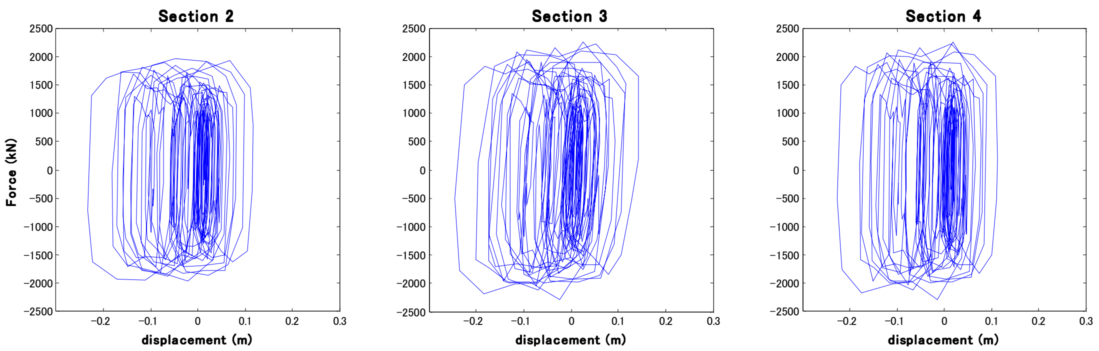

Figure 4.26 Hysteresis of the VD in the piers –case: Nonlinear VD-

4.2.5 FINAL COMMENTS

The presented examples was solved 30 times with a different artificial earthquake compatible with the displacement spectra (Chapter 2), Table 4.2 shows the average values. In most cases, no iterations were required in the design of single piers. In some cases, due to the variation of the resulting displacements after the first iteration, an additional one was required. This behavior then, suggests the influence of the compatible earthquakes in the accuracy of the results.

In a more general view, the accuracy of the presented method is influenced by the inherent errors presented in each of the equations and in the tools used in its derivation: a) One comes from the earthquakes used as input; in the example, artificial motions compatible with the displacement spectra were used. The use of real earthquakes and their corresponding displacement spectrum is recommended so the spectral displacement at period T_{eq} would be nearly the exact value. b) In this example, the displacement spectrum was derived from the acceleration spectrum. However, spectra generated in this way are not necessarily compatible (Boomer et al., 2000). For this reason, the use of a displacement spectrum compatible with the acceleration spectrum is strongly recommended, especially in the neighborhood of the corner period. c) The damping reduction defined by Equation 2.30 is an approximation of the real damped spectra. More accurate results can be obtained with more realistic damped spectra. d) The different assumptions involved in the rest of the equations used (Equations 2.12 and 2.21).

The method however, provides an accurate enough process to calculate the coefficients of the viscous dampers to limit the displacement under allowable predefined values.

4.3 Summary

In this Chapter, a new displacement-based design procedure for concrete bridges on bilinear isolated devices with viscous dampers was developed. The limit state considered in this study is such that the piers and the deck remain elastic, while the isolated devices are allowed to behave inelastically. In this approach, the dampers can either be linear or nonlinear. The proposed methodology has two advantages: the direct calculation of the design forces on the piers, and the fast calculation of the damping coefficient of the viscous dampers to limit the maximum displacement of the structural elements under the target value, avoiding the iterative nonlinear calculations of the current force-based design. The application of the proposed methodology was presented and their results were validated by nonlinear time history analysis.

References

American Association of State Highway and Transportation Officials (AASHTO). (1999), *Guide Specifications for Seismic Isolation Design*, Washington, D.C.

Bardakis V. G. and Fardis M. N. (2008), "Displacement-based seismic design of concrete bridges" *Proceedings of the 14th World Conference on Earthquake Engineering*, Beijing, China, October.

Bommer, J. J., Elnashai, A. S. and Weir, A. G. (2000), "Compatible acceleration and displacement spectra for seismic codes", *Proceedings of the 12th World Conference on Earthquake Engineering*, Auckland, New Zealand, February.

Building Seismic Safety Council (BSSC), (1997), "NEHRP Guidelines for the Seismic Rehabilitation of Buildings," Report FEMA 273/274, Federal Emergency management Agency, , Washington, D.C.

BSSC, (2000), "Prestandard and Commentary for the Seismic Rehabilitation of Buildings", Federal Emergency management Agency, Washington, D.C.

Calvi G. M. and Kingsley G. R. (1995), "Displacement-based seismic design of multi-degree-of-freedom bridge structures", *Earthquake Engineering and Structural Dynamics*, **24**(9):1247–1266.

Calvi, G. M. and Pavese, A. (1995), "Displacement based design of building structures", *Proceedings of the Fifth SECED Conference*, Exeter, UK, 127-132.

Cardone D., Dolce M. and Palermo G. (2009), "Direct displacement-based design of seismically isolated bridges", *Bull Earthquake Eng* 7:391–410

Chopra A. K. and Goel R. K. (2001), "Direct Displacement-Based Design: Use of Inelastic vs. Elastic Design Spectra", *Earthquake Spectra*, **17**(1): 47-64.

Japan Road Association (JRA), (2002), *Seismic Design Specifications for Highway Bridges* (in Japanese)

Jara M. and Casas J. R. (2006), "A direct displacement-based method for the seismic design of bridges on bi-linear isolation devices", *Engineering Structures* 28: 869–879.

Kim J. and Choi H. (2006), "Displacement-Based Design of Supplemental Dampers for Seismic Retrofit of a Framed Structure", *Journal of Structural Engineering*, 132(6):873-883

Kowalsky, M. J., Priestley M. J. N. and MacRae G. A. (1995), "Displacement-based design of RC bridge columns in seismic regions", *Earthquake Engineering and Structural Dynamics*, **24**(12):1623–1643.

Lin Y. Y., Chang K. C. and Chen C. Y. (2008), "Direct displacement-based design for seismic retrofit of existing buildings using nonlinear viscous dampers", *Bull Earthquake Eng* **6**(3):535–552.

Medhekar M. S. and Kennedy D. J. L. (2000), "Displacement-based seismic design of buildings—theory", *Engineering Structures* **22**(3):201–209

Moehle J. P. (1992), "Displacement-based design of R/C structures subjected to earthquakes", *Earthquake Spectra* **8**(3), 403-427.

Panagiotakos T. B. and Fardis M.N. (2001), "A Displacement-based Seismic Design Procedure of RC Buildings and Comparison with EC8", Journal of Earthquake Engineering and Structural Dynamics, **30**(10): 1439-1462.

Pang W. and Rosowsky D. (2007), "Direct displacement procedure for performance-based seismic design of multistory woodframe structures", *NESSWOOW* Report NW-02

Pietra D., Calvi G. M., Pinho R. Displacement-based seismic design of isolated bridges, Research Report No. ROSE 2008/01. IUSS Press 2008

Priestley M. J. N., Calvi G. M. and Kowalsky M. J. (2007), *Displacement-based seismic design of structures*, IUSS Press, Pavia, Italy.

Priestley M. J. N., Seible F. and Calvi G. M. (1996), *Seismic design and retrofit of bridges*, John Wiley & Sons, New York, USA.

Roesset J.M., Whitman R.V., Dobry R. (1973), "Modal analysis for structures with foundation interaction", *Journal of the Structural Division*, ASCE, **99**(ST3):399–416.

SEAOC (1995), "Performance-based seismic engineering", Vision 2000 Committee, *Structural Engineers Association of California*, Sacramento, CA.

Shinde J. K., Symans M. D., Pang W. C. and Rosowsky D. V. (2008), "Displacement-based design of woodframed structures with linear viscous fluid dampers", *Proceedings of the 14th World Conference on Earthquake Engineering*, Beijing, China, October.

Singh M. P., Verma N. P. and Moreschi L. M. (2003), "Seismic analysis and design with Maxwell dampers", *Journal of Structural Engineering*, **129**(3):273-282.

Wallace J. W. (1995a), "Seismic design of RC structural walls. Part I: new code format", *Journal of Structural Engineering*, ASCE, **121**(1):75–87.

Wallace J. W. (1995b), "Seismic design of RC structural walls. Part II: applications", *Journal of Structural Engineering*, ASCE, **121**(1):88–100.

Yun H. B., and Tasbighoo F., Masri S. F., Caffrey J. P., Wolfe R. W., Markis N. and Black C. (2008), "Comparison of modeling approaches for full scale nonlinear viscous dampers", *Journal of Vibration and Control*, 14:51-7

CHAPTER 5

BIDIRECTIONAL DISPLACEMENT-BASED DESIGN OF SKEWED ISOLATED PIERS WITH VISCOUS DAMPERS

5.1 GENERAL REMARKS

The effects of the multidirectional earthquake phenomenon are very complex and involve a large amount of variables. In the absence of near-source effects, it is valid to assume that ground motions have one strong principal direction so in the perpendicular one the ground motion acts with a lesser magnitude (Penzien and Watabe, 1975). These motions are regarded to be statistically independent of each other acting simultaneously in two perpendicular directions. For seismic design of bridges subjected to multidirectional earthquakes, the representative maximum response of interest for design (displacement or acceleration) can be obtained by combining the corresponding maximum individual modal responses derived from the response spectrum method (Chopra 2001, Clough 2003). Once the seismic forces are calculated they can be applied in two orthogonal directions.

In general, it is unlikely that the maximum individual modal responses would all occur at the same time during an earthquake. Thus, it is necessary to identify appropriate combination methods to obtain the representative maximum response of interest from the maximum individual modal responses. The methods utilized to combine seismic responses of individual modes obtained from the response spectrum method can provide only approximate representative maximum values, which do not necessarily correspond to the time history method.

The multidirectional effect of the earthquakes on global seismic response is more prominent for skewed bridges. The complexity of this phenomenon is influenced by several factors including bridge skew angle, deck flexibility, number of spans, number of columns per bent, column ductility, soil-abutment-superstructure interaction, soil-structure interaction, characteristics of the abutments, and characteristics of the earthquake. Moreover, skewed bridges subjected to multidirectional earthquakes tends to rotate causing excessive transverse movement, unseating of the superstructure, and pounding the abutment backwall (Maleki and Bisadi, 2006).

In displacement-based design of bridges, it is common to assume the earthquake acting in only one direction (transverse or longitudinal), design the structure and combine the responses from each direction following the Code requirements. Although this approach may be acceptable for uniformly straight bridges, for skewed ones it may give inaccurate results. In spite of its importance, however, there is still not a robust methodology to account for bidirectional effects in skewed bridges within the framework of displacement-based design. For this reason, in the following section a methodology to estimate the maximum response of skewed piers subjected to bidirectional earthquakes is presented, exemplified and verified.

5.2 REVIEW OF THE PREVIOUS STUDIES

5.2.1 FOR SPECTRAL AND TIME HISTORY ANALYSIS

i. The simplest and most conservative combination for the bidirectional seismic response is the Absolute Sum Method (ASM). This approach assumes that the maximum modal values, for all modes, occur at the same point in time. Due to the conservative results obtained, it is not often used in engineering practice (Maleki and Bisadi, 2006). Consider R_T as the resulting action (shear force, bending moment, displacement, etc.) due to the earthquake, and R_x and R_y as the actions in the direction x and y respectively. The ASM is defined by the following equation:

$$R_T = |R_x| + |R_y| \tag{5.1}$$

ii. Another method used is the square-root-of-the-sum-of-squares (SRSS). The basic assumption of this method is that R_x and R_y are statistically independent, thus there is no correlation between the horizontal components (Reyes-Salazar et al. 2008). The results obtained in this method are independent of the chosen reference axis and are generally conservative (Wilson and Habibullah, 1995). This rule would be accurate if the assumed horizontal ground motion components were along the principal axes of the earthquake, or the inputs in each of the perpendicular directions are the same (Menun and Der Kiureghian, 1998). However, for three-dimensional structures in which a large number of frequencies are almost identical, this assumption is not justified.

The total response considering the contribution of the first mode is given by the following expression (Wilson *et al.* 1995):

$$R_T = \sqrt{(R_x^{\ 2} + R_y^{\ 2})} \tag{5.2}$$

When R_x and R_y are given by different spectra, the critical angle (θ_{cr}) for which the action R_T will be maximum or minimum is given by

$$\theta_{cr} = \frac{1}{2}\tan^{-1}\left(\frac{\pm 2R_x R_y}{R_x^{\ 2} + R_y^{\ 2}}\right) \tag{5.3}$$

However, when the same spectrum is applied along any arbitrary set of directions, the structural response does not depend of the angle of incidence, and therefore, any value of θ_{cr} is a critical value (Lopez and Torres, 1996).

iii. Complete quadratic combination (CQC). This method based on random vibration theories requires that all modal response terms be combined by the application of the following equations (Wilson et al. 1981):

$$\text{For displacements } u_k = \sqrt{\sum_i^N \sum_j^N u_{ki} \rho_{ij} u_{kj}} \tag{5.4}$$

$$\text{For forces } f_k = \sqrt{\sum_i^N \sum_j^N f_{ki} \rho_{ij} f_{kj}} \tag{5.5}$$

where the correlation coefficient ρ_{ij} is given by

$$\rho_{ij} = \frac{8\sqrt{(\xi_i \xi_j)[\xi_i + (\omega_j/\omega_i)\,\xi_j]}\,(\omega_j/\omega_i)^{3/2}}{[1-(\omega_j/\omega_i)^2]^2 + 4\xi_i\xi_j\,(\omega_j/\omega_i)[1+(\omega_j/\omega_i)^2]4(\xi_i+\xi_j)^2\,(\omega_j/\omega_i)^2} \tag{5.6}$$

where ξ and ω are the damping and frequencies in the corresponding modes i and j respectively, and u_{ki} is a typical component of the modal displacement response vector, $U_{i,max}$, and f_{ki} is a typical force component which is produced by the modal displacement vector, $U_{i,max}$.

iv. Improved complete quadratic combination (CQC3). It is an extension of the CQC rule defined by the following equations (Menun and Der Kiureghian, 1998):

$$R_T = \sqrt{\left[(R_x^{\ 2} + R_y^{\ 2}) - (1-\gamma^2)\left(R_x^{\ 2} - \frac{1}{\gamma^2} R_y^{\ 2}\right)\sin^2\theta_{cr} + \left(\frac{1-\gamma^2}{\gamma} R_{xy} \sin\theta_{cr} \cos\theta_{cr}\right)\right]} \tag{5.7}$$

where $R_x \leq R_y$

$$\gamma = \frac{R_x}{R_y} \tag{5.8}$$

$$\theta_{cr} = \frac{1}{2}\tan^{-1}\left(\frac{\frac{2}{\gamma} R_{xy}}{R_x^{\ 2} - \frac{1}{\gamma^2} R_y^{\ 2}}\right) \tag{5.9}$$

$$R_{xy} = \sum_i \sum_j \rho_{ij} a_{xi} a_{yi} S_{xi} S_{yi} \tag{5.10}$$

with the terms *a* representing the participation factors of the modes *i* and *j* along the directions *x* and *y*.

v. Concurrent Orthogonal Excitations. The bi-directional seismic effects are combined according with the 1-λ rule. In this rule, λ times of the response in one direction is added to the total response in the perpendicular direction as

$$R_R = R_x + \lambda R_y \tag{5.11}$$

$$R_R = \lambda R_x + R_y \tag{5.12}$$

In the 100%-30% rule, λ=0.3 (Rosenblueth and Contreras 1977, AASHTO 2008, CALTRANS 2006).

In the 100%-40% rule, λ=0.4 (ATC 1996, Newmark 1975, NCHRP 2001).

For single span skewed bridges with elastomeric bearings the 100%-40% combination of input motion produces reasonable results (Maleki and Bisadi, 2006).

vi. Bidirectional spectra. This type of spectra has been adopted by some design codes (NEHRP, 2009). The bi-directional seismic effects are taken into account in the design spectra by the following relationship

$$S_A = \sqrt{S_{A,x}{}^2 + S_{A,y}{}^2} \tag{5.13}$$

where S_A is the total acceleration and $S_{A,x}$ and $S_{A,y}$ are the acceleration in directions *x* and *y*, respectively. Although the bidirectional spectra is easy to implement for practical applications, the bidirectional displacement spectrum is still not well established for long periods. Then, its application is not recommended for static analysis on displacement-based design. Moreover, in near-fault earthquakes the influence of the orientation in the maximum response has been recognized as significant factor (Huang *et al*. 2009). Therefore, the definition of the horizontal ground motion from the peak response of a single lumped mass oscillator regardless of direction is still controversial (Stewart *et al*. 2010),

5.2.2 FOR DISPLACEMENT-BASED DESIGN

In the current conception of DBD, the structural elements resist the earthquake effects undergoing deformations exclusively within the plane of the earthquake input. Therefore, the bridge is designed for the most unfavorable direction (transverse or longitudinal), and the less critical direction is checked to be within allowable limits (Priestley, 2007). Another option commonly used in force-based design can be applied in DBD. It consists of designing the bridge in both longitudinal and transverse directions. Then, the responses are combined by using any of the methods described in sections 5.2.1 (Figure 5.1).

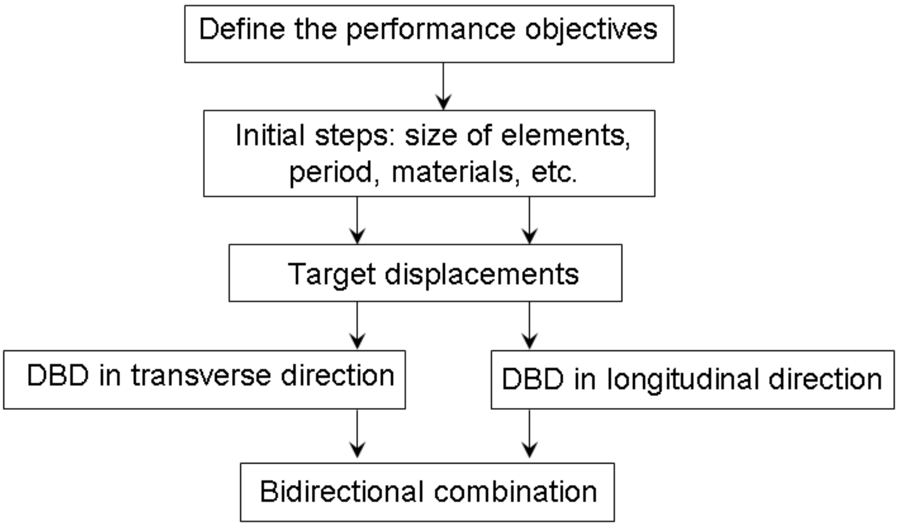

Figure 5.1. Current bidirectional DBD

One attempt to explicitly account for bidirectional earthquakes in DBD was presented by Suarez (2008). This approach considers that the in-plane and out-of plane response parameters of abutments and piers in a skewed configuration are no longer oriented in the principal design directions of the bridge (Figure 5.2.). Then, the effects of the skew can be considered in DBD by the projection of the response parameters such as yield displacement δ_y, target displacement δ_T, and others with respect to the transverse and longitudinal direction of the bridge. To consider these effects, Suarez (2008) proposed an elliptical interaction function between the in-plane and out-of-plane response, given by the following equations:

$$rp_L = rp_{out} + skew\frac{(rp_{in} - rp_{out})}{90} \tag{5.14a}$$

$$rp_T = rp_{in} + skew\frac{(rp_{out} - rp_{in})}{90} \tag{5.14b}$$

where, rp_{in} is the value of the response parameter in the in-plane direction of the element, rp_{out} is the response parameter in the out-of-plane direction of the element, rp_T is the projection of the response parameter in the transverse direction of the bridge and rp_L is the projection of the response parameter in the longitudinal direction of the bridge.

For isolated bridges with additional dampers, no method that explicitly accounts for the combination of bidirectional earthquakes in displacement-based design has been found.

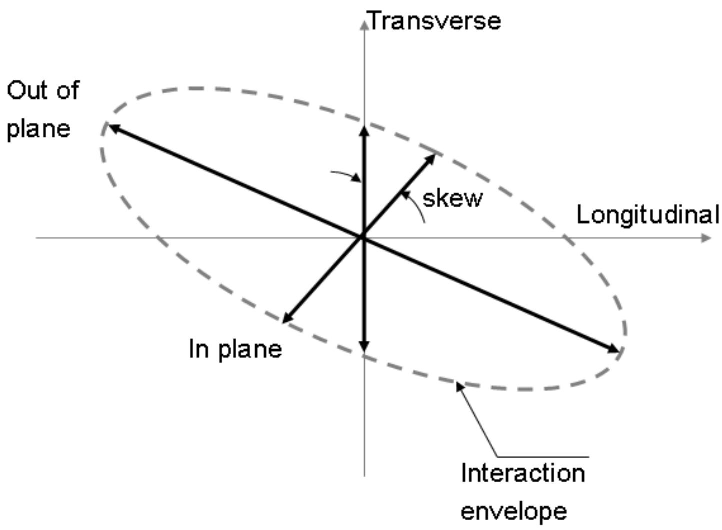

Figure 5.2. Design axes in skewed elements (Suarez, 2008)

5.3 DISPLACEMENT-BASED DESIGN OF SKEWED PIERS

5.3.1 CONCEPTUAL SCOPE

Most of the methods presented in section 5.2.1 were developed to combine the response of multiple modes for MDOF systems. For isolated bridges designed under the displacement-based design philosophy, the following simplifications can be done (Figure 5.3):

- Only the contribution of the fundamental mode is assumed.
- The piers must remain elastic during seismic events (section 4.2.2). Then, the inelastic behavior of the system can be assumed to be in the isolators and the projections by Suarez (2008) are valid for transverse and longitudinal directions for the elastic piers.
- The torsional effects produced by the skewed angle are assumed to small so they can be neglected. This is valid since the rotation is absorbed by the isolators and the main source of rotation is given in the ends of the bridges by pounding between the deck and the abutments (Maleki and Bisadi, 2006).
- The rotation of the damper (φ) and the variation of the stroke are the only movements considered. Deformation of the damper due to other effects (buckling, manufacturing deficiencies, etc.) are not considered. The location of the damper shall be calculated for a specific design earthquake. Then, introducing the mathematical optimal orientation of the damper goes beyond the scope of this dissertation. The limitations in fact, do not come from the design methodology itself. The restrictions are due the lack of reliable records that well represent a family of earthquakes with specific site characteristics for which, the displacement spectra would be compatible with the corresponding acceleration spectra as recommended in Chapter 3 and Chapter 4.
- To account for the bidirectional effects in the calculation of the maximum displacements, the maximum displacement demands ($\delta_{x,max}$, $\delta_{y,max}$) are defined in terms of the skewed angle θ_{skw}, and the maximum responses of the bridge in the direction x and y are projected by Equations 5.14 (Figure 5.2). Then, $\delta_{max}(\theta_{skw}, R_x, R_y)$.

In this study, the objective is to calculate the damper coefficient in such a way that the resulting displacement does not exceed the target one, for this reason the simplification of the equivalent structure shall account for the bidirectional effects.

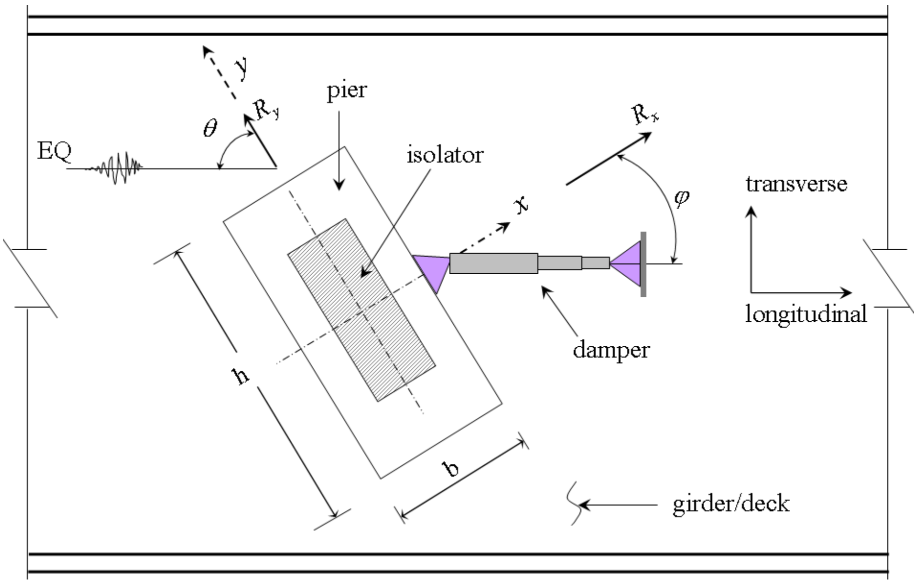

Figure 5.3 Skewed isolated pier with viscous damper

5.3.2 NUMERICAL SCOPE

- The response quantities of interest for the system under consideration are the absolute displacement of the superstructure and the relative displacement of the isolators and dampers.
- The isolators are characterized by bilinear model considering bilinear coupling effects (Huang *et al*, 2000) with the typical behavior shown in Figure 5.4 and defined by the following equation for the two orthogonal directions *x* and *y*:

$$\left(\frac{F_x}{F_{x,y}}\right)^n + \left(\frac{F_y}{F_{y,y}}\right)^n = 1 \tag{5.15}$$

where the factor *n* is the coupling factor.

- The rotational effects are assumed to be small enough so they can be neglected.
- The artificial earthquakes generated in Chapter 2 do not account for multicomponent ground motions, then, the two components as well as the elastic displacement spectra of the Kobe earthquake (Figure 5.5) are used as input. These records are filtered, to eliminate low frequencies avoiding base line problems, using the Hodder filter (Hodder, 1983):

$$H_H(f) = \begin{cases} 0 & if \quad f < f_s \\ \sin^2\left(\dfrac{\pi(f - f_s)}{0.3}\right) & if \quad f_s < f < f_s + 0.15 \\ 1 & if \quad f > f_s + 0.15 \end{cases} \tag{5.16}$$

  where f represents the frequency components, and f_s the cut-off frequency. A detailed explanation on this filter can be found in Hodder (1983).
- The NS component of the Kobe earthquake is applied in the x-direction, and the EW component is applied in the y-direction of the system (Figure 5.3). This conditions is referred as *two-component* excitation and the response calculated. The response is also obtained for the same components acting independently in each direction (referred to as *single-component)* in which there is no interaction between them.

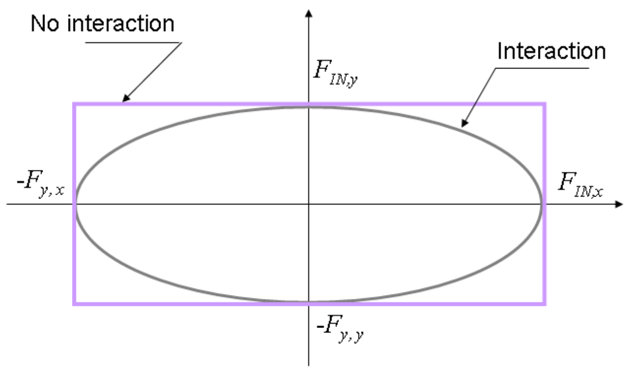

Figure 5.4. Bilinear Model with Bidirectional Interaction

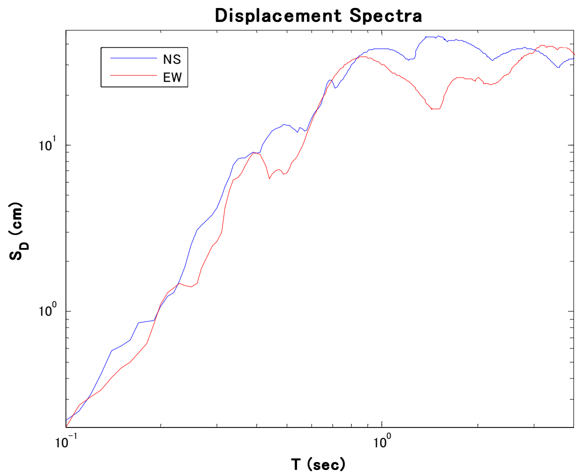

Figure 5.5 Displacement spectra for the Kobe earthquake

5.4 Design of single isolated piers with viscous dampers

5.4.1 Methodology

Basically, the displacement-based design methodology developed in Chapter 4 is still valid for skewed piers. There are, however, some basic differences: a) the target (yielding) displacement of the piers, b) the target (maximum) displacement of the isolator considering the bidirectional earthquake, and c) the influence of the damper orientation on the overall response. The main performance objectives are the same to those mentioned in Chapter 4: the gravitational system (pier and girder) remains elastic during a seismic event and the isolator behaves inelastically.

In order to account for the differences aforementioned, the step *iv* in the general algorithm (Figure 5.6) was modified.

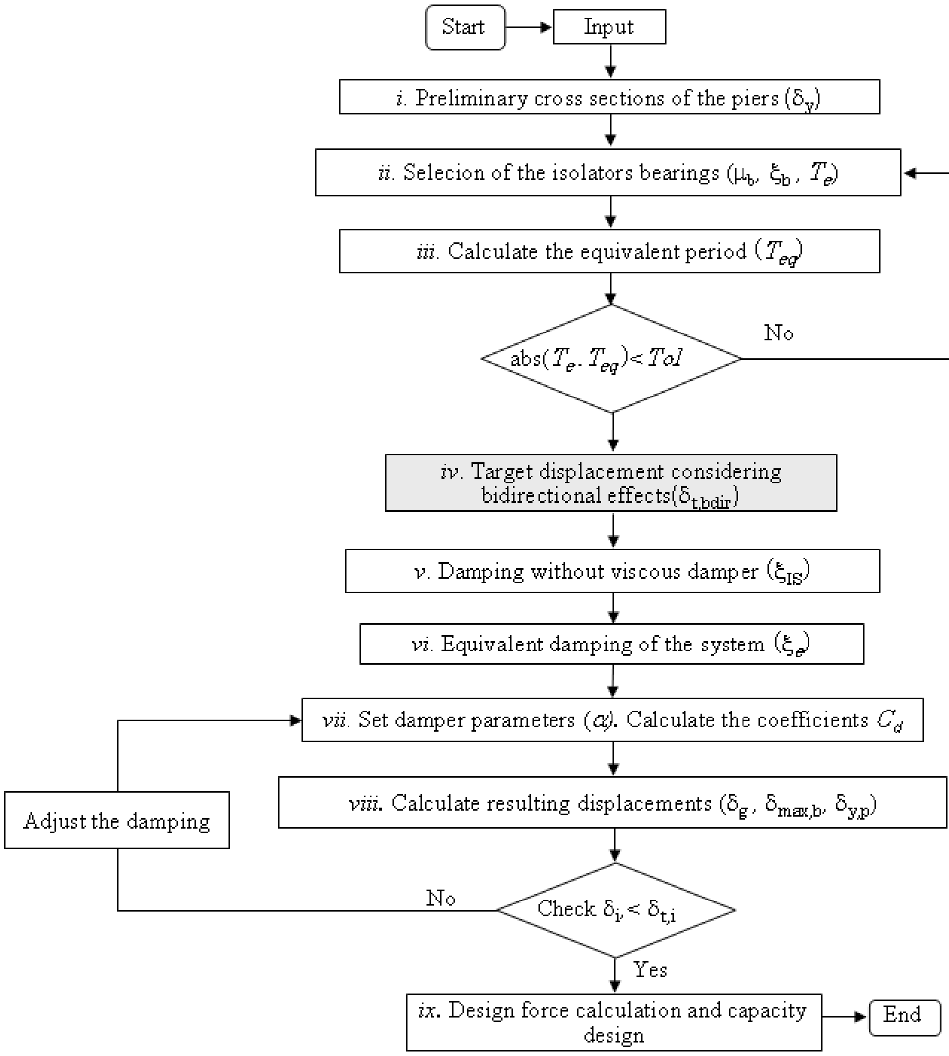

Figure 5.6 Proposed bidirectional DBD methodology

The design algorithm can be described as follows:

i. Selection of the preliminary pier cross section.

Once the selection of the pier is done and its yielding displacement is calculated as described in Section 4.2.3.1, the projections given by Equations 5.12 have to be calculated.

ii. Selection of the isolator bearings

Similar to the steps described in section 4.2.3.1. However, the maximum allowable displacement is calculated with the coupling model of Equation 5.15.

iii. Calculation of the period of the 2DOF systems

The equivalent period of the pier can be straightforwardly calculated for any skewed angle by the following equation:

$$T_e = \sqrt{\frac{m_e}{k_{skw}}} \tag{4.17}$$

where m_e is the mass calculated with the procedure of Section 4.2.3.1 assumed independent of the skewed angle ϕ, and the equivalent skewed stiffness k_{skw} is the stiffness of the skewed pier.

iv. Target displacement of the pier-IS-deck system

The new target displacement of the skewed system is calculated with the projections of the yielding displacements of the pier and the maximum displacement of the isolator subjected to bidirectional earthquakes. To this end, the envelope of total displacements have to be calculated and the maximum displacement $\delta_t=\delta_p+\delta_b$ at the time t should be calculated (Figure 5.7).

Once the magnitude and orientation of the maximum response is obtained for a two component excitation with a single earthquake, the location of the damper can be taken in the same direction of the maximum displacement (Figure 5.8). The structure, however, may be subjected to different types of earthquakes during its useful life. Then, it is recommended that the optimal location of the damper would be determined from analysis with several design earthquakes.

v. Equivalent damping of the pier-IS system

It can be calculated with Equations 4.11 and 4.12 (Section 4.2.3.1) with $k_p= k_{skw}$. In Equation 4.12, the terms, $\xi_{f\theta}$, k_{fh}, $k_{f\theta}$ should take into account the orientation φ, or they can be simplified as a the projection given by Equations 5.14.

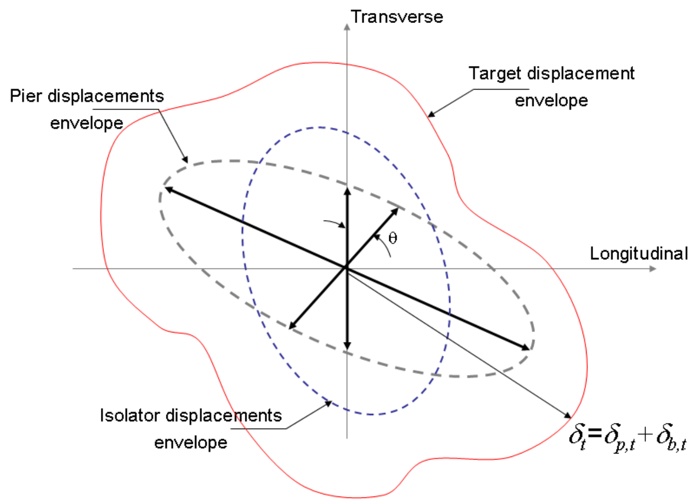

Figure 5.7 Target displacement from the total displacement envelope

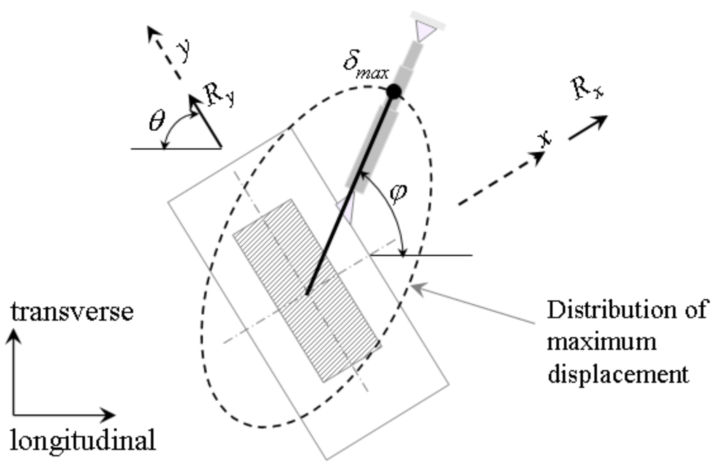

Figure 5.8 Damper orientation

vi. Maximum response of the pier-IS-deck system

The maximum response of the pier-IS-deck system has to be determined to evaluate the amount of supplemental damping required. In general, it can be done by nonlinear time history analysis or it can be approximated by linear static analysis or simplified dynamic analysis. In the present model, since the pier remains elastic and the only inelastic element is the isolator, the analysis is done by considering the coupling effects due to the bidirectional earthquake on the simplified model implemented in the software BISPEC (Engineering Solutions, 2010).

vii. Equivalent damping of the pier-IS-VD systems

Similar step to that described in Section 4.2.3.1.

viii. Coefficient of viscous dampers

Similar step to that described in Section 4.2.3.1.

ix. Verification of the target displacement and

x. Capacity design of the structural element.

Similar to the steps mentioned in Section 4.2.3.

5.4.2 Example No. 3

This example shows the design of the central pier of the bridge shown in Figure 5.9 (modified from Suarez, 2008). The bridge has two spans of 38.20 m and total length of 76.40 m. The superstructure is continuous with weight of 130 kN/m. To take advantage of the isolation and viscous dampers, the central bent is modified from the original example presented by Suarez (2008). In the present example, the central bent has one pier with rectangular cross section (b=1.25 m, h=2 m) with free height H = 6.80 m. The cap-beam height is 1.37 m and its width is 1.2 m. The reinforced concrete in columns has a compressive strength, f'_c=26.5 MPa. The reinforcing steel has a yield stress, f'_y= 414 MPa, a hardening ratio of 1.35 and a damage control strain, ε_s= 0.06. The foundation has cast-in-place reinforced concrete piles. All substructure elements are skewed 18 degrees. Unlike the example from Suarez (2008), the bridge is assumed isolated with a viscous damper in the pier location.

Firstly, the pier is independently designed in both, the transverse and longitudinal directions under single component excitation. Secondly, the design is made under two-component excitation.

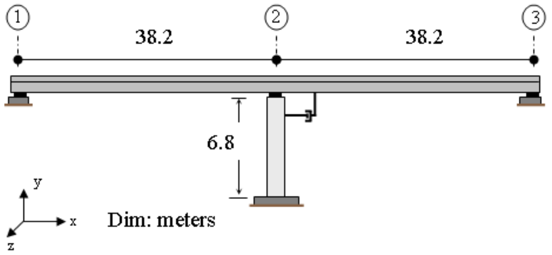

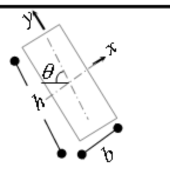

Pier section		
b (m)	h (m)	θ deg
1.25	2.0	18

Girder-deck		
Area (m²)	Ix (m⁴)	Wg (kN/m)
8.5	100	130

General		
Earthquake	Concrete	Period (sec)
Kobe EW: x Kobe NS: y	fc=30 MPa fy=414 Mpa	T_{0x}=0.51 $T_{ex}\approx 2T_0\approx 1.0$ T_{0y}=0.32 $T_{ey}\approx 2T_0\approx 0.65$

Figure 5.9 Bridge of Example 3 (Suarez, 2008)

The resulting damper coefficients are C_d=620 kN·s/m and C_{dNL}=501 kN·s/m for linear and nonlinear dampers (α=0.3), respectively as indicated in Table 5.1.

The resulting displacements are verified by bidirectional time history analysis. Figures 5.10 and 5.11 show the displacement configuration of the pier and the associated error. It can be observed the resulting displacements are smaller than the target displacement previously defined. For this specific earthquake, the viscous damper can be placed approximately at 135° with reference to the longitudinal direction (Figure 5.3). Figures 5.12 and 5.13 show the displacement history of the isolator and its displacement orbit with coupling effects, respectively. The Figure 5.14 shows the hysteretic loop for the isolator with coupling effects.

Element	ξ	δ_t (m)
System	ξ_e=30%	δ_e=0.20
Pier	ξ_p=5%	δ_p=0.05
IS	ξ_b=16%	δ_b=0.15
VD linear (φ=135°)	C_d=620 kN*s/m	δ_{LVD}=0.15
VD nonlinear (α=0.3) (φ=135°)	C_{dnl}=501 kN*s/m	δ_{NLVD}=0.15

Table 5.1 Damping and target displacements

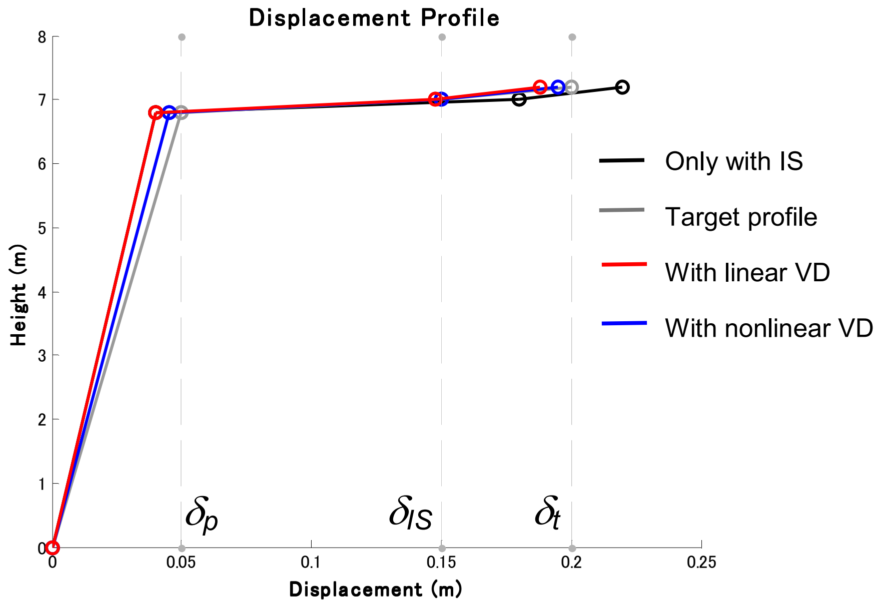

Figure 5.10 Maximum displacement profile –skewed pier-

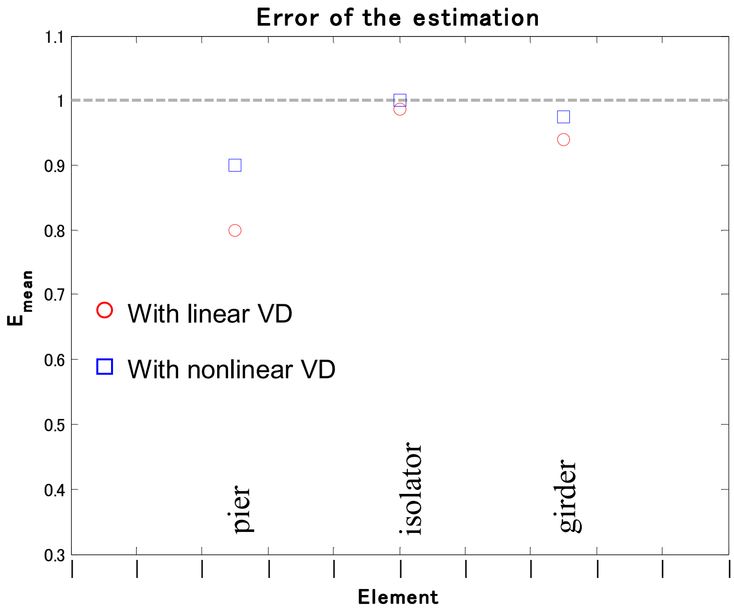

Figure 5.11 Error of the estimation –skewed pier-

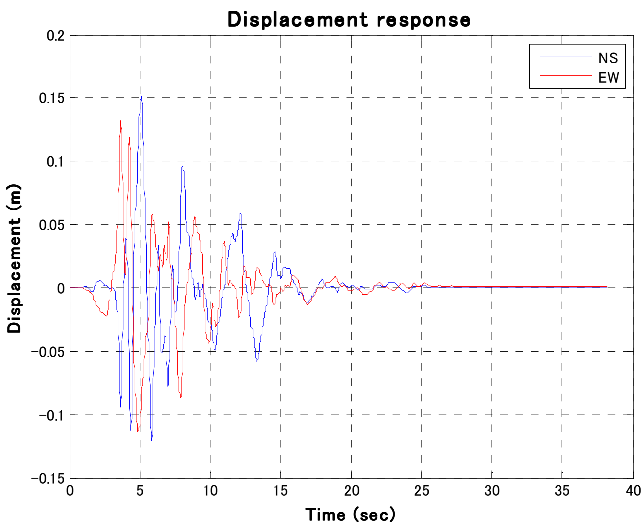

Figure 5.12 Displacement history of isolator

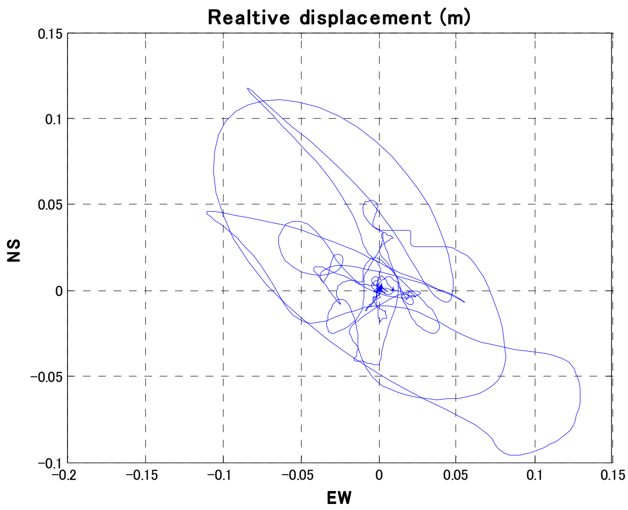

Figure 5.13 Orbit displacement of the isolator with coupling

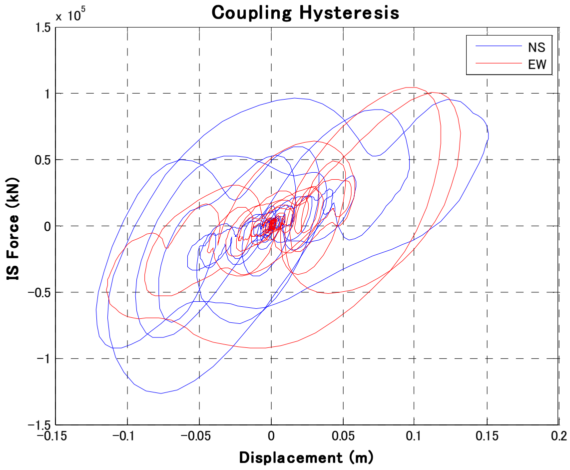

Figure 5.14 Hysteretic loop for the isolator

5.5 Final Comments

It is important to mention that although the proposed methodology limits the displacements under a predefined value, the selection of the isolator modeling may influence the accuracy of the maximum response and therefore, the dampers coefficients values may be affected. Under the modeling assumptions adopted in this Chapter, the value of the exponent n greatly affects the performance of the isolator. Therefore, a conservative value that realistically represents the bidirectional influence should be adopted.

5.6 Summary

In this Chapter, a new displacement-based design procedure for skewed isolated-piers with viscous dampers was developed. In the limit state, the piers and the deck remain elastic, while the isolated devices behave inelastically. In the proposed methodology, the dampers can either be linear or nonlinear. The methodology has been proved to be effective for single isolated piers; however, its application to a whole bridge should be complemented with additional tools to take into account the torsional effects in the pier due the skewed angle and the interaction with the abutments.

REFERENCES

Chopra A. K. (2001), Dynamics of Structures: Theory and Applications to Earthquake Engineering, 2nd Edition, Prentice Hall, New Jersey.

Clough, R.W. and Penzien, J. (2003), *Dynamics of Structures*, Computer and Structures, Inc.

Der Kiureghian A. (1981): “A response spectrum method for random vibration analysis of MDF systems”, Earthquake Engineering and Structural Dynamics, 9, 419-435.

Dhakal, R.P., Mander, J.B., Mashiko, N. (2006): “Performance of ductile highway bridge piers subjected to bi-directional earthquake attack”, *San Francisco: Eighth US "National Conference on Earthquake Engineering (8"CEE)*, 18-22 April.

Earthquake Solutions, (2010), *Bispec Version Student version*, http://eqsols.com/default.aspx

Grant D. (2004), Bidirectional modeling of high damping rubber bearings, PhD Dissertation, ROSE School.

Hodder, S. B. (1983), “Computer processing of New Zealand strong-motion accelerograms”, *Proceedings of the Third South Pacific Regional Conference on Earthquake Engineering*,1: 36-53.

Huang, W., Fenves, G.L., Whittaker, A.S. and Mahin, S.A. (2000), “Characterization of seismic isolation bearings for bridges from bi-directional testing”, *Proceedings of the 12th World Conference on Earthquake Engineering*, New Zealand.

Huang Y., Whittaker A. S., and Luco N. (2009), “Orientation of Maximum Spectral Demand in the Near-Fault Region”, *Earthquake Spectra*, 25(3): 707–717

Lopez O. A. and Torres R. (1996): “Discussion of “A clarification of the orthogonal effects in a three-dimensional seismic analysis by E. L. Wilson, I. Suharwardy, and A. Habibullah””, *Earthquake Spectra*, 12(2), May, 357-361.

Maleki S. and Bisadi V. (2006): “Orthogonal effects in seismic analysis of skewed bridges”, *Journal of Bridge Engineering*, 11(1), Jan., 122-130.

Menun C. and Der Kiureghian A. (1998): “A replacement for the 30%, 40%, and SRSS rules for multicomponent seismic analysis”, *Earthquake Spectra*, 14(1), 153-163.

Penzien J., and Watabe M. (1975): “Characterization of 3-dimensional earthquake ground motions”, *Earthquake Engineering and Structural Dynamics*, 3, 365-373.

Stewart J. P., Abrahamson N. A., Atkinson G. M., Baker J. W., Boore D. M., Bozorgnia Y., Campbell K. W., Comartin C. D., Idriss I. M., Lew M., Mehrain M., Moehle J. P., Naeim F., Sabol T. A., and M.EERI (2010): "Representation of bi-directional ground motions for the design spectra in buildings codes", Submitted to *Earthquake Spectra*

Suarez V.A., (2008), "Implementation of the Direct Displacement Based Design Method for Highway Bridges", PhD Dissertation, North Carolina State University.

Tena-Colunga A. and Escamilla-Cruz J.L, (2008), "Torsional Amplifications in Asymmetric Base Isolated Structures", *Journal of Engineering Structures*, 29(2): 237-247.

Tena-Colunga A. and Gomez-Soberon L. (2002), "Torsional Response of Base Isolated Structures due to Asymmetries in the Superstructures", *Journal of Engineering Structures*, 24(2), pp 15871599.

Warn G. (2003), *Performance Estimates in Seismically Isolated Bridge Structures,* M.S. Thesis, University at Buffalo, May.

Wilson E. L., Suharwardy I. and Habibullah A. (1995): "A clarification of the orthogonal effects in a three-dimensional seismic analysis", *Earthquake Spectra*, 11(4), Nov., 659-666.

CHAPTER 6

CONCLUSIONS

Throughout the years, extensive research on seismic design methodologies and seismic energy dissipation devices to mitigate the damage of structures subjected to earthquakes has been conducted. However, the current state-of-practice does not include yet some advances on new design methodologies with seismic energy dissipation devices. For this reason, this study attempted to contribute with some developments to the implementation of the displacement-based design in the current practicing engineering. The conclusions of this research are presented as follows:

In Chapter 3, a set of equations to calculate the equivalent period and damping of SDOF systems was derived by statistical procedures on equivalent linearization. The equations were derived from nonlinear analyses of systems with modified Clough hysteretic behavior for ductility ratio values of 1, 1.5, 2, 3, 4, 5, and 6. Families of artificially generated ground motions compatible with the acceleration spectra for earthquakes level 2, as defined by the Japanese Seismic Design Specifications for Highway Bridges, were used in the time response analysis. The results confirm the dependency on the initial period of both the equivalent period and the equivalent damping. The results indicate the proposed equations can estimate the maximum inelastic displacement between the limits of conservative errors set as -10% and 20%. In general, although there is a trend to overestimate the maximum displacements, the maximum error is always smaller than 20%. The results also suggest that the equivalent properties should be derived for specific type of earthquakes, for one hysteretic model and for specific soil conditions. Moreover, in order to capture the period shift at long periods, the use of displacement spectra compatible with the acceleration spectra is strongly recommended.

In Chapter 4, a new Displacement-Based Design (DBD) methodology for continuous and multi-span bridges with base isolation and viscous dampers was presented. The performance level of the bridge was defined by the elastic behavior of the piers and deck and the inelastic behavior of the isolators characterized by a bilinear model. The design procedure was applied to a 4-span continuous simply supported bridge, characterized by an irregular layout of pier heights. The predictions of the displacement-based design method were compared with the results obtained by nonlinear time-history analyses. To this end, a set of 30 spectrum compatible accelerograms were used. From this comparison, it was verified that the bridges and piers designed with the proposed DBD method satisfied the desired performance level by achieving the target displacements of the structural elements (girder, piers and isolators) while the piers remain elastic. Based on the results, the method was proved to be efficient and accurate so it can be used for preliminary design to avoid the iterative nonlinear analysis required in the current force-based design to calculate the viscous damper coefficients. The proposed design procedure, however, is not intended to cover all the aspects related to the design of bridges with seismic isolation and viscous dampers. It establishes the fundamental steps under a rational methodology for the effective calculation of the viscous damper coefficients to control displacements under severe earthquakes. Moreover, the design methodologies are general enough so they are compatible with any design Code. For this reason, the safety factors were intentionally omitted. In the current form, the presented methodologies can be straightforwardly implemented in any computational program.

In Chapter 5, a methodology for the design of skewed isolated piers of bridges with viscous dampers was presented. The proposed methodology is consistent with the others obtained in Chapter 4 in such a way that it can be straightforwardly implemented. The presented method can be directly use in the effective design of single piers or in the preliminary design of skewed bridges. Although the presented methodology has been proved to be effective for single isolated piers, its application to a whole bridge should be complemented with the torsional effects on the pier due the skewed angle and the interaction with the abutments. Additionally, a carefully selection of the coupling exponent for the isolator is strongly recommended.

This study attempts to contribute with some developments to the implementation of the displacement-based design in the current practicing engineering with the development of –easy-to-implement tools derived by the Japanese Design Specifications for Highway Bridges, although the developed algorithms are valid for other Design Codes.

The research objectives were completely achieved. However, it is important to mention that displacement-based design methodologies are still under development. Therefore, further research is needed before the implementation in major codes of a robust displacement-based design of isolated-bridges with seismic energy dissipation devices. Especially, additional studies on more accurate simplifications for the equivalent structure in MDOF bridges, and on skewed bridges subjected to multidirectional earthquakes to evaluate the optimum orientation of the seismic dampers.